

DEVELOPMENT AND APPLICATION OF A METHODOLOGY FOR  
MEASURING ATMOSPHERIC MERCURY BY INSTRUMENTAL  
NEUTRON ACTIVATION ANALYSIS

by

Michael R. Ames

B.S. Nuclear Engineering, Massachusetts Institute of Technology (1984)  
M.S. Nuclear Engineering, Massachusetts Institute of Technology (1986)

Submitted to the Department of Nuclear Engineering  
in partial fulfillment of the requirements for the degree of

Doctor of Science  
in Nuclear Engineering

at the  
Massachusetts Institute of Technology  
June 1995

© Massachusetts Institute of Technology 1995. All rights reserved.

Signature of Author \_\_\_\_\_  
Department of Nuclear Engineering  
May 17 1995

Certified by \_\_\_\_\_  
Ilhan Olmez, Thesis Advisor  
Principal Research Scientist, Nuclear Reactor Lab

Certified by \_\_\_\_\_  
Michael J. Driscoll, Thesis Reader  
Professor Emeritus, Nuclear Engineering

Accepted by \_\_\_\_\_  
Allan F. Henry  
Chairman, Department Committee on Graduate Students

Science  
MASSACHUSETTS INSTITUTE  
OF TECHNOLOGY

JUN 07 1995

LIBRARIES

DEVELOPMENT AND APPLICATION OF A METHODOLOGY FOR  
MEASURING ATMOSPHERIC MERCURY BY INSTRUMENTAL  
NEUTRON ACTIVATION ANALYSIS

by

MICHAEL R. AMES

Submitted to the Department of Nuclear Engineering on May 17, 1995  
in partial fulfillment of the requirements for the degree of

Doctor of Science in Nuclear Engineering

**ABSTRACT**

A complete methodology has been developed and tested for the collection of atmospheric vapor phase mercury by activated charcoal sorbents, and its measurement by instrumental neutron activation analysis (INAA). Automatic air samplers were constructed and used for two years to obtain four samples weekly at five locations across Upstate New York. A total of 1149 measurements were made from 2120 possible sampling dates. Mercury concentrations were found to be between 0.6 and 9.0 ng/m<sup>3</sup>, with a typical analytical error of  $\pm 0.3$  ng/m<sup>3</sup>.

The vapor phase mercury concentrations at all five sampling sites displayed similar, distinctive seasonal trends of higher winter and lower summer levels. This commonality indicates that vapor phase mercury in the region is affected by large, regional changes in either the relevant sources, or in atmospheric transformations. Though particulate phase mercury concentrations also exhibited a maximum in the winter, the same temporal changes were not seen at all five sites, and these maxima did not coincide with those for the vapor phase. Thus particulate phase mercury concentrations are being influenced by different nearer range source variations or weather patterns.

Source identification was performed using multivariate factor analysis and by observing distinct elemental source profiles in particulate samples obtained on the same dates as the vapor phase samples. This analysis indicated a strong impact on the area's mercury concentrations from smelters, precious metals works, and aluminum plants. Wind trajectories from industrialized areas in Canada and the U. S. matched with the highest levels of these influences.

precious metals works, and aluminum plants. Wind trajectories from industrialized areas in Canada and the U. S. matched with the highest levels of these influences.

An inverse relationship between vapor phase mercury and tropospheric ozone measured at the sampling locations was also observed. Though a causal link cannot be concluded from the available data, the heterogeneous oxidation rate of metallic mercury by ozone is estimated to be large enough to account for this correlation.

Thesis Supervisor: Dr. Ilhan Olmez

Title: Principal Research Scientist, MIT Nuclear Reactor Lab, and  
Department of Nuclear Engineering

Thesis Reader: Dr. Michael J. Driscoll

Title: Professor of Nuclear Engineering (Emeritus)

## **BIOGRAPHICAL SKETCH**

Name: Michael Richard Ames

Born: March 11, 1961; New York, New York

### Education:

Doctor of Science, in Nuclear Engineering, M. I. T., June 1995  
Thesis Title: Development And Application Of A Methodology For  
Measuring Atmospheric Mercury By Instrumental Neutron Activation  
Analysis

Master of Science in Nuclear Engineering, M. I. T., February 1986  
Thesis Title: A Characterization of the Post-Irradiation Properties of  
Copper Alloys for Fusion Applications

Bachelor of Science in Nuclear Engineering, M. I. T., June 1984  
Thesis Title: Observations of the Soft X-Ray Emissions of the Versator  
II Tokamak During Lower Hybrid Current Drive

Secondary Education, Ossining Public Schools, Ossining New York, 1979

### Employment:

M. I. T. Nuclear Reactor Lab September 1986 - September 1990  
Research Engineer, Coolant Corrosion Loops

Universal Voltronics Corp., Mt. Kisco, NY Summer 1981

Harrick Scientific Corp., Ossining NY, July 1978 - August 1980

### Affiliations:

Sigma Xi, Scientific Research Society, associate member since 1986.  
American Nuclear Society, student member since 1991.  
Alpha Nu Sigma, Nuclear Engineering Honor Society, member since 1992.  
Health Physics Society, student member since 1993.

### Publications and Proceedings:

"A Methodology for Determining Vapor Phase Mercury by Instrumental  
Neutron Activation Analysis", M. Ames, I. Olmez, S. Meier and P. Galvin,  
Second International Conference on Managing Hazardous Air Pollutants,  
Electric Power Research Institute, Washington, D.C, (1993).



"Elemental Composition of Charcoal Sorbants", I. Olmez, M. Ames and J. Che, Second International Conference on Managing Hazardous Air Pollutants, Electric Power Research Institute, Washington, D.C, (1993).

"Mercury Determination in Environmental Materials: Methodology for Instrumental Neutron Activation Analysis" I. Olmez, M. Ames and N. K. Aras, The Measurement of Toxic and Related Air Pollutants, EPA, Durham, N. C. (1993).

"In-Pile PWR Loop Coolant Chemistry Studies in Support of Dose Reduction", G. E. Kohse, R. G. Sanchez, M. J. Driscoll, M. Ames and O. K. Harling, The Second JAIF International Conference on Water Chemistry, Fukui City, Japan (1991).

"Materials and Water Chemistry Research in Support of LWR Technology at MIT", O. K. Harling, M. J. Driscoll, G. E. Kohse, R. G. Ballinger, I. S. Hwang, M. Ames, S. Suzuki, S. T. Boerigter and P. Stahle, The JAIF International Conference on Water Chemistry, Tokyo, Japan (1991).

"Neutron Irradiation Scoping Study of Twenty-five Copper-Base Alloys", O. K. Harling, N. J. Grant, G. E. Kohse, M. Ames, T. -S. Lee and L. W. Hobbs, Journal of Materials' Research, 2, No. 5 (1987).

"Progress in Developing DBTT Determinations from Miniature Disk Bend Tests", G. E. Kohse, M. Ames and O. K. Harling, Journal of Nuclear Materials, 141 - 143, pp. 513 - 517. (1986).

"Microstructural Evolution and Swelling of High Strength, High Conductivity RS-PM Copper Alloys Irradiated to 13.5 dpa with Neutrons", T. -S. Lee, L. W. Hobbs, G. E. Kohse, M. Ames, O. K. Harling and N. J. Grant, Journal of Nuclear Materials, 141 - 143, pp. 179 - 183 (1986).

"Mechanical Property and Conductivity Changes in Several Copper Alloys after 13.5 dpa Neutron Irradiation", M. Ames, G. E. Kohse, T. -S. Lee, N. J. Grant and O. K. Harling, Journal of Nuclear Materials, 141 - 143, pp. 174 - 178 (1986).

## ACKNOWLEDGMENTS

This research was supported by the Empire State Electric Energy Research Corporation (ESEERCO), the New York State Department of Environmental Conservation (NYSDEC) and the Adirondack Lakes Survey Corporation (ALSC). Special thanks are due to Sandra Meier of ESEERCO and Philip Galvin of NYSDEC.

Without the careful and dedicated work of the NYSDEC and ALSC field operators none of this would have been possible. Thanks are deeply owed to Paul Aery and Tom Dudones of ALSC and to Hollis Potter, Terry Novak and Jim Wolfe of NYSDEC for two years of sample changing in wind, rain, and snow.

As supervisor for this thesis Dr. Ilhan Olmez has been a teacher, a colleague, and a friend. It has been an enriching and demanding pleasure to have worked with him on this and other projects.

Professor M. J. Driscoll has been extremely helpful in preparing this document by employing his legendary skill as a thesis reader.

The operations staff of the MITR-II performed all of the irradiations for the analysis and testing used in this thesis, and deserve generous thanks for their consistent performance and accommodating efforts.

The other members of the ER&R lab have been helpful in their technical discussions and for the way they have helped this lab function as a family. Additional particular thank you's to Jack Jec-Kong Gone, Xudong Huang, and S. Sinan Keskin, for late night sample changing; Jianmei Che for spectral peak fitting, and Gülen Güllü for help with the factor analysis.

For giving me the chance to prove myself at times when others might not have, thanks are due Professor O. K. Harling, MITR-II Director.

As this is the formal end of my career as a student, I would like to express my gratitude to those who began me on this path by expecting the best: Ms. Betty Davis. Dr. Arthur Margro, and Ms. Mirla Morrison of the Ossining Public Schools, and Dr. N. J. Harrick of the Harrick Scientific Corporation.

I am most grateful for the eternal love and support of my family and especially my mother Dr. Rose G. Ames who has made all things possible.

For every day making my life full of happiness and hope, thank you to my wife Cynthia Woolworth and my daughter Charlotte Woolworth Ames.

This thesis is dedicated to the memory of my father Dr. Richard C. Ames, from whom I have always learned the most important lessons.

## TABLE OF CONTENTS

ABSTRACT.....	2
BIOGRAPHICAL SKETCH.....	4
ACKNOWLEDGMENTS.....	6
TABLE OF CONTENTS.....	7
LIST OF FIGURES.....	9
LIST OF TABLES.....	11
1. INTRODUCTION.....	12
1.1 Historical Perspective.....	12
1.2 Project Motivation, History and Objectives.....	15
1.3 Thesis Overview.....	17
2. ATMOSPHERIC MERCURY.....	19
2.1 Sources.....	20
2.2 Atmospheric Transformations.....	23
2.3 Fate.....	27
2.4 Overall Cycle and Budget.....	30
3. SAMPLING FOR ATMOSPHERIC MERCURY.....	36
3.1 Current Standard Methods for Vapor Phase Mercury Analysis.....	37
3.2 Sampling Requirements for INAA.....	41
3.3 Charcoal Testing for Composition.....	42
3.4 Charcoal Testing for Collection.....	47
3.5 Field Use of the Charcoal.....	50
3.6 Collection Efficiency Problems.....	52
3.7 Sampler Equipment Design.....	65
3.8 Field Operations.....	73
4. INSTRUMENTAL NEUTRON ACTIVATION ANALYSIS (INAA)....	79
4.1 Basic INAA Theory.....	80
4.2 The Past Use of NAA for Mercury Determination.....	84
4.3 The Optimization of INAA for Mercury Determination.....	91
4.4 Analytical Difficulties.....	96
4.5 The Analytical Methodology for Mercury Determination by INAA.....	99

5.	RESULTS AND DISCUSSION.....	112
5.1	Mercury Concentrations and Initial Interpretations.....	113
5.2	Factor Analysis and Source Identification.....	120
5.3	Atmospheric Transformations and Fate.....	129
6.	SUMMARY AND SUGGESTIONS FOR FUTURE RESEARCH.....	135
7.	REFERENCES.....	140
APPENDIX A.	ELEMENTAL CONCENTRATIONS OF ACTIVATED CARBON SORBENTS.....	145
APPENDIX B .	SITE OPERATING PROCEDURES AND SAMPLE DATA SHEET.....	152
APPENDIX C.	VAPOR PHASE MERCURY CONCENTRATIONS.....	160

## LIST OF FIGURES

Figure 1.	Local and regional atmospheric mercury cycle.....	32
Figure 2.	The global atmospheric mercury cycle and budget.....	33
Figure 3.	Elemental mercury over the mid-Pacific Ocean.....	34
Figure 4.	The pre-industrial global atmospheric mercury cycle and budget.....	35
Figure 5.	Concentrations of selected trace elements in 18 charcoal sorbents.....	44
Figure 6.	Concentrations of arsenic, selenium, and barium in 18 charcoal sorbents.....	44
Figure 7.	Concentrations of sodium and zinc in 18 charcoal sorbents.....	45
Figure 8.	Mercury concentrations in 18 charcoal sorbents.....	46
Figure 9.	Radioactive mercury tracer experiment, type 1.....	48
Figure 10.	Sorbent collection tube for vapor-phase mercury sampling,.....	51
Figure 11.	Radioactive mercury tracer experiment, type 2.....	54
Figure 12.	Radioactive mercury tracer experiment, type 3.....	56
Figure 13.	Mercury's vapor pressure in torr and its equilibrium concentration in $\text{mg}/\text{m}^3$ as a function of temperature.....	58
Figure 14.	Radioactive mercury tracer experiment, type 4.....	59
Figure 15.	A front view of the complete vapor-phase mercury sampling system.....	67
Figure 16.	Sample assembly.....	71
Figure 17.	Schematic flow diagram of the vapor-phase mercury sampling system.....	72
Figure 18.	Atmospheric sampling locations in Upstate New York.....	74
Figure 19.	Schematic spectrum of single, high energy gamma ray source obtained using a germanium detector.....	83
Figure 20.	The full collected INAA spectrum of an atmospheric mercury sample.....	86
Figure 21.	INAA spectrum of an atmospheric mercury sample on 100 mg charcoal, expanded around the 77 keV.....	87
Figure 22.	INAA spectrum of an atmospheric mercury sample on 100 mg charcoal, expanded around the 279 keV.....	88
Figure 23.	Composite spectrum showing reduction of lead X-rays by lining detector's shielding.....	93

Figure 24.	Schematic diagram of aluminum and copper shielding liners.....	93
Figure 25.	A schematic of the peak and background areas used in a gamma spectrum.....	95
Figure 26.	Calculated error of 77 keV peak determination as a function of cooling time.....	95
Figure 27.	Vapor phase mercury measurements at Belleayre.....	115
Figure 28.	Vapor phase mercury measurements at Moss Lake.....	115
Figure 29.	Vapor phase mercury measurements at Perch River.....	116
Figure 30.	Vapor phase mercury measurements at Westfield.....	116
Figure 31.	Vapor phase mercury measurements at Willsboro.....	117
Figure 32.	Smoothed average mercury measurements at all five sites.....	117
Figure 33.	Vapor phase mercury factor score plots for Belleayre, Moss Lake, Westfield, and Willsboro.....	124
Figure 34.	Perch River factor score plots for three identified source types.....	127
Figure 35.	Wind trajectories ending at Perch River and associated with high factor scores.....	128
Figure 36.	Smoothed vapor phase mercury , ozone , and particulate mercury concentrations at Belleayre NY.....	130
Figure 37.	Smoothed vapor phase mercury , ozone , and particulate mercury concentrations at Moss Lake NY.....	130
Figure 38.	Smoothed vapor phase, fine and coarse particulate mercury concentrations at Perch River NY.....	131
Figure 39.	Smoothed vapor phase mercury , ozone , and particulate mercury concentrations at Westfield NY.....	131
Figure 40.	Smoothed vapor phase, and particulate mercury concentrations at Willsboro NY.....	132

## LIST OF TABLES

Table 1.	Typical concentrations of mercury species in the atmosphere....	24
Table 2.	Chemical reactions of atmospheric Mercury.....	25
Table 3.	Selected efficiency tests of Calgon Carbon sorbents, type 3.....	62
Table 4.	Selected efficiency tests of Calgon Carbon sorbents, type 4.....	63
Table 5.	Efficiency test of Calgon Carbon charcoal using parallel samples taken with iodated charcoals.....	64
Table 6.	Sample corrections for spectral interferences when using 279 keV for mercury determinations.....	91
Table 7.	Seasonal and overall averages of vapor phase mercury concentrations in ng/m <sup>3</sup> at all sites.....	114
Table 8.	Seasonal and daily variations, and overall standard deviation in the mercury concentrations for two years at all sites.....	118

## 1 INTRODUCTION

Mercury is familiar to almost everyone due to its use in thermometers, electrical equipment, and perhaps from old high school chemistry demonstrations. Indeed, though they probably don't realize it, most people have a small amount in their mouths in the form of dental amalgams. Mercury's toxicity is also widely known, though less understood, from frequent warnings and restrictions on the consumption of fresh water fish caught in certain areas. Over the past forty years it has moved from being a long recognized occupational toxin to being an acutely poisonous local industrial pollutant to its current status as a regional or even global public health hazard. This latest state was realized when relatively elevated levels of mercury were found in areas very far from known sources.

Mercury contamination in remote regions can occur through long range atmospheric transport. Existing in the air as an atomic vapor, mercury's high vapor pressure and low solubility give it an atmospheric lifetime of up to one year. The concentration in ambient air is however extremely low, and elevations above the natural background level are small. This makes the measurement and analysis of ambient atmospheric mercury troublesome. The present work involves the development of a methodology for determining atmospheric mercury at levels which have caused great difficulties for standard techniques. Through the use of activated charcoal sorbents and direct instrumental neutron activation analysis (INAA), vapor phase mercury determinations can now be routinely and simply performed at the natural background level of about one nanogram per cubic meter of air.

### 1.1 Historical Perspective

Among the vast number of chemicals known to mankind, mercury is one of the most unique due to its long history, its toxicity, and its chemical and physical properties. It was known to the ancient Chinese and Hindus, and has been found in Egyptian tombs from 1500 B. C. The Phoenicians traded cinnabar ( $\text{HgS}$ , used as the pigment vermilion) from around 700 B. C. and the medicinal use of 'liquid silver' (*Hydrargyrum* in Latin) is described by Aristotle. Mercury's ability to separate precious metals such as gold and silver from their ores by amalgamation was known as early as 500 B. C. and is still



employed today for gold extraction in the Amazon region. Through the Middle Ages, alchemists regarded the metal as the key to transforming base metals into gold (ironically the detection method developed in this thesis is based on turning mercury itself into gold).

Mercurialism as an occupational disease was recognized by the Romans who sentenced slaves and prisoners to work the mines of Almaden in Spain. Mercury poisoning, either acute or chronic, affects the central nervous system, with early signs ranging from tingling in the hands and feet, slurring of speech, loss of coordination, and difficulties in vision and hearing. In the organic form (methyl mercury,  $\text{CH}_3\text{Hg}^+$ ) mercury can pass through the blood/brain barrier and through the placenta (Lindqvist, 1985). With the increased use of mercury and its compounds in crafts, industry and for the treatment of such ailments as syphilis, the toxic effects of mercury became more common. The expression "mad as a hatter" stems from the use of mercuric nitrate in the making of hat felts from rabbit fur. Mercuric chloride (the corrosive sublimate  $\text{HgCl}_2$ ) was used as an antiseptic, but its toxicity was further employed as a violent poison through the Middle Ages.

The modern realization of mercury as a public health hazard came about because of the Minamata disaster of 1953-1956. Fifty-two deaths and over seven hundred poisonings resulted in a year (and many more over the next several years) when the fish which were the staple of the local community's diet became contaminated with dimethyl mercury sulfide ( $\text{CH}_3\text{HgSCH}_3$ ). It was not until 1958 that the mercury was found to be the source of the poisonings and to have originated from a local chemical works where mercury salts were used inefficiently as a catalyst and discharged into the shallow Minamata Bay in an inorganic form (Kurland, 1960). The use of mercury containing fungicides has also caused numerous deaths world wide when treated seeds meant for planting were inadvertently consumed directly. The most notable case here occurring in rural Iraq in 1971 when 459 deaths resulted from alkyl mercury poisoning.

It is consumption of mercury contaminated fish as in Minamata which continues to keep mercury pollution a matter of scientific interest, public concern, and government regulation. As mentioned above, the general airborne concentration of mercury is extremely low, well below any level where it might be considered a direct hazard. However, once the mercury reaches open waterways, it enters a complex web of chemical reactions and

microbial activity where it may eventually be transformed into methyl mercury. In this form, which is resistant to environmental degradation, mercury is ingested and retained by aquatic organisms. In fish, the mercury accumulates preferentially in the muscles with proportionately much less in neural tissues than in birds or mammals. Traveling up the food chain, through the process of bio-accumulation the concentration of mercury in large fish can reach several micrograms per gram or ppm (the fish which caused acute poisonings at Minamata contained an average of 50 ppm mercury). The death of at least one Florida panther has been attributed to the consumption of raccoons who in turn consumed mostly fish (Douglas, 1994).

Consumption of fish with this level of mercury constitutes a significant health risk to humans, especially small children and developing fetuses. Game fish in many areas exceed state, national, and international public health guidelines for mercury levels. The U.S. Food and Drug Administration removes fish from stores if its mercury level exceeds one ppm. It is somewhat surprising though fortunate that this is the general public's only source of exposure to hazardous levels of mercury. Public knowledge of mercury contamination of local fish may be gauged by the fact that the subject is frequently covered by the press (e.g. The Boston Globe ran a lengthy story including measured concentrations beginning on the front page, September 2, 1992). General concern in industrial circles can be judged by the level of funding in mercury research by organizations such as the Electric Power Research Institute (EPRI), which has been studying mercury for ten years as part of the PISCES (Power Plant Integrated Systems: Chemical Emissions Studies); MTL (Mercury in Temperate Lakes) projects (Moore, 1994; and Douglas, 1994); and this study supported by the Empire State Electric Energy Corporation (ESEERCO) and the New York State Department of Environmental Conservation (NYSDEC) through the Adirondack Lakes Survey Corporation (ALSC).

Initial governmental reaction to elevated mercury levels in fish is generally the issuance of warnings covering certain locations and some types of fish. The next step, aimed at reducing the amount of mercury in fish, is the reduction in the emissions of mercury into the environment. Though discharging mercury directly to waterways has been prohibited for about two decades (Douglas, 1994), releases to the atmosphere continue and are now estimated to exceed direct aquatic inputs by at least an order of magnitude

(Lindberg, 1986). The appearance of elevated mercury levels in remote waters further indicates atmospheric transport as the means of contamination (Nater, 1992; Slemr, 1985; and Sorenson, 1990). The Clean Air Act Amendments of 1990 (CAAA) thus requires the EPA to perform major studies regarding mercury's health risks, its deposition to large lakes, and its emissions from electric utilities.

Mercury is one of only eight hazardous air pollutants for which the EPA set emissions standards under the initial Clean Air Act of 1970, and it is among the 189 hazardous air pollutants requiring maximum achievable control technology (MACT) under Title III of the CAAA (BNA, 1991). This is where a better understanding of mercury transport and fate is essential. The EPA's decisions regarding control measures will be based in part on the results of studies such as those mentioned above. Knowing the significant sources of atmospheric mercury and identifying the areas which have become contaminated is not enough. What is needed is to link the two so that emissions reductions will indeed result in reduced human exposures.

Further complicating the need for a cradle to grave understanding of atmospheric mercury however are uncertainties in determining its concentration. Historically, analytical errors and contamination of samples have meant that many mercury measurements were of questionable merit. Stack emissions quoted by the EPA in 1989 for bituminous coal plants varied by a factor of one hundred (Moore 1994). Measurements in natural waters during the 1970's range from zero to one thousand nanograms per liter (Lindqvist, 1985). Previous to 1985 anthropogenic emissions to the atmosphere were thought to be small compared to natural sources based on measurements of pre-industrial Greenland ice cores whose values turned out to be too high by a factor of ten (Lindqvist, 1985). Even though there is currently a much better appreciation of the need for clean sampling and analytical protocols, the anthropogenic contribution to the atmosphere is perhaps only known to within a factor of two (Expert Panel, 1994).

## **1.2 Project Motivation, History, and Objectives**

The central question with regard to mercury, is to find its pathways from emissions, through the atmosphere, into wet and dry deposition, and eventually to human (and wildlife) exposure. In order to help answer this

question several areas of research are in need of further development. These are well laid out in a recent EPRI report "Mercury Atmospheric Processes: A Synthesis Report" (Expert Panel, 1994) which was prepared by an international expert panel convened by EPRI in March 1994. Among those needs the ones primarily addressed in this work are improvements in the tools used for mercury determination, and in a long range, long term monitoring program for identifying trends and improving current models. Past problems in mercury sampling and analysis using standard techniques have been somewhat overcome in recent years through the use of ultra-clean protocols, but INAA is still one of the most sensitive methods for mercury determination in many samples, and the refinements developed here have kept this methodology in the forefront of the mercury field. There is also a great need for improved source sampling capabilities, and this methodology has been successfully applied in a number of stack sampling inter-laboratory comparisons, as well as in the analysis of coal and various oil samples (Olmez, 1995). Interestingly, these 'dirtier' samples are more difficult for other analytical techniques, but are generally easier to analyze than environmental samples when using INAA.

In 1990 the M.I.T. Nuclear Reactor Lab's Environmental Research & Radiochemistry group (NRL-ER&R, then known as the Trace Analysis and Radiochemistry or TAR division) began taking samples of atmospheric particulates and wet deposition across upstate New York and analyzing them for trace elements. The work was sponsored by the Empire State Electric Energy Research Corporation (ESEERCO) and the Adirondack Lakes Survey Corporation (ALSC). The primary goal of this research was to determine the impact of various anthropogenic sources on the region by using elemental markers and source signature profiles. The analysis of atmospheric particulates by INAA allows up to forty elements to be determined routinely. Sampling was performed daily at five sites using automated PM-10 dichotomous samplers. These follow the U.S. EPA's standards for collection of particulates less than ten microns in size, and further segregates the particle into fine ( $< 2.5 \mu\text{m}$ ) and coarse ( $2.5 \mu\text{m} - 10 \mu\text{m}$ ) fractions. The significance of these sizes is that particles smaller than ten microns are considered inhalable, and those less than  $2.5 \mu\text{m}$  are more generally of anthropogenic origin and are also able to travel greater distances through the atmosphere.

It was soon recognized that a better understanding of the sources, transport, and fate of atmospheric mercury could be an important part of this research. The need for this information was evidenced by the general public awareness of the problem, the impending re-evaluation of federal regulation of mercury emissions, and by a call in the literature for better measurements of long term and regional mercury concentrations as mentioned above. However, the determination of mercury in these particulates was not initially undertaken due to the special precautions needed; the problems of mercury analysis by INAA or by other methods was mentioned specifically in the original project's proposal. Although mercury determination by INAA is extremely sensitive, mercury's high volatility and nuclear recoil energy typically require that samples be encapsulated in quartz tubes for irradiation. This would be expensive and extremely time consuming if it were required for all of the samples involved in this study.

Additionally, of the total mercury in the atmosphere, only a few percent of it is associated with particulate matter, the vast majority is in the vapor phase and so is not collected by the PM-10 sampling systems. Therefore, a separate study was proposed in 1991 to develop a complete program for determining particulate and vapor phase mercury at the five New York locations. The collection of particulate samples was covered by the above mentioned trace elements program, but the need for special handling and preparation of the samples was specifically outlined. The collection of vapor phase mercury would require a new sampling system and analytical procedures. The design of this system, the development of the analytical methodologies, and the implementation of these for samples from Upstate New York, is the work covered by this thesis.

### **1.3 Thesis Overview**

This thesis is comprised of six chapters. As an introduction, chapter one has offered a brief history of mercury, particularly as it pertains to the environment and public health, followed by an account of the beginnings of this project. Chapter two provides a background in the current understanding of atmospheric mercury's sources, transport, and fate, with particular emphasis on the role this thesis' research will provide in identifying and quantifying these. Chapter three covers the details of the

design, testing and operation of the sampling system, especially the use of activated carbon as a collection medium. Chapter four will discuss the development of a methodology for the routine determination of mercury at trace levels by instrumental neutron activation analysis (INAA). Chapter five will then present the results of the mercury measurements made at the five New York sampling sites and discuss their significance. Chapter six will conclude with a summary of the thesis, offer some improvements to the current methodologies, and outline some proposals for future research.

## 2     ATMOSPHERIC MERCURY

As mentioned above, the general concern with mercury in the environment is due to its tendency to accumulate to hazardous levels in fish. If consumed in sufficient quantities mercury causes neurological disorders in humans and other carnivores (deaths of rare Florida panthers and large fish eating birds of the Atlantic have been attributed to mercury poisoning, Douglas, 1994). The previous cause of such contamination was the direct discharge of mercury to waterways. Though such practices have been reduced or eliminated, mercury continues to be found at elevated levels in many areas. Some of this may be residual contamination from previous episodes, and some due to the changing chemistry or topography of waterways (e.g. the damming of the Colorado River). The presence of mercury in remote and undisturbed waters, and the increase in measured mercury emissions, concentrations, and deposition indicate that long range atmospheric transport of mercury is responsible for some of the current contamination problems (Keeler, 1992; Nater, 1992; and Sorenson, 1990).

In order to lessen the impact of anthropogenic sources of atmospheric mercury on the environment the initial regulatory response is to require reduced emissions from the larger identifiable point sources (BNA, 1991). However, the relative contributions of local, regional, and global sources is both location and site specific. Emissions of mercury bearing particulates may deposit locally if they are of sufficient size, or may travel hundreds of miles. Soluble species have a widely variable lifetime depending on local meteorological conditions. Vapor phase mercury, which in some cases (e.g. coal fired power plants) comprises the bulk of the emissions, has a lifetime of up to one year, meaning that its local or regional impact may not be significant. Local deposition may be made up of a particular form of mercury which is not a major part of the total, so even large reductions in emissions, if improperly targeted, may have little local effect. If the control technologies are to provide a significant improvement in environmental and public health, the sources, transformations, and fate of atmospheric mercury need to be well understood.

## 2.1 Sources

As there is a significant abundance of natural mercury, both crustal and aquatic, there is of course a natural amount of mercury in the atmosphere as well. The mercury content of typical rocks range from a few up to several hundred parts per billion, with some common mineral ores as high as a few hundred parts per million. The levels near the sites of active mercury mines such as those near Almaden Spain are as high as 20% (D'Itri, 1972). The general worldwide distribution of mercuriferous belts tends to follow regions of geological activity. Natural waters, including the oceans and inland fresh waters have on the order of 0.5 to 5 nanograms per liter with the mercury in ocean waters being stabilized as  $\text{HgCl}_4^{2-}$  (Lindqvist, 1985). The natural vaporization and evasion of these large mercury pools result in a globally averaged atmospheric mercury concentration of about 1.6 nanograms per cubic meter ( $\text{ng}/\text{m}^3$ ). The flux of mercury to the atmosphere is driven by its availability at the surface since at  $20^\circ\text{C}$  its equilibrium vapor concentration is  $\approx 20 \text{ ng}/\text{m}^3$ .

It is somewhat misleading however to consider this as the natural concentration level for atmospheric mercury because anthropogenic emissions over the past one hundred years greatly outweigh the pre-industrial abundance of available mercury. It is estimated that since 1890 two hundred thousand tons of mercury have been emitted to the atmosphere (Expert Panel, 1994), whereas the current atmospheric burden is perhaps only five thousand tons (the troposphere is  $3.1 \times 10^{18} \text{ m}^3$ ). Thus a great deal of what may appear to be natural emissions of mercury especially from the oceans is actually the re-emission of anthropogenically produced mercury. The specifics of this storage and re-emission will be addressed at the end of this chapter, but an estimate of the present 'natural' global emission rate is one thousand tons from land and two thousand tons from the oceans annually (ref Mason 1994).

Anthropogenic sources can be categorized in a variety of ways, the first being to divide them into diffuse and point sources. Point sources constitute the largest mercury emissions, are the easiest to measure, and the most likely to be addressed by regulation. World-wide mercury consumption is on the order of ten kilotons [metric] per year; up to one half of this is lost to the environment though source estimates vary by as much as a factor of two (ref



Expert Panel). The EPA has recently attempted to inventory airborne mercury releases in the U. S. (for the first time in twenty years) with the intent of using these figures as a basis for new regulations on emissions (ref Raloff 1994a). Of a total 341 tons annually they ascribe 117 to coal fired and 4.4 to oil fired power plants. The mercury released from these plants originates as naturally occurring impurities in the fuels, and emissions are frequently estimated by analyzing plant feed stocks. Municipal and medical incinerators are estimated as annually contributing 64 tons each and commercial and industrial boilers generating 30 tons. Presently, none of these sources are under regulatory control and power plants are specifically exempt under the 1990 CAAA, though this may obviously be changing soon.

Globally, the largest source component is fossil fuel combustion for industrial applications, which contributes about 1200 tons per year. Waste incineration accounts for 600 tons and electricity production about 300 tons annually (about 60 tons from U.S. plants) (ref Douglas). The concentration of mercury at the outlet of a 500 MW coal fired power plant is on the order of a few micrograms mercury per cubic meter, which corresponds to about 200 kilograms of mercury per year. Industrial sources include chlor-alkali production, metal ore roasting, refining and processing are also significant in some areas. Canadian base and precious metals recovery accounts for 45% of that country's emissions, and these sites are frequently upwind of the Upstate New York sampling locations in this work (Peterson, 1990).

Diffuse sources are, in general, much harder to quantify, but some mass balance based estimates are possible and it appears that the global sum of these many small sources is up to 1000 tons per year. The EPA estimates from the emissions inventory cited above an annual U.S. release of 8.8 tons from the breakage of fluorescent and other lamps, 4.4 tons from latex paints where mercury has been used as a bio-cide, and one ton from dental uses including the release of mercury used in fillings of people who are cremated (Raloff, 1994b). Other common small scale sources include the disposal of dry cell batteries and other electrical equipment. (Mercury levels in both paints and batteries have been decreasing over the past years, partly through regulation and partly through consumer preference.) The use of mercury compounds in agricultural and lumber fungicides, and its use in primitive gold extraction in the Amazon are possibly large but diffuse semi-industrial sources (Pfeiffer,

1988). Finally the small amount of mercury present in motor fuel and lubricating oils may be a significant and widespread source (Olmez, 1995).

The physical size of the sources is not as critical in determining the fate of the mercury emissions as the chemical and physical form of the emissions. While many of the difficulties associated with measuring total mercury have been solved, the speciated measurements of mercury sources continues to be problematic and rare despite the fact that this information is critical in determining mercury's short and long range fate. Part of the difficulty in making speciated measurements is the volatility of mercury which creates problems of inter-species conversion during sampling periods. Generally speaking, sources emit mostly gaseous elemental mercury. If significant chlorine is present such as in incinerators, paper mills, and chlor-alkali plants a sizable fraction of mercury can be emitted as  $\text{HgCl}_2$  which is volatile, but also highly soluble. The amount of soluble mercury present in a plant's emissions is important both in terms of the mercury's ultimate fate, and in terms of the ability of current clean-up technologies to remove it from flue gasses. A pilot scale coal plant run by EPRI achieved almost total capture of ionic mercury using an electrostatic precipitator followed by wet limestone flue gas desulphurization (Moore, 1994), though only a small fraction of the elemental mercury was removed. The proportion of ionic to elemental mercury however varies with coal type, plant design and operation, and location along the flue gas path. Central sewage facilities may be a significant source of organic mercury such as  $\text{CH}_3\text{HgCl}$  and  $(\text{CH}_3)_2\text{Hg}$  (Soldano, 1975). The mercury likely enters the facilities as inorganic mercury having been previously ingested and excreted by humans. The emission levels vary widely and are dependent on the specific biological activity present and the population load on the facility.

The other important characteristic concerning mercury emissions from a specific source is the percent mercury associated with airborne particulates and also the size distribution of those particulates. As will be discussed shortly, an aerosol's size drastically affects its atmospheric range (i.e. coarse particles settle locally, while fine ones can travel hundreds of miles). Measurements very close to the stack of a coal-fired power plant near Oak Ridge Tennessee indicate that mercury particulate emissions may be as high as 9% of the total, but drop to 3% and then 1% at seven and twenty-two kilometers respectively (Lindberg, 1980); 1 - 2% particulate is a usual ambient

level. The fraction of mercury associated with particulates is also important because of how it affects control strategies. Emissions of particulates from coal plants for example are usually controlled through the use of electrostatic precipitators (ESP) and/or fabric filters which effectively reduce trace metal concentrations in the plant's effluent. The reduction in the mercury emissions for these systems vary widely (0 - 60%) depending on the amount of particulate mercury and the specific placement and temperature of the control systems (Moore, 1994).

## **2.2 Atmospheric Transformations**

Atmospheric mercury may be operationally defined as existing in three states based on the primary mechanism by which it is removed from the air. Particulate mercury is removed by gravitational settling or Brownian diffusion depending on its size, or by inclusion into wet deposition as insoluble species, gas phase mercury is removed by diffusion and surface adsorption, and soluble mercury is removed by wet deposition. Because these removal processes occur at very different rates, the lifetimes and hence spatial importance of the associated mercury species are also very different. As mentioned above, the settling of atmospheric particulates is dependent almost entirely on their size. Further, though some solid phase reactions have been identified, these particulates can generally be regarded as chemically inert (Seigneur, 1994). Physically, the two changes which particulate mercury can make are the desorption of vapor phase mercury, and the inclusion of particulates into precipitation by either nucleation or scavenging: the latter of these will be covered in the next section, 2.3 Atmospheric Fate. The physical loss of mercury from aerosols has been inferred from measurements within the plume of a coal-fired power plant by Lindberg (Lindberg, 1980). In this study the ratio of vapor phase to particulate mercury increased from eleven at 0.25 km downwind from the stack to 100 at 22 km. Total suspended particulates were also measured to compensate for differing dispersion rates between the particulates and the vapor phase mercury. At the distance of 22 km the vapor phase to particulate ratio was the same as for ambient samples at the same location indicating that further conversion was unlikely. Though more study is perhaps necessary, one may assume that particulate mercury behaves as a conserved species in the

atmosphere. Indeed this fact is put to use in the trace metals in airborne particulate study which the ER&R lab is also conducting.

What really drives the atmospheric part of the mercury cycle are the chemical reactions that make it more or less available for deposition, and the most important changes are the reduction reactions which convert elemental mercury into soluble ionic mercury. This can be seen by comparing the typical gas and liquid-phase concentrations of Hg(0) and Hg(II) (the liquid phase Hg(0) concentration is calculated by means of Henry's law (Seigneur, 1994).

Table 1. Typical concentrations of mercury species in the atmosphere.

Mercury species	Typical gas-phase concentration (ng/m <sup>3</sup> )	Typical liquid-phase concentration (ng/L)
Hg(0)	2 - 5	6 - 27 x 10 <sup>-3</sup>
Hg(II)	0.09 - 0.19	3.5 - 13.3

The vast difference in concentrations of the two species in both media is of course due to solubility differences; what is really important however is the equally large difference in the atmospheric lifetime of the two. Elemental mercury has an atmospheric lifetime of about one year (as has already been mentioned), while aqueous mercury has a tropospheric lifetime on the order of days (Slemr, 1985). Thus Hg(0) may be thought of as a reservoir for the production of short-lived Hg(II) by various oxidation reactions. There are of course a large number of reactions, both gas and aqueous phase, oxidation and reduction. Table 2 lists the most significant reactions and equilibria, their estimated rate or equilibrium parameters (or the upper limit of these, Seigneur, 1994). It does not include reactions involving organic mercury because these compounds are not generally produced anthropogenically, and there is no information regarding their reaction products or kinetics. Likewise solid-phase mercury reactions are not included because the concentrations are very low and the reaction rates are not known at room temperature (as mentioned above particulate atmospheric mercury is generally considered a conservative species)

Table 2. Chemical reactions of atmospheric Mercury

<u>Gas-phase reactions</u>		<u>Rate (cm<sup>3</sup> / molecule second)</u>
1.	$\text{Hg}^0(\text{g}) + \text{O}_3(\text{g}) \rightarrow \text{Hg}(\text{II})(\text{g})$	$<8 \times 10^{-19}$
2.	$\text{Hg}^0(\text{g}) + \text{Cl}_2(\text{g}) \rightarrow \text{HgCl}_2(\text{g})$	$<4.1 \times 10^{-16}$
3.	$\text{Hg}^0(\text{g}) + \text{H}_2\text{O}_2(\text{g}) \rightarrow \text{Hg}(\text{OH})_2(\text{g})$	$<4.1 \times 10^{-16}$
4.	$\text{Hg}^0(\text{g}) + \text{SO}_2(\text{g}) \rightarrow \text{products}$	$<6 \times 10^{-17}$
5.	$\text{Hg}^0(\text{g}) + \text{NH}_3(\text{g}) \rightarrow \text{products}$	$<1 \times 10^{-17}$
6.	$\text{HgCl}_2(\text{g}) + h\nu \rightarrow \text{products}$	slow
7.	$\text{Hg}(\text{OH})_2(\text{g}) + h\nu \rightarrow \text{Hg}^0(\text{g})$	not available
<u>Aqueous-phase reactions</u>		<u>Equilibrium or Rate</u>
8.	$\text{Hg}^0(\text{aq}) + \text{O}_3(\text{aq}) \rightarrow \text{Hg}(\text{II})(\text{aq}) + \text{O}_2(\text{aq})$	$4.7 \times 10^7 \text{ M}^{-1}\text{s}^{-1}$
9.	$\text{Hg}^0(\text{aq}) + \text{H}_2\text{O}_2(\text{aq}) \rightarrow \text{HgO}(\text{s}) + \text{Hg}^{2+} + \text{H}_2\text{O}(\text{l})$	$6.0 \text{ M}^{-1}\text{s}^{-1}$
10.	$\text{Hg}^{2+} + \text{SO}_3^{2-} \leftrightarrow \text{HgSO}_3(\text{aq})$	$5 \times 10^{12} \text{ M}^{-1}$
11.	$\text{HgSO}_3(\text{aq}) \rightarrow \text{Hg}^0(\text{aq}) + \text{SO}_4^{2-}$	$0.6 \text{ s}^{-1}$
12.	$\text{HgSO}_3(\text{aq}) + \text{SO}_3^{2-} \leftrightarrow \text{Hg}(\text{SO}_3)_2^{2-}$	
13.	$\text{Hg}(\text{SO}_3)_2^{2-} \rightarrow \text{Hg}^0(\text{aq})$	$1.0 \times 10^{-4} \text{ s}^{-1}$
14.	$\text{HgCl}_2(\text{s}) \leftrightarrow \text{HgCl}_2(\text{aq})$	$0.27 \text{ M}$
15.	$\text{HgCl}_2(\text{aq}) \leftrightarrow \text{Hg}^{2+} + 2\text{Cl}^-$	$10^{-14} \text{ M}^2$
16.	$\text{HgCl}_2(\text{aq}) + 2\text{Cl}^- \leftrightarrow \text{HgCl}_4^-$	$70.8 \text{ M}^{-2}$
<u>Gas/liquid equilibria</u>		<u>Henry's law constant (M/atm)</u>
17.	$\text{Hg}^0(\text{g}) \leftrightarrow \text{Hg}^0(\text{aq})$	0.11
18.	$\text{Hg}(\text{OH})_2(\text{g}) \leftrightarrow \text{Hg}(\text{OH})_2(\text{aq})$	$1.2 \times 10^4$
19.	$\text{HgCl}_2(\text{g}) \leftrightarrow \text{HgCl}_2(\text{aq})$	$1.4 \times 10^6$
20.	$\text{CH}_3\text{HgCl}(\text{g}) \leftrightarrow \text{CH}_3\text{HgCl}(\text{aq})$	$2.2 \times 10^3$
21.	$(\text{CH}_3)_2\text{Hg}(\text{g}) \leftrightarrow (\text{CH}_3)_2\text{Hg}(\text{aq})$	0.13
<u>Solid/liquid equilibria</u>		<u>Solubility (<math>\mu\text{g}/\text{L}</math>)</u>
22.	$\text{HgO}$	$5.3 \times 10^4$
23.	$\text{HgS}$	10
24.	$\text{Hg}_2\text{Cl}_2$	$2 \times 10^3$
25.	$\text{HgCl}_2$	$6.9 \times 10^7$

Although the oxidation of mercury by ozone, reaction 1, was first identified by P'yankov in 1949 it can be seen that the rates for the gas-phase reactions (1-7) are only known as upper bounds due to the difficulty in ruling out surface effects in lab scale experiments. Reaction 2 is included primarily due to its importance in creating soluble mercury within the hot stack gasses of sources containing both mercury and chlorine such as incinerators. Aqueous-phase reactions are much more critical, with the wet oxidation of mercury by ozone, reaction 8, being by far the most important pathway for the removal of elemental mercury from the troposphere (Iverfeld, 1986). Though the concentration of  $\text{Hg}^0(\text{aq})$  is extremely low, as it is removed by oxidation it is replaced by  $\text{Hg}^0$  entering from the gas-phase. The kinetics of this gas to aqueous dissolution are not well characterized, but as a heuristic model it may be considered a rapid process. It has been noted that the solubility of  $\text{Hg}^0$  is enhanced by the presence of  $\text{O}_2$  and low pH in rain (Lindberg, 1986). The aqueous-phase oxidation of mercury by ozone may thus be thought of as a chemical pump which takes mercury from the air where it is present as a gas and deposits it into water droplets as the soluble species  $\text{Hg}(\text{II})$ .

Because these reactions occur in rain, cloud, or fog water the actual rates at which they proceed in the atmosphere depends on the air's liquid water content which ranges from  $10^{-4}$  to  $1 \text{ g/m}^3$  (the reactions can also take place in the moisture associated with hygroscopic aerosols). However, this fact also means that the oxidized mercury is then in a phase which is directly deposited to the ground over a relatively short time scale. It is also worth noting that all of the information necessary to evaluate the importance of this reaction in the field will be available after this project is completed. Atmospheric ozone is routinely measured at NYSDEC sites, the Henry's law constants for ozone and mercury can be used to calculate their aqueous-phase concentrations, and the concentration of the reaction's product, soluble  $\text{Hg}(\text{II})$  in rain waters will soon be available.

Balancing the oxidation of elemental mercury by ozone is the reduction of mercury(II) by sulfite ions ( $\text{SO}_3^{2-}$ ) shown in the successive reactions 10 - 13. The presence of HCl in the atmosphere stabilizes the  $\text{Hg}(\text{II})$  by complexing it as  $\text{HgCl}_2$ , with  $\text{HgCl}_4^-$  only occurring at the high chlorine levels present in the oceans. Recent computer simulations of atmospheric mercury chemistry (Seigneur, 1994) indicate the sensitivity of the system to several key variables, i.e., liquid water content, pH,  $\text{SO}_2$  concentration, and

HCl concentration. Computed Hg(0)/Hg(II) ratios range from 10 to  $10^6$  and the gas/liquid ratios for Hg(II) were from  $3.5 \times 10^{-3}$  to 36 for various realistic values of the parameters. However, because of the uncertainty of many of the equilibrium and rate parameters, and the scarcity of field measurements of all the necessary species, it is not clear how accurate these figures are.

### 2.3 Fate

As mentioned above none of the mercury species present in the atmosphere are at levels where they are of direct concern; the only reason to measure their presence and study their interactions is to better understand their deposition and transfer to the biosphere. Atmospheric deposition is usually divided into dry and wet deposition, with wet deposition further divided into rainout, which includes various in-cloud processes, and washout, which is the below-cloud process of scavenging by falling precipitation.

Dry deposition refers to the transfer of gaseous and particulate airborne material to the earth's surface and its subsequent removal from the atmosphere. It can be thought of as having three distinct stages. First there is the aerodynamic stage which involves the turbulent diffusion and/or gravitational settling through the bulk of the atmosphere. This is followed by the diffusion of the material within the laminar sublayer directly adjacent to the surface. Though this layer may be only 0.1 mm thick, action here can determine the overall rate of deposition. Finally there is transfer of the material to water, soil or vegetation at the surface. This final stage is very location and species specific, non-reactive gasses for example may not undergo dry deposition at all because they are not absorbed at the surface, particulates are considered to have deposited once they reach the surface. Because of the complexity of these processes dry deposition is empirically determined and expressed as a proportionality constant between the atmospheric concentration of a material and its vertical flux; this is called the deposition velocity.

Dry deposition rates for aerosols are very sensitive to the particle's size. Large particles ( $> 20\mu\text{m}$ ) deposit mainly by gravitational settling, while very small particles ( $< 0.1\mu\text{m}$ ) behave aerodynamically like gasses and are governed by Brownian diffusivity. Between 0.1 and  $1.0\mu\text{m}$  particles fall in a

velocity trough, not being affected very much by either of these two mechanisms. There is considerable uncertainty in the deposition velocity for these sizes though it is probably in the range from 0.1 to 1.0 cm/sec, with wind velocity and surface roughness being locally variable parameters which may determine the actual rate.

It should be mentioned here that on a weight per volume basis aerosols tend to have a bi-modal distribution, with one peak in this low deposition region and one around 10 $\mu$ m (Seinfeld, 1986). Part of the fine fraction peak may be due to the lower settling rates, but it is also somewhat due to the fact that anthropogenic particulate emissions are usually in this size region. The ER&R lab's particulate sampling program takes advantage of this by collecting aerosols smaller than 2.5 $\mu$ m and between 2.5 and 10 $\mu$ m separately. The fine fraction samples represent largely anthropogenic and long-range influences, and the coarse fraction particles are more often locally produced and crustal material.

Both the mechanisms and rates associated with dry deposition of gas-phase mercury are still somewhat uncertain. In general non-reactive gas species such as mercury have low deposition rates due to the difficulty with which they are chemically absorbed by soil, water and vegetation at the earth's surface. Elemental mercury is believed to be absorbed by vegetation directly through the pores of leaves, or stomatally, especially near sources where the Hg<sup>0</sup> level may be high or through interaction with dew-saturated surfaces (Lindberg, 1992). This uptake is likely regulated by the ambient concentration and its relation to a deposition/emission compensation point, which is the atmospheric concentration above which the leaves will absorb mercury and below which they will emit mercury, resulting in a negligible net uptake. Though the specific values for this deposition mechanism are not well established, it appears that the compensation point for many species is higher than regional ambient concentrations and thus long-term dry deposition rates may be comparable to those for wet deposition (Iverfeldt, 1991).

Wet deposition of particulate mercury occurs by two processes, either through nucleation and subsequent rainout, or by the below-cloud scavenging of falling precipitation. The difference between the two is not of great practical importance though unless the sources of the particulates differ. Further, it is usually impossible to distinguish between them, although current research in the ER&R lab using cloud and rain samples from the



summit and base of Mount Washington (New Hampshire) may be able to separate these. A more significant distinction in the evaluation of mercury in wet deposition is the separation of inert, particulate mercury and reactive, soluble mercury, because these originate from different atmospheric species and possibly different original sources. This has been done by Fitzgerald et al. (Mason, 1992) for samples collected over the remote Pacific and Wisconsin. Particulate mercury in the rain was determined as the difference between total and reactive measurements, and though it makes up only a few percent of total atmospheric concentration it contributed about half of the deposited mercury. The direct measurement of particulate mercury in wet deposition samples is also being studied in the ER&R lab, but no actual measurements have been made yet.

A practical distinction may thus be made among four types of deposited mercury on the basis of species, sources, scale and mechanisms. First there is elemental mercury which is deposited directly to the biosphere by its uptake through the pores of vegetation. This is the least well understood in terms of its importance and mechanisms, it is certainly dependent on location, and its magnitude will rise or fall slowly as the long range concentration of vapor-phase mercury changes both spatially and temporally. If high concentrations are present downwind of large sources this type of deposition may also have significant local effects. Vapor-phase mercury can also be deposited by its conversion to the soluble Hg(II). Though this mercury is from the same sources as the first example, and thus is affected by long term trends and long distance sources, its deposition can be affected by short term, local atmospheric conditions such as moisture content, pH, and ozone, chlorine and SO<sub>2</sub> concentrations. Indistinguishable by analysis from this converted Hg<sup>0</sup> is the deposition of Hg(II) which was originally emitted in this form. The distinction between the two is that mercury emitted in a soluble form has an atmospheric lifetime of only a few days, and so is deposited locally or regionally. The identification of other species in the deposition samples or the prior knowledge of source speciation is necessary to determine the importance of this type of deposition on a case by case basis. Finally there is the deposition of particulate mercury (possibly subdivided into wet and dry processes). This may be a local problem if the particles are very coarse, though the measurement of high concentrations of non-reactive species in rain over

the remote Pacific indicates that the phenomenon also has regional and global implications.

Once mercury has reached the ground, if it is not re-emitted to the air, what happens to it is no longer relevant within the scope of this work. But because the only reason we are concerned about mercury is its effect on humans and animals through the food chain, a brief description of the rest of its biological and chemical cycle is in order. The mercury species of interest because of its toxicity and ability to bio-accumulate is methyl mercury  $\text{CH}_3\text{Hg}$ . Though it is present in fish and in fresh and ocean waters, it is not deposited there to any great extent from the atmosphere or introduced by runoff. Methyl mercury is instead produced locally by sulfate-reducing anaerobic bacteria. The activity of these organisms can be increased by the presence of sulfate and low pH (both products of acid rain, Fitzgerald, 1993). Part of the pH effect might be due to the increased reduction of  $\text{Hg}(\text{II})$  to  $\text{Hg}^0$  under higher pH conditions; this mercury is then emitted back to the atmosphere. As one moves up the food chain from these micro-organisms, the methyl mercury concentration increases until it is on the order of three million times more concentrated in the flesh of large fish than it is in the surrounding water. Failing the loss of the mercury to the atmosphere or the consumption of mercury laden fish by birds or mammals, the mercury is finally deposited to the underlying sediments. Whether the mercury in these sediments is re-released is largely an unanswered question, but effects such as this could prolong the existence of highly contaminated fish long after any reduction in atmospheric or other input to the system.

## **2.4 Overall Cycle and Budget**

It should be appreciated from the previous sections that there is a considerable amount of uncertainty in almost every aspect of atmospheric mercury's pathway, from its sources to its final consumption (and also with regard to its health effects at low levels, which were not covered). Nevertheless, estimates of mercury's concentrations and fluxes are becoming more reliable. In 1985 global fluxes reported in a review by Lindqvist (Lindqvist, 1985) gave uncertainty ranges up to a factor of 17 for total emissions and deposition. At a recent international expert panel convened by EPRI (Expert Panel, 1994) there was some disagreement about current

uncertainty bounds, but it is probably on the order of a factor of two or better. This uncertainty is possibly large enough to call into question the validity of any specific conclusions derived from current atmospheric models. However, the overall form of these models and the general sizes of the reservoirs and fluxes are probably understood well enough to both provide insight into the relative importance of the various mechanisms, and to point out the areas which are in need of further study.

A simplified local and regional mercury cycle is shown schematically in Figure 1. Looking at the model from the source end, three forms of anthropogenic emissions are shown, elemental  $\text{Hg}^0$ , particulate Hg, and soluble  $\text{Hg(II)}$ . Though some sources emit other species as well, these are the major types and are illustrative of the variety of processes in the cycle. Most sources emit primarily elemental mercury ( $\approx 95\%$ ), which because of its low solubility and high vapor pressure is not deposited locally, but combines with the global background mercury. The conversion of global elemental mercury to soluble mercury is shown by the most prevalent mechanism, the wet oxidation by ozone. On the other hand, if the source's emission height is low or atmospheric conditions create an inversion which brings a high concentration of mercury into contact with local vegetation, dry uptake of the gas-phase could result, but this process is not currently well quantified. Coarse particulate mercury will deposit locally, but finer particulates will combine with the regional and global background. The removal of these fines by wet deposition is clearly dependent on meteorological conditions; they may be removed locally or be transported thousands of kilometers. Soluble mercury, which can make up a significant portion of the total emissions is generally deposited on a local scale.

The most important feature of the local and regional mercury cycle is that the location where the mercury deposits is largely dependent on the chemical and physical form in which it is emitted. The total amount of mercury coming from a stack is not a sufficient measure for determining its effects. Accurate speciated measurements are necessary because even though soluble or particulate mercury may make up a small fraction of a plant's output they may be the most critical portion in terms of local and regional impacts. Further, regulations and control technologies based on total mercury reduction may provide little or no local benefits if only long range species are reduced.

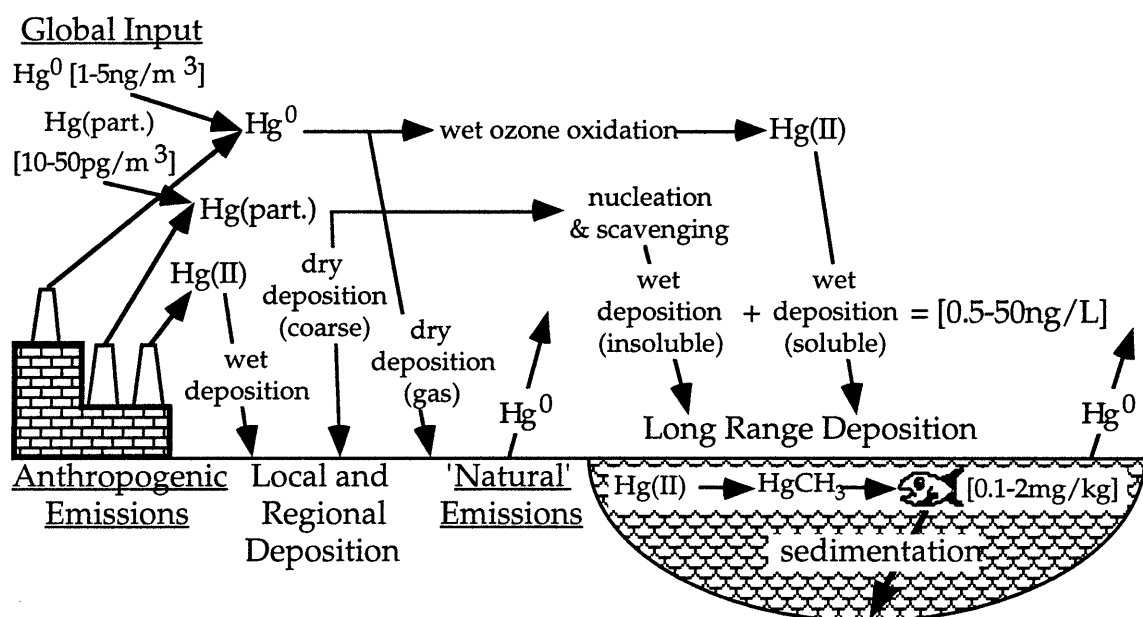


Figure 1. Local and regional atmospheric mercury cycle. Some typical concentrations are shown in brackets. 'Natural' emissions include the re-emission of accumulated mercury from historical anthropogenic activity.

From the receptor end of the cycle, several other features are evident, or should be mentioned. First, as with mercury sources, a simple measure of the presence of mercury does not provide very much information about the path the mercury has taken. Even a measurement of soluble  $\text{Hg}(\text{II})$  in wet deposition does not indicate whether a local source of this species or the oxidation of  $\text{Hg}^0$  is responsible. The deposition and evasion fluxes of  $\text{Hg}^0$  are not directly measurable, but must be inferred from changes and spatial gradients in the relevant concentrations, and in accumulated samples such as ice cores and peat bogs; and the separation of the various other deposition pathways requires the simultaneous collection and analysis of several sample types. The presence of particulate mercury in Pacific Ocean rain (mentioned above) shows that this species can travel thousands of kilometers before being deposited, and its measurement at a particular site may thus arise from the global background. Finally the eventual sedimentation of the atmospheric mercury deposited to local and regional waters provides a long term reservoir which may extend the problem of high concentrations in fish long after the sources of the mercury are eliminated (Bothner, 1980). This phenomenon is suspected in remote areas where the observed deposition rate has already

dropped from a maximum in the 1950's, and where high levels of mercury were discharged directly to waterways (Douglas, 1994).

Moving up to a global scale, Figure 2 includes total mercury burdens for the troposphere, oceanic mixed layer, and annual fluences. The values are from the measurements and models employed by Mason (Mason, 1994). and several of the numbers require some explanation. The anthropogenic emissions, global terrestrial and marine deposition rates, river runoff to the oceans, and the oceanic sedimentation rate were all determined using actual concentration and flow measurements. The marine evasion and natural terrestrial input rates were determined using measured surface mercury concentrations and gas exchange models.

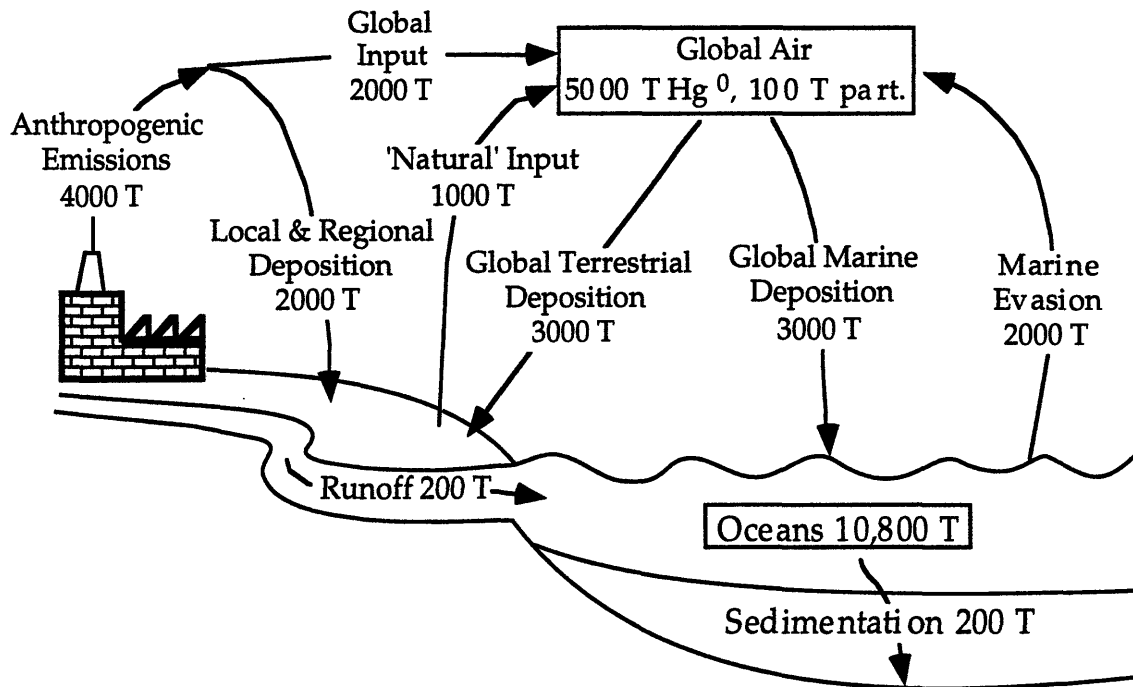


Figure 2. The global atmospheric mercury cycle and budget. Boxed titles are total global mercury burdens of these pools, plain titles are annual mercury fluences along particular pathways (all numbers are in metric tons). 'Natural' input includes re-emission of previously deposited anthropogenic mercury. Adapted from Mason et al. (1994).

Perhaps the most important balance here, between the contribution of anthropogenic emissions to global and regional deposition, is calculated by

applying conservation of mass to the terrestrial part of the system. Specifically, half of the anthropogenic emissions contribute to the global air mass and half are deposited locally and regionally (4000 T anthropogenic + 1000 T natural terrestrial emissions - 3000 T global terrestrial deposition = 2000 T local and regional deposition). The impact of anthropogenic emissions on the global atmospheric concentrations can be seen by observing the higher mercury levels in remote regions of the northern hemisphere as compared to the southern hemisphere (inter-hemispheric mixing is very slow). This is shown in Figure 3 (Fitzgerald, 1993).

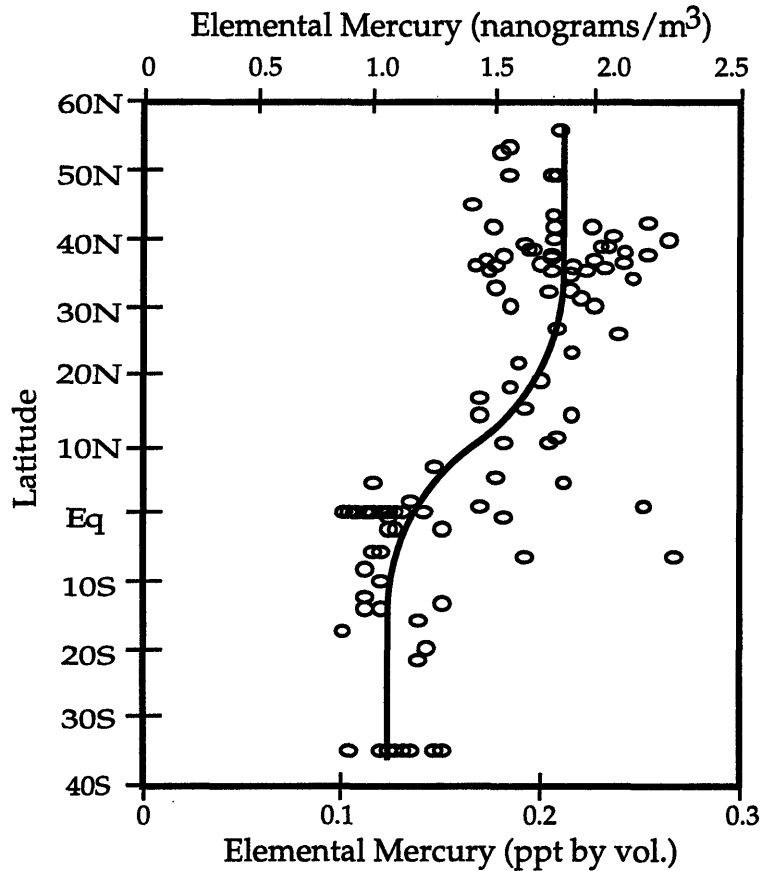


Figure 3. Elemental mercury over the mid-Pacific Ocean. The higher mercury concentrations in the Northern Hemisphere are due to the greater presence of industrial activity and mercury emissions (adapted from Fitzgerald 1993).

Other data related to the temporal increase in global atmospheric mercury due to human activities are shown in Figure 4, the pre-industrial mercury cycle, also adapted from the measurements and models employed by Mason (Mason, 1994). These numbers were calculated based on two assumptions: First that current terrestrial evasion rates are not significantly different than pre-industrial rates because little of the mercury deposited to land is re-emitted to the atmosphere; and second that all other fluxes are simply proportional to concentrations, that is that the mechanisms have not changed.

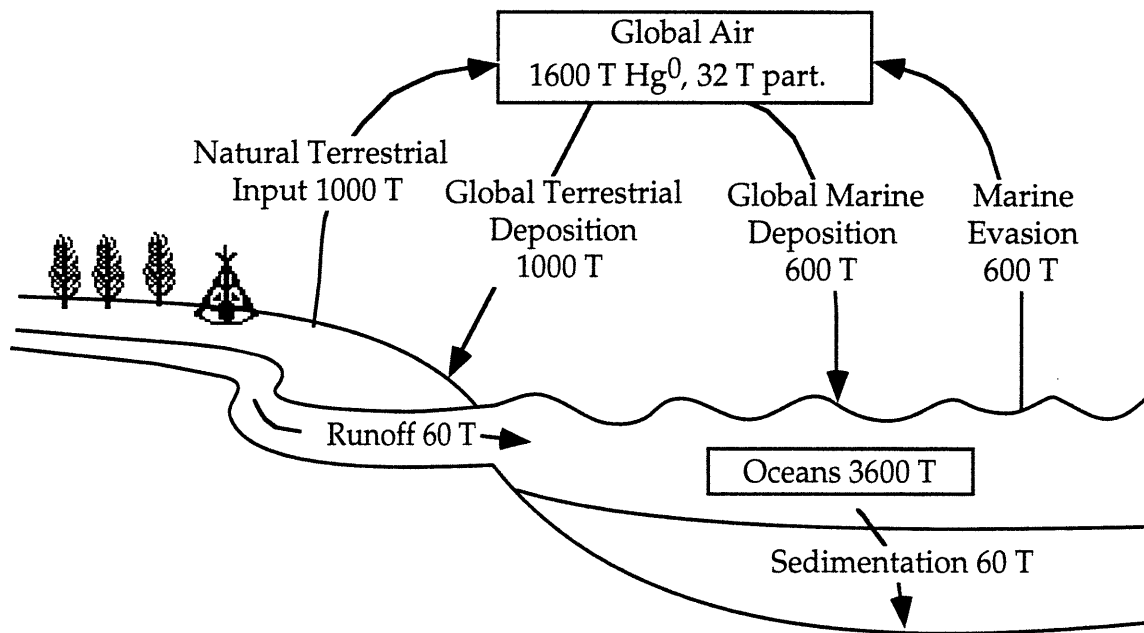


Figure 4. The pre-industrial global atmospheric mercury cycle and budget. Boxed titles are total global mercury burdens of these pools, plain titles are annual mercury fluxes along particular pathways (all numbers are in metric tons). (Adapted from Mason 1994).

When compared with Figure 2 the most obvious changes due to industrialization are the three-fold increase in the reservoir masses and most of the fluxes and the five-fold increase in total terrestrial deposition. Not directly shown in these figures but important in their derivation is the fact that cycling of mercury between the atmosphere and the oceans is relatively rapid, while the recycling of terrestrially deposited mercury is rather slow. A result of the increased mercury within these recyclable reservoirs is the future

persistence of high global mercury concentrations even after any future reduction in anthropogenic emissions. This is similar to the effects seen with the sedimentation and release of mercury in local and regional waters as mentioned above. Like many pollutants, the effects of mercury's introduction to the environment may long out-live current concerns with its release.



### 3 SAMPLING FOR ATMOSPHERIC MERCURY

Because the concentration of mercury in ambient air and even in factory emissions is so low (on the order of 1-5 ng/m<sup>3</sup> for remote air samples) it is almost always necessary to extract the mercury from the air and concentrate it on or within a collection medium before it can be analyzed. The basic requirements for the collection medium are dictated by sampling logistics, such as location, frequency, duration, handling and automation needs, by the temperature, moisture, or presence of other impurities in the air, and by the analytical technique to be used. Further, because of the low total amount of mercury typically collected (i.e. a few nanograms) the medium must be very efficient and the amount of mercury present within it, or the blank value, must be low and consistent from one collector to another. The actual sampling procedure needs to be reliable, non-contaminating, and to represent a known amount of air. These qualities are generally important in all types of environmental analysis, but particularly in the measurement of atmospheric mercury.

#### 3.1 Current Standard Methods for Vapor Phase Mercury Analysis

Most current techniques for mercury measurement operate by observing the emission or absorption of 253.6 nanometer UV radiation in an electronic transition of elemental mercury vapor. Methods for the direct detection of atmospheric mercury have been developed using differential absorption lidar (light detection and ranging, Edner, 1989) and folded light path enclosures (Jepsen, 1972). The former however requires a high-power, narrow-bandwidth tunable laser mounted on a small truck, and the latter has only been applied to characterize the high mercury concentrations near large sources.

If the collected mercury vapor is to be analyzed in a lab after its sampling in the field, as is more usually the case, then the collection media must be able to quantitatively release the mercury for analysis as a vapor. Mercury which is initially in the vapor phase can be absorbed by a number of materials including: activated carbon both plain and treated (Germani, 1988; and Schroeder, 1985), magnesium oxide (BITC, 1979) or magnesium-copper oxide (SKC, 1992), lead sulfide (Alexandrov, 1985), and liquid impingers (e.g.

4%  $\text{KMnO}_4$ /10% $\text{H}_2\text{SO}_4$ , DeVito, 1993). Owing to mercury's unique properties it may also be collected by amalgamation with gold or silver (Taylor, 1983; Shierling, 1981; and Fitzgerald, 1979). Speciated atmospheric sampling can be accomplished through the use of different collection media which have high efficiencies for only one form of mercury. The collection of mercury by gold also makes possible several novel techniques for analysis such as thin film resistivity measurement (Murphy, 1979), and gold coated quartz resonant oscillators (currently being developed at this lab). Because particulate mercury is also of importance in the atmosphere, several sampling and analytical procedures have also been developed to determine the concentration of mercury in this form. Aerosol collection is more straightforward than gas phase collection and is performed routinely for the determination of a variety of chemicals other than mercury. Filters of quartz or glass fibers, or of cellulose acetate are frequently used (Breinska-Paudyn, 1986; and Dumarey, 1979) and are available in a wide range of filter and pore sizes.

The two methods for the release of mercury vapor from charcoals and from particulates and filters are wet digestion and pyrolysis. Acid digestion is usually performed in a Teflon® pressure vessel followed by a reduction-aeration vessel. As an example Bloom (1993) uses 5 mL of 7:3  $\text{HNO}_3$ / $\text{H}_2\text{SO}_4$  diluted with 0.02N  $\text{BrCl}$  at 70°C to digest 150 mg charcoal sorbents used for vapor-phase collection. Reduction of ionic mercury species collected in sorbants or in impingers is carried out using either  $\text{SnCl}_2$  or  $\text{NaBH}_4$  (Bloom, 1993; and DeVito, 1993 respectively). Problems associated with this digestion are the long times required to completely digest the samples, the possibility of incomplete digestion, and the relatively large and sometimes variable blank values present in the digestion and reduction reagents. Pyrolysis is more efficient and straightforward, but the organics which may also be collected and which result from the destruction of the filter can cause serious interference and need to be removed from the analytical stream (Dumarey, 1979).

In order to shorten the release time of mercury into the actual detection device and to purify it from such interfering species, a gold amalgamation stage is commonly inserted between the sample collection media and the detector. Fitzgerald (1979) actually employs a two-stage gold amalgamation technique using gold-coated glass beads, where the initial field mercury is collected on one column and then the mercury is released by

controlled heating to 500°C and absorbed by a second analytical column. In addition to the advantages mentioned above the two-stage procedure also means that the analytical column is used repeatedly for introducing the mercury into the detector, so it is only necessary to calibrate the heater-column-detector once. Another method for achieving a more uniform release of the mercury, and also perform speciated measurements without the use of several types of collectors is to employ a small gas chromatography column before the detector. The mercury species are transferred to the column which is cooled in liquid nitrogen and then eluted sequentially in increasing order of polarity by ramping the column temperature to 180°C over 20 minutes.

Once the mercury is appropriately vaporized it can be detected by atomic absorption or atomic fluorescence, the former being simpler and more commonly available, and the latter being more sensitive but also more complex and expensive. These analytical techniques are more usually performed by atomizing a sample and introducing it into a flame, but because mercury has such a high vapor pressure it can be analyzed without the use of an ionizing flame. Thus the methods are referred to as cold vapor atomic absorption spectroscopy and cold vapor atomic fluorescence spectroscopy (CVAAS and CVAFS respectively). They are basically similar in that a collimated mercury vapor UV light source is coupled with a photo-multiplier tube (PMT) detector. In CVAAS the reduction of 253.6 nanometer radiation absorbed by the mercury is used for detection (the source and detector are co-linear), while in CVAFS the re-emission of radiation by excited mercury atoms is measured (the source and detector are perpendicular).

All of the above sampling and analytical techniques have some common requirements and difficulties. Because of the low concentrations typically measured, contamination is by far the greatest problem during sampling, handling, transfer or analysis, as mentioned within several of the references. Indeed it was the contamination of Greenland ice core samples taken in the early 1970's which led to a gross over-estimate of global pre-industrial mercury deposition from the atmosphere (Lindqvist, 1985). Fitzgerald (1979) notes that airborne mercury concentrations within his lab can approach 1000 ng/m<sup>3</sup> which can easily result in small but significant amounts of contamination of analytical equipment. Bloom mentions the fact that much of the blank in his method comes from added reagents (Bloom,

1993) which can vary from lot to lot and must be checked frequently when used. In methodologies using sorbents the need for low and consistent mercury blank values is vital. Various activated carbons analyzed by this lab (Olmez, 1993a) ranged in mercury blank values from 2 to 100  $\mu\text{g}/\text{kg}$ , even if only 100 mg of sorbent is used for atmospheric collection the blank value can easily be of the same order as the sample. Taylor also notes that commercially available sorbent tubes of hopcalite, even those of the same batch, show unacceptably high blank variations (Taylor, 1983).

Mercury loss, which produces the opposite result of contamination, is also a problem through all stages of measurements. An initial concern is that during sampling volatile mercury species will be lost from the collection media. This is usually checked through the use of a back-up collector either during testing or routinely. The back-up is meant to capture all or part of the mercury which has either been evolved or simply passed by the primary collector (breakthrough). This is not often a problem even in the collection of particulate material which might be expected to lose mercury by volatilization. Collection media which are particularly sensitive to storage losses such as liquid impingers are handled by cooling and rapid analysis, but difficulties with sample loss to container surfaces remains. The most likely measurement stage for mercury loss is during analysis when the sample is returned to the vapor-phase. The potential here is mostly for mercury to be adsorbed onto glass or metal surfaces during analysis, and most detailed accounts of analytical methodologies prescribe cleaning and conditioning procedures for lab apparatus. If such adsorption occurs it can cause contamination problems, as well as high levels of mercury possibly deposited by standards are re-released during the analysis of low level samples. The identification of mercury loss as a problem during sampling or analysis is generally more difficult than the identification of contamination. Because the amount of mercury in a typical analysis can be on the order of a few nanograms, contamination significantly over this amount is easily spotted as an anomaly. On the other hand, even the worst case of sample loss will appear only to give a result below the detection limit, which may not be much lower than a normal result.

### 3.2 Sampling Requirements for INAA

Because Instrumental Neutron Activation Analysis is fundamentally different than any other method for measuring low concentrations of mercury, the requirements for sample collection are also different. The vast majority of methodologies in use and described above require that the mercury in the sample be volatilized as elemental mercury before actual analysis. (The few exceptions rely on the separation of the mercury from the rest of the sample by amalgamation before analysis.) The vaporization is necessary because the initial pre-concentration of the mercury from air leaves the sample in the solid state which is the most difficult form for chemical analysis. In contrast, INAA is the easiest to perform using solid samples, with liquids and gasses being more difficult to handle. Thus there is no need for the mercury to be removed from whatever substance is used for its collection. The collection media no longer needs to be able to be chemically digested, or to release the mercury upon heating, its only critical property is the ability to capture and retain sampled mercury.

However, since the collection media is analyzed along with the sample, and because of the nuclear nature of the analysis several properties of the collector which were previously unimportant are critical in determining whether it is useful for INAA. Physically, it is important that the collected samples be small in size so that several may be irradiated simultaneously. The containers used for irradiation, or rabbits, have inside dimensions of 1 inch (25 mm) diameter and 3 inches (75 mm) length. The price for irradiating samples in the MITR-II for six hours using these rabbits is currently \$156, regardless of the number of samples it contains; thus the smaller the sample size the more economically it can be irradiated. Also, because it is best to transfer the samples to new containers after irradiation, the collection media should be easy to handle using tweezers to reduce radiation exposure, and should present little likelihood of spillage or loss to prevent radiological contamination of personnel or equipment.

While the amount of mercury in the collector is important regardless of the type of analysis, the only relevant measurement of this amount is by the detection method actually used. For example if there is a significant mercury impurity within the glass or sand substrates beneath a gold amalgamation layer this is not important if the mercury does not diffuse out

during normal analytical procedures. Because both the activation and analytical steps used in INAA penetrate the matrix completely, the presence of otherwise unavailable mercury will contribute to the blank value.

As will be described within Chapter 4, mercury is determined in INAA by measuring the emission of 77.3 keV gamma rays by Hg-197. In a typical INAA spectrum this energy falls in an area of relatively high background radiation (due to the incomplete collection of higher energy gamma rays by the detector). Therefore it is beneficial to select a collection material which will not produce many of these high energy gamma rays and thus not produce a high background under the mercury signal. Immediately many types of commonly used collectors are removed from consideration. Gold and silver are among the most easily detected elements by INAA due to their high neutron absorption cross sections; any technique using the amalgamation of mercury with these is not applicable because of the huge background even a small amount of these materials would create in the spectrum. The porous sorbents based on metal oxides such as hopcalite (copper-manganese oxide) do not contain unusually high amounts of elements which produce elevated background radiation, but the activation of manganese results in a very strong though short-lived (2.6 hours half-life) radiation hazard.

### **3.3 Charcoal Testing for Composition**

With the above prerequisites in mind it was decided that activated carbon would be the best substance to use for mercury collection. Activated coconut charcoal had also been previously used by Germani and Zoller (Germani, 1988) for the analysis by neutron activation of vapor-phase emissions from a coal fired power plant stack. Also, commercially manufactured sorbent tubes and bulk quantities of activated carbon are readily available for such applications. They are produced from a variety of carbon sources including wood, coal, oil, lignite, coconut shell and peat. The source material is carbonized by thermal decomposition in the absence of oxygen, producing the sorbent's basic pore structure and carbon matrix. Activation is the removal of the less tightly bound carbons, which increases overall porosity and opens up micro-pores within the matrix. These micro-pores are of the size of a single carbon ring and are the most effective sites for

trapping species which diffuse into the structure. This also greatly increases the effective surface area of the charcoal, with typical values for the specific area being from 1000 to 1500 m<sup>2</sup> per gram. Activating agents include phosphoric or sulfuric acid, zinc chloride, carbon dioxide, oxygen, and steam. Physically, activated carbons are available as powders, various sized grains and spheres, treated with organic and inorganic substances, or coated with polymers. Eighteen types of activated carbon were obtained for analysis by neutron activation to determine which type would be best suited for mercury collection and determination. Though the specific process involved in producing activated carbons is often proprietary, some relevant information is usually provided, and some was inferred from the analysis. (A complete reference for the analysis can be found in Olmez 1993a.)

Because we were only concerned with the charcoals' composition as it related to mercury determinations, the irradiation and counting were the same as for these measurements. That is six hour irradiations, several days cooling, and six hour countings; no short irradiations were performed. The specifics of the INAA procedures used are covered in the next chapter, but in addition to the usual mercury standards four National Institute of Standards and Testing (NIST) standards were used for the analysis of other elements. These were the Standard Reference Materials (SRM's) 1633 fly ash and 1572 orchard leaves. Two samples of each of the charcoals were analyzed to perform an initial check on the homogeneity of 100 mg amounts (the size to be used for the sorbants) taken from the batches.

Though very little was known about the charcoals initially, the results of these analyses made evident some striking similarities and differences among them. Appendix A gives a description of the charcoals and the full results of the analyses. In Figures 5 through 8 (and in Appendix A) the charcoals are in order of increasing iron concentration; an additional charcoal which will be discussed later, labeled CYAK, is also included. Figure 5 shows the measured concentrations of a selected group of trace elements within the charcoals. It is clear that there is a distinction between the charcoals to the left which are derived from vegetative carbon sources, and those to the right which come from mineral sources. The SKCMER is hopcalite, a copper-manganese oxide, not a charcoal, but was included in the analysis for reference. Five of the charcoals (SPECGRAN through SIGGRAN excepting

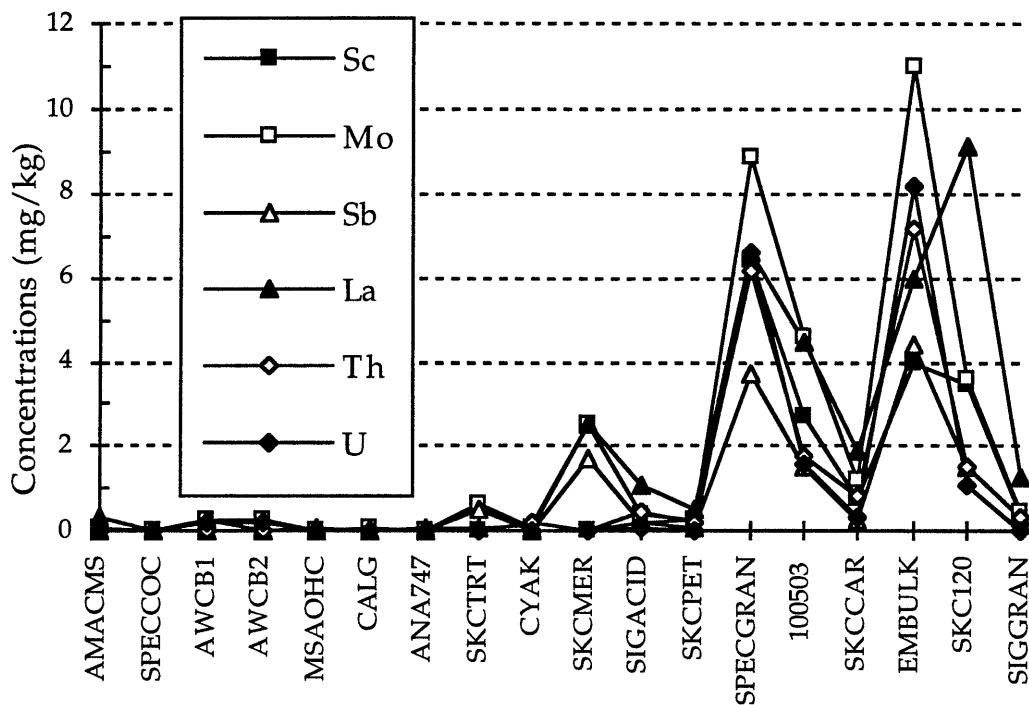


Figure 5. Concentrations of selected trace elements in 18 charcoal sorbents as determined by INAA. For charcoal descriptions see text and Appendix A.

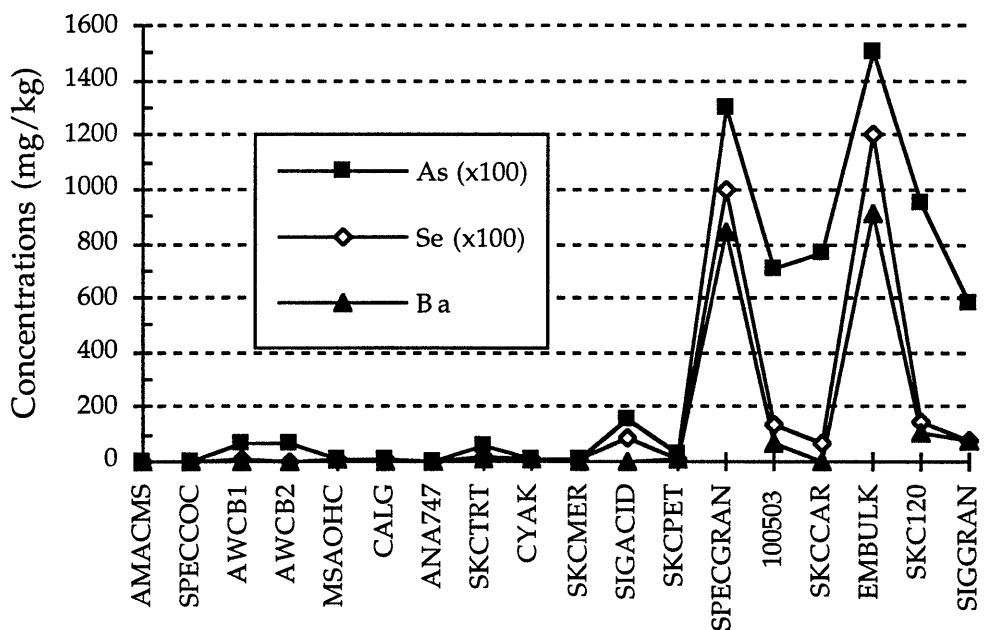


Figure 6. Concentrations of arsenic, selenium, and barium in 18 charcoal sorbents as determined by INAA. For charcoal descriptions see text and Appendix A.



SKCCAR) are likely derived from coal or lignite, and as the names imply SKCPET is made from petroleum and SCKCAR is from a carbide. Three elements frequently of concern in atmospheric trace analysis are shown in Figure 6. Arsenic is partially present in the atmosphere in the vapor phase, and can be collected by activated carbon sorbents much like mercury. Selenium is usually observed with arsenic and the ratio between the two is important in distinguishing various source types. In the past it also caused difficulties in determining mercury by INAA because of its spectral interference with the activation product Hg-203; this will be discussed in detail in chapter 4. Zinc concentrations are shown in Figure 7, indicating the possible use of zinc chloride as an activating agent. Sodium is also shown here because of its high concentration in many of the charcoals and because during INAA its presence results in the production of Na-24 which creates most of the background under the Hg-197 signal. This too will be discussed in detail in chapter 4. In contrast to the previous figures, the differences in concentration from the vegetative and the mineral charcoals is not very large for these elements.

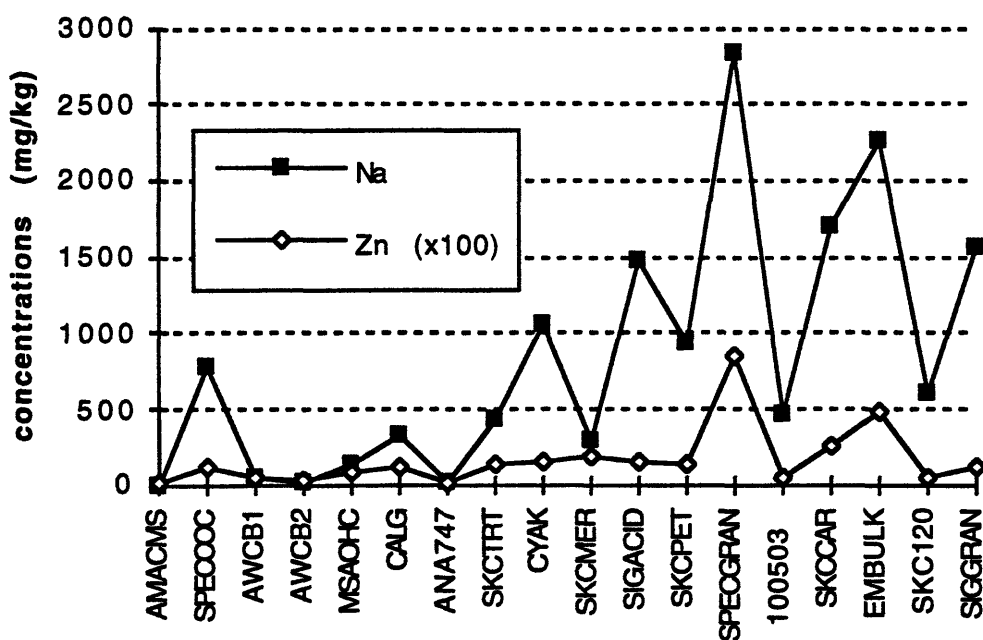


Figure 7. Concentrations of sodium and zinc in 18 charcoal sorbents as determined by INAA. For charcoal descriptions see text and Appendix A.

The most obvious concern when selecting a charcoal for this project in terms of its elemental content was the blank mercury value. All else being equal a lower value would be preferred, but of more importance is the consistency of this figure from one sample of the charcoal to the next. A large variation in the measured blanks, or a large error band in the measurement may make an otherwise promising charcoal useless. Figure 8 shows the measured mercury concentrations for the eighteen charcoals tested, giving the errors associated with each measurement and the individual results from the two rounds of testing. Several of the samples were so inhomogeneous that the measurements do not even overlap in their error bars. Though not shown this was also the case for many of the other elements in Figures 5 - 7, but the levels of these elements were mostly of informational interest only.

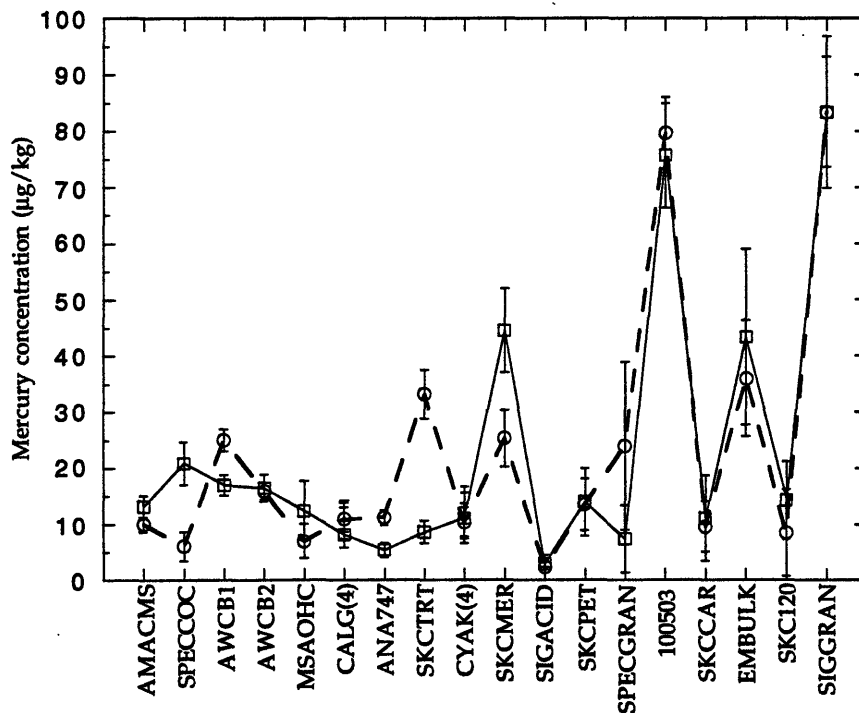


Figure 8. Mercury concentrations in 18 charcoal sorbents as determined by INAA. The two lines connecting the data points represent two sets of measurements and difference between these for some samples indicates the degree of inhomogeneity of the charcoals.

The error bars shown in Figure 8 arise from two sources, as will be discussed further in Chapter 4, first there is the uncertainty of the measurement of the Hg-197 peak area which is determined solely by the size of the peak. The error in measuring the background under the peak is also included in this figure, and this is due to the presence of elements, most notably Na-24, which produce high energy gamma rays following irradiation; this can be seen in the large errors associated with SPECGRAN and EMBULK. In practical terms, because the size of the sorbents used for atmospheric sampling is 100 mg, each 10 µg/kg of blank mercury results in one nanogram of blank mercury in the sorbent. Further, each µg/kg of uncertainty in this value results in a final measurement uncertainty of 0.1 ng for an actual sample. Both of these can be significant considering that the amount of mercury routinely collected is on the order of 5 - 10 nanograms. Of the initial charcoals CALG (a steam activated coconut charcoal from Calgon Carbon) was selected for use in the samplers. Following some problems with this charcoal to be discussed shortly, CYAK (an iodated steam activated coconut charcoal from Cameron-Yakima) was used.

### 3.4 Charcoal Testing for Collection

The requirements for the charcoal from the point of view of collection are very simple: the sorbent should absorb all of the vapor-phase mercury which passes through it, and it should not lose the collected mercury during normal operation and handling. Even for charcoals with a low efficiency, the first condition can usually be met by increasing the size of the sorbent column or by lowering the gas flow rate. These solutions produce other problems however, increasing the blank level and decreasing the sample size respectively. Thus testing for a sorbent's collection efficiency is mainly intended as a way of determining a practical minimum sorbent size and maximum sampling flow rate. The other concern in terms of the required sorbent size for full sample collection is whether the charcoal will become saturated with mercury or some other chemical which it might collect simultaneously.

In order to test the efficiency, capacity, and retention of charcoals a series of simple experiments were performed using irradiated metallic mercury as a tracer. A schematic diagram of the initial test set-up is shown in

Figure 9. The mercury, indicated by  $\text{Hg}^*$ , was a small drop of about 15 mg, irradiated in the MITR-II short irradiation facility for ten minutes. This allowed any mercury which was volatilized in the flask and collected by the sorbants to be measured by counting the activity in the sorbent. The absence of other radionuclides in the spectra made the measurements very easy. The heating jacket was rated at 60 Watts but was operated at a reduced voltage using a variac for better control at the moderate operating temperatures (the maximum temperature used was  $80^\circ\text{C}$ ). A K-type (chromel-alumel) thermocouple between the jacket and flask was used to measure the temperature. Air flow was measured at the inlet to avoid radioactive contamination of the flow meter, and the inlet tube was a narrowly tapered pipette to prevent backflow. The connections from the flask to the sorbent and the vacuum pump tubing were made with flexible silicone tubing.

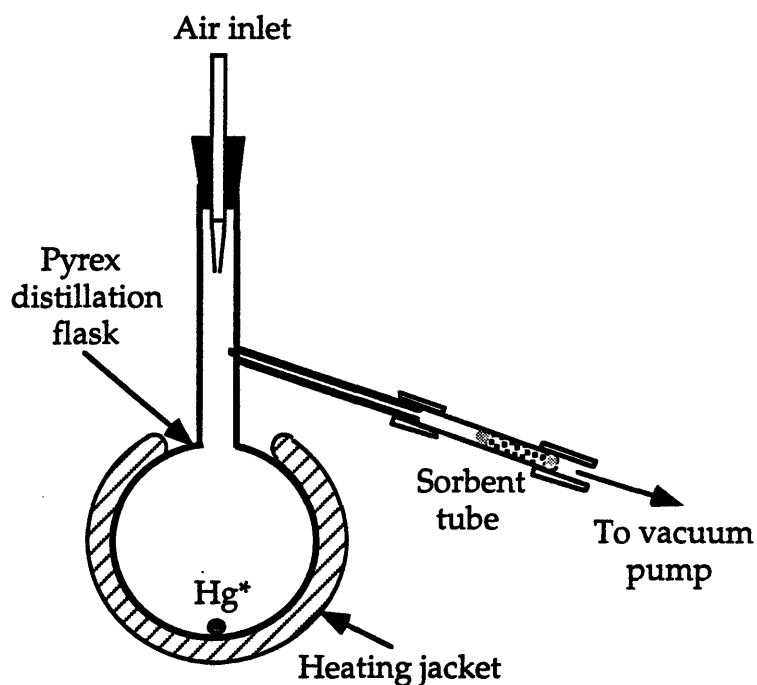


Figure 9. Radioactive mercury tracer experiment, type 1. By heating the flask some of the radioactive mercury ( $\text{Hg}^*$ ) is volatilized and can easily be detected in the sorbent tube.

The first experiments which were performed with this set-up were very simple, used commercially available sorbent tubes, and were primarily

aimed at determining whether saturation would be a problem in 100 mg of charcoal, and whether the charcoal would retain the collected mercury. The sorbent tubes were made of coconut charcoal from SKC (referred to as SKC120 in the previous section) with a 100 mg front section followed by a 50 mg backup. This configuration of two separate sorbent stages is common in commercial collection tubes as it allows for a routine check for breakthrough. The sorbents labeled SKC and MSA in the previous section all were in this configuration, and are sealed in a glass tube with two tapered ends which are broken open before sampling. They are designed as occupational exposure monitors for use with small battery operated pumps which are worn on a workers belt. For comparison with the experiments and atmospheric sampling, when used for their designed purpose the sorbents are run at 100 - 200 ml/min, and the National Institute of Occupational Safety and Health (NIOSH) average mercury concentration limit for an eight hour working day is 0.05 mg/m<sup>3</sup> (SKC, 1992).

In the first test with this set-up it was uncertain how much of the mercury would be volatilized by the heating so, after no mercury was measured on the sorbents after a 30 min run at room temperature and a flow rate of 800 ml/min, the flask was heated to 80°C for 30 minutes which vaporized most of the mercury in the flask. Of the 10.7 mg of Hg tracer initially in the flask, 8.1 mg was measured on the sorbent, with between 90 and 95% of the Hg in the front of the tube. A subsequent test using a new tracer at 30°C, a flow rate of 1800 ml/min, and two 50 mg sorbent tubes in series was run for one hour with about 20 µg of Hg collected on the front sorbent and 0.5 µg Hg on the backup. Passing clean air (without any activated mercury) over the sorbants for 18 hours did not change the mercury levels in the charcoal. Despite the fact that these tests were very brief and at much higher mercury concentrations than found in the atmosphere (≈400 µg/m<sup>3</sup> vs. 1-2 ng/m<sup>3</sup>), it was felt that activated coconut charcoal would be a suitable sorbent for atmospheric sampling. This judgment was also based on its previously mentioned use by Germani and Zoller (Germani, 1988), and on Dr. Olmez's past experiences with it. The time frame when this decision was made was in late April 1992 with the experiments having begun in February. At that time the most pressing issue was the design and construction of the sampling units (to be covered in section 3.6) in time for testing and delivery to the New York sites in June. The assumption was made that the charcoal

would not present any difficulties as a collection medium, and that activated coconut charcoals from different sources, but of the same grain size and type would behave similarly.

### 3.5 Field Use of the Charcoal

The first charcoal used for sampling at the New York sites was the previously labeled MSAOHC, which was obtained from Mine Safety Associates in sealed 6 mm glass tubes with a 100 mg charcoal section followed by a 50 mg section as described above. Because of measured inhomogeneities in the mercury concentrations among the sorbent tubes, the charcoal was removed from 200 sorbents, homogenized and re-packed into the tubes with only one 100 mg section of charcoal. These tubes were only used as the initial test sorbents to check the performance of the samplers, which covered the last two weeks of June 1992, and in the first full month of actual sampling, July 1992.

Since August 1992 the entire sorbent tubes have been made in this lab from a bulk supply of charcoal packed into Teflon® FEP (fluorinated ethylene polypropylene) tubes. The tubing is 1/4 inch outside diameter with a 1/32 inch wall (6.4 mm x 0.8 mm) and is purchased as a 25 foot roll. It is first cut to a length of roughly 2-1/4 inches (57 mm), then one end is heated and closed shut so the piece looks like a small test tube. This closed end is then center drilled using a 3/32 inch (0.24 mm) bit and any excess material trimmed away. A batch of 100 tubes is usually made at one time. The tubes are cleaned by soaking in 1:4 nitric acid for two hours and then rinsed four times with de-ionized water (resistivity  $\geq 2 \text{ M}\Omega\text{-cm}$ ). Drying is performed in a Class-100 laminar flow clean hood. A small retaining plug ( $\approx 3/16$ " or 5 mm) is inserted into the bottom of the tube; 100 mg of charcoal is poured in using a polyethylene funnel which fits tightly onto the top of the tube; and another plug is lightly tamped down onto the top of the charcoal. The amount of charcoal in the tube is only roughly 100 mg because it is measured out by volume in a small scoop made from the end of a polyethylene vial cut to size; a sample of 35 tubes showed an average charcoal weight of  $106 \pm 6 \text{ mg}$ . Figure 10 shows a full size sorbent tube.

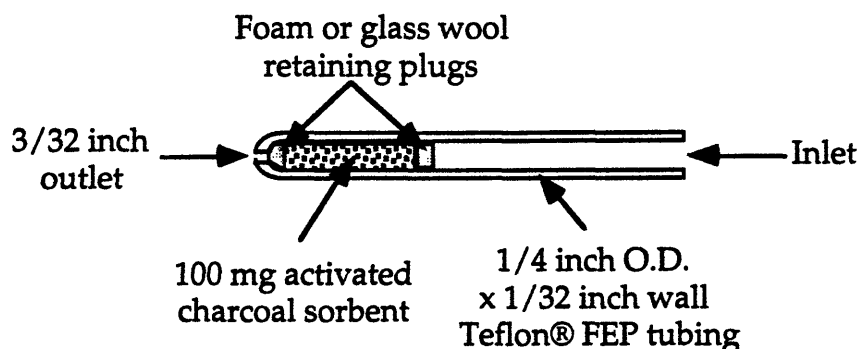


Figure 10. Sorbent collection tube for vapor-phase mercury sampling, approximately full size. For specifics concerning the charcoal used and the retaining plugs see text.

The first bulk activated charcoal used in the tubes produced in this lab was a 20 - 35 mesh size coconut charcoal purchased from EM Science, previously referred to as EMBULK. Before being packed into sorbent tubes it was heated to 400°C for two hours in an attempt to reduce the mercury blank value. This charcoal was used from August 1992 through July 1993. After problems in the mercury analysis were found and resolved in April 1993, the charcoals were re-analyzed for elemental composition as discussed in Section 3.3 (the analytical problems will be discussed in Chapter 4). It was then decided to switch to another steam activated coconut charcoal obtained from Calgon Carbon (type PCB 12 x 30). Efficiency tests using irradiated metallic mercury similar to those described in Section 3.4 were performed using this new charcoal in early July 1993, and was used for field sampling from August 1993 until the end of the ESEERCO Upstate New York project.

The retaining plugs used in the sorbent tubes were initially both made of fine glass wool rolled into a ball, but in January 1993 they were both switched to acid-washed open-cell polyurethane foam, because this is much easier to handle, forms a more consistent and reproducible plug, and can be analyzed for mercury using INAA (glass wool contains boron which would cause excessive heating if irradiated with neutrons). Following problems with the results from the field to be discussed shortly, the front plug was switched back to glass wool in April 1994. This return to glass wool packing was out of concern that the polyurethane might be collecting vapor-phase mercury upstream of the charcoal since polyurethane is sometimes used as a

collection medium for volatile organic compounds (SKC, 1992). Also, glass wool is used for the front packing of all the commercially available sorbent tubes seen in this lab and used by other investigators that we know even though the back packing is sometimes made of foam. After analyzing some of the foam plugs from the field it appeared that they were not collecting a significant amount of mercury, but the glass wool was retained so the sorbents from this lab would be as similar as practical with commercial tubes and those used by other investigators.

### **3.6 Collection Efficiency Problems**

Due to delays in analysis caused by uncertainties regarding blank values and INAA procedures to be discussed in Chapter 4, there was a large gap between the time samples were being received from the field and when they were being analyzed in the lab. Thus, in the spring of 1994 a concerted effort was made to analyze a large number of samples as quickly as possible. When the results of these analyses were examined it was clear that some problem existed which was causing the results to show unrealistically low mercury levels, generally below any of the ambient concentrations reported in the literature. Furthermore, a calculation error made it appear that the measurements changed suddenly beginning in February 1993. Though the numerical mistake was not discovered until much later, these two unusual results prompted an investigation into what was causing the low measured concentrations.

Several explanations were immediately considered. The first was that some systematic error was being made in the analysis or in the lab. A mistake in the element library file in the MicroVAX used for spectrum storage and data reduction (covered in Chapter 4), or some discrepancy in the reference material's mercury concentration or counting could easily produce consistently low measurements. However the element library file was in good order, and by checking the measured activity of the standards with a calculated value based on the appropriate neutron flux, activation cross section, and detector efficiencies, it was determined that no systematic analytical mistakes were causing the problem. To check that the mercury was not being lost during storage, samples which had just been received from the field were analyzed along with some which were eighteen months old. There



was no significant difference between the measured mercury concentrations of these groups.

Suggestions that the low concentrations were due to problems in the field or in an actual reduction in atmospheric mercury concentrations were the next to be ruled out. The field operations were performed at that time by four different people from two organizations, and the five sampling sites are separated by up to 350 miles, so any mishandling or error in the samplers' performance that could have affected all of them simultaneously, seemed extremely unlikely. An actual change in the atmospheric mercury concentration would have affected all five locations identically because of the long range nature of the species. It is however, this global nature of vapor phase mercury which rules out the likelihood that the concentrations measured in New York would be below the lower bounds of reported measurements from any site including those from the remote Pacific.

It was thus inferred that the drop was due to a change in the preparation of the sorbents or the sample assembly. One suspicion was that some part of the sample assembly (the entire sorbent tube, the particulate filter and its holder) upstream of the charcoal was collecting the missing mercury. The only pieces of equipment in front of the sorbent are the particulate filter, its support backing, and the front retaining plug in the sorbent tube itself. Three different types of tests were performed on these parts to determine whether any of them were absorbing mercury which should have been reaching the charcoal. To complicate matters somewhat, two different materials had been used for both the front retaining plug and the particulate filter. This meant that both types of filters and plugs needed to be tested.

The first and quickest tests which were run were those using a radioactive mercury tracer. The set-up shown in Figure 9 was found to be too hard to control for the entrained mercury concentration, so a second arrangement was assembled as shown in Figure 11. The first changes were that the heated part of the set-up containing the mercury was much smaller than before, and the mercury primarily stays in the vial in which it was irradiated (the ends of the vial had small holes in them, made by poking a small syringe through the plastic). The advantages gained by this are that it is very easy to change the mercury source without contamination problems, and the air flow over the mercury is much more direct than before. The

heater for this part was run at very low voltage (about 5 VAC) and was regulated using a feedback controller receiving input from the K-type thermocouple which also served to hold the polyethylene vial in place. The tee fitting used compressed O-rings (not shown) to seal the air

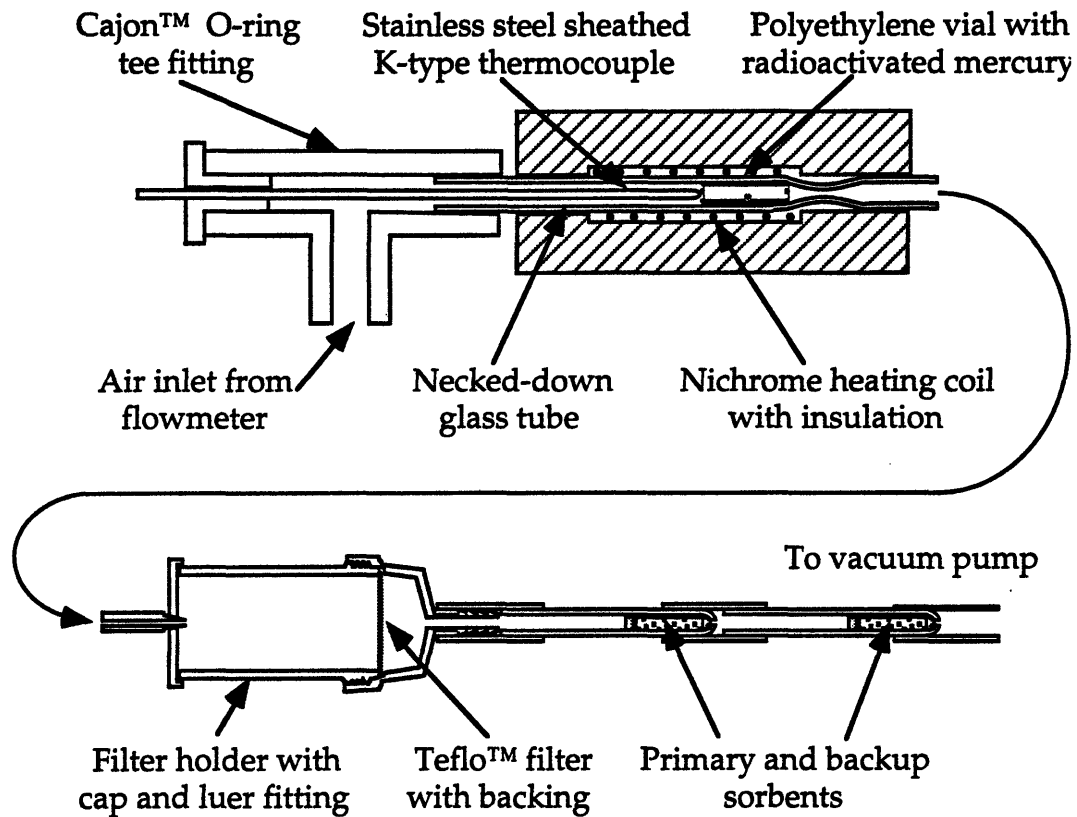


Figure 11. Radioactive mercury tracer experiment, type 2. Shown on top is the mercury source which passes air through a heated polyethylene vial containing 10 - 20 mg of irradiated mercury. Below there is a complete sample assembly with a luer fitting inlet to the filter holder to close the system.

inlet line (which included a variable area flow meter, not shown), the thermocouple, and the glass tube holding the mercury source. After some initial tests, the insulation was extended to cover the sampling assembly as well as the mercury source so that mercury would not be collecting in the sample assembly's parts by simple condensation. The temperature of the source, and later for the source and collection assembly was set between room

temperature ( $\approx 20^{\circ}\text{C}$  in the hood) and  $35^{\circ}\text{C}$  so it was never very far from realistic field levels.

The second type of test was to analyze by neutron activation as many of the parts from the field samples as was possible to look for mercury in places other than the charcoal. Although this is an obvious way to look for problems with past samples, not all of the parts from the returned sample assemblies were archived, and the glass wool packing can not be irradiated due to its boron content as mentioned above. Nevertheless, the Teflo™ filters, their paper support backings, front and rear foam retaining plugs, the charcoal itself, and even the Teflon® tubes from old and new field samples as well as lab and field blanks were all analyzed for mercury.

The final type of tests performed involved the collection of samples here at MIT, both in one of our labs (NW13-269), and on the roof of building NW13. By using different combinations of filters, support backings, retaining plugs, and tubes for the sorbents it was hoped that the problem could be identified.

These three types of tests were run basically in parallel over a period of two months from September through the end of October 1994. The results from each test were used to adjust the specific materials and conditions for the subsequent tests. The details of most of the work are not particularly relevant however, because in terms of finding sufficient amounts of mercury in some part of the sampling system other than the charcoal, all the results were negative. It was from one of the tests and the experiments that followed it, that an explanation for the low mercury measurements was found though almost by luck more than design. The analysis of samples from a 24 hour collection in our lab, NW13-269, suggested that there was a problem of break-through in the charcoal sorbents, i.e. that not all of the mercury passing through was being collected. This was inferred because when different amounts of charcoal were used to collect mercury in parallel sampling, the measured concentrations were greater in the larger sorbents.

Thus, lab sampling and radioactive tracer experiments were begun with two sorbent tubes running in series so that any mercury which was not captured on the first sorbent would be found on the back-up. The tracer experimental set-up was changed yet again because the one in Figure 11 was still too hard to control, and had the further problem that, when heated, the

polyethylene vial sometimes extruded itself into the taper of the glass tube, thus closing off its exit holes. The third source configuration is shown in

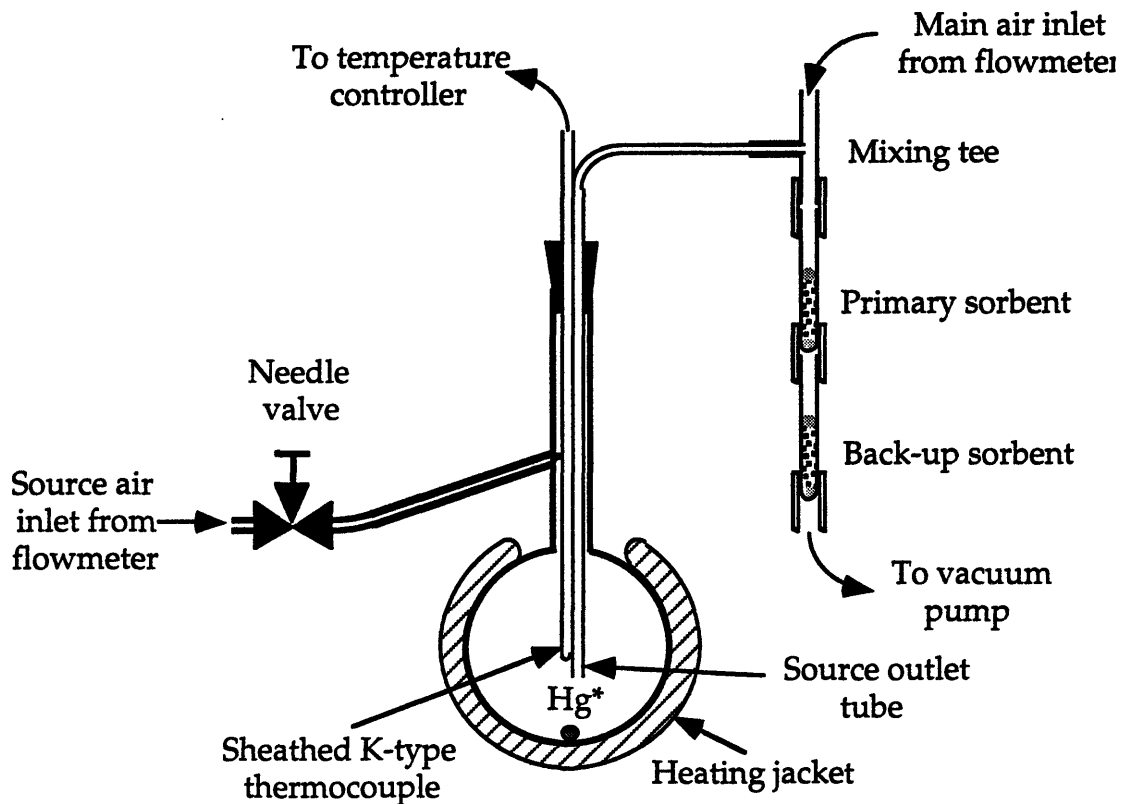


Figure 12. Radioactive mercury tracer experiment, type 3. Most of the air passing through the sorbents comes from the main inlet at the top right. A small amount of air containing the radioactive mercury is drawn into the mixing tee by the flow induced pressure drop. This way the mercury concentration in the flask can be more accurately diluted.

Figure 12, along with two sorbent tubes run in series, so that the charcoal's collection efficiency or break-through can be detected. The main air flow was measured with a variable area flow meter, and was run between 1 and 4 liters per minute. The source flow was much lower, usually between 10 and 100 milliliters per minute, and was measured using an optically timed soap bubble flow cell, with a small bubbler installed at first to allow a visual check for the flow. When the apparatus had run for a few days with no problems or flow changes the bubbler was removed. As with the previously shown tracer experiments, mercury is present in the air stream in sufficient amounts to be

measured because of its high vapor pressure. The actual concentration of mercury in the past set-ups was limited by the kinetics of the vapor leaving the liquid drop because all of the air flowing through the sorbents was passing the tracer. This flow rate ( $\approx 1 - 4$  liters per minute) was too high for liquid/vapor equilibrium to be reached. In this new arrangement however, the amount of mercury in the sampled air is largely determined by the ratio of the main flow rate to the tracer flow rate, and the equilibrium vapor concentration of mercury at the temperature of the source flask.

The vapor pressure in torr and the equilibrium concentration in  $\text{mg}/\text{m}^3$  are shown in Figure 13. At room temperature the concentration is about  $22 \text{ mg}/\text{m}^3$ , and the smallest ratio between the source and total flow possible with this arrangement was 1:400, thus a final concentration of  $54 \text{ }\mu\text{g}/\text{m}^3$  was as low as this set-up could reach. Though still four orders of magnitude higher than ambient concentrations this was much lower than previous experiments could obtain, and more importantly the concentration was easy to estimate, reproducible, and controllable. Using this equipment the problem of the low measured mercury concentrations was finally solved.

Because the mercury concentrations produced in these tests could be estimated, by using the measured specific activity of the source mercury (counts per milligram) this allowed the expected activity on the charcoal to be estimated. When the actual activity on the charcoals turned out to be much lower than expected, this led to a real indication that not all of the mercury was being collected by the charcoal, and the beginning of further tests with two sorbent tubes in series as seen in Figure 12. The first round of tests used two identical sorbents, and because the irradiated mercury was of a low specific activity and the mercury concentration in the air was low, no counts were measured on the backup sorbent. Finally a commercially produced iodated charcoal, the one previously referred to as MSAMER was inserted as a backup. After 20 minutes of sampling, with a source flow of  $26 \text{ mL}/\text{min}$  and a total flow of  $3.3 \text{ L}/\text{min}$ , the backup sorbent had 2.5 times more activity than the primary sorbent, and so the collection efficiency of the charcoal was identified as the root of the low mercury measurements. The remaining task was to accurately quantify the efficiency so that the data from the 'low mercury' measurements could be corrected.

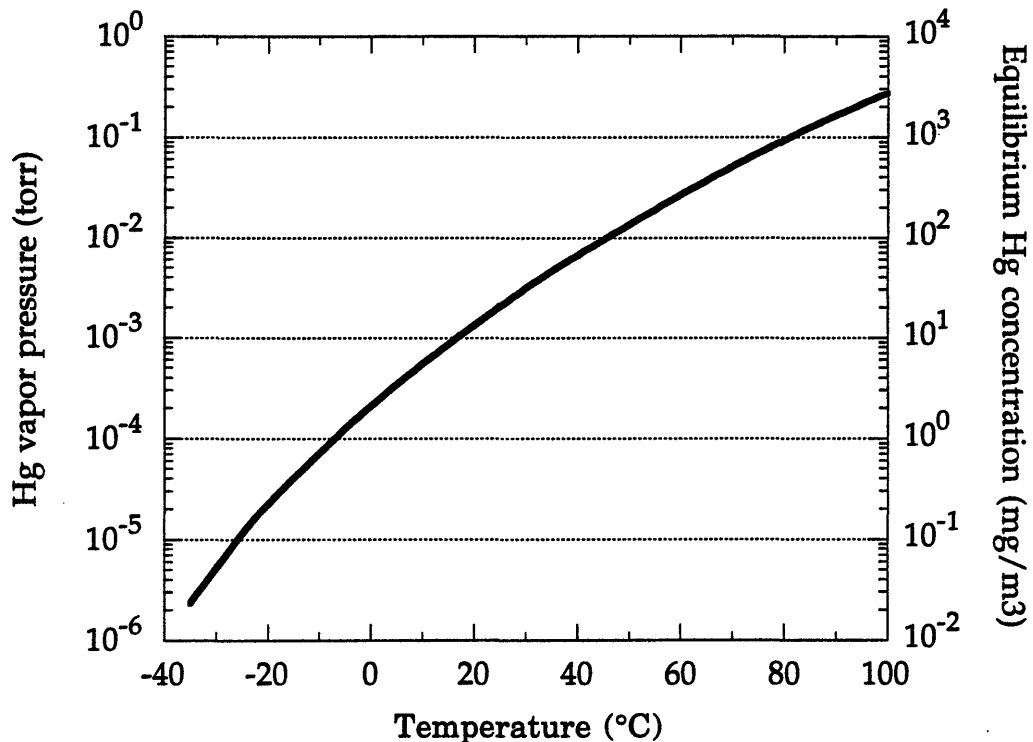


Figure 13. Mercury's vapor pressure in torr and its equilibrium concentration in  $\text{mg}/\text{m}^3$  as a function of temperature. The line shows the vapor pressure; in these units, the equilibrium concentration is 11,800 times the vapor pressure at standard conditions rather than 10,000 times as implied by the graph, but the difference is too small to be seen clearly on the logarithmic scale shown.

Approximately 30 radio-tracer tests were performed and two comparative sets of roof and lab samples were taken in order both to establish the collection efficiency of the standard charcoal which had been in use in the field, and to create a test for the efficiency of a replacement charcoal. The mercury source was run at three temperatures which corresponded to three convenient equilibrium vapor concentrations:  $35.4^\circ\text{C}$ , which is  $50 \text{ mg}/\text{m}^3$ ;  $24.1^\circ\text{C}$ , gave  $20 \text{ mg}/\text{m}^3$ ; and  $0^\circ\text{C}$ ,  $2.5 \text{ mg}/\text{m}^3$ . A  $0^\circ\text{C}$  source was established by replacing the heating jacket shown in Figure 13 with an ice bath. The source flow rate for the first series of tests was either  $\sim 25$  or  $\sim 10 \text{ mL}/\text{min}$ , and the total flow was either 1 or  $\sim 2.5 \text{ L}/\text{min}$ . These temperatures and flows were

used to produce final mercury concentrations from 1.8 mg/m<sup>3</sup> down to 250 µg/m<sup>3</sup>. When it became clear that the efficiency of the standard charcoal was a function of the mercury concentration, yet another experimental arrangement was needed to produce very low levels of radio-activated mercury; this is shown in Figure 15.

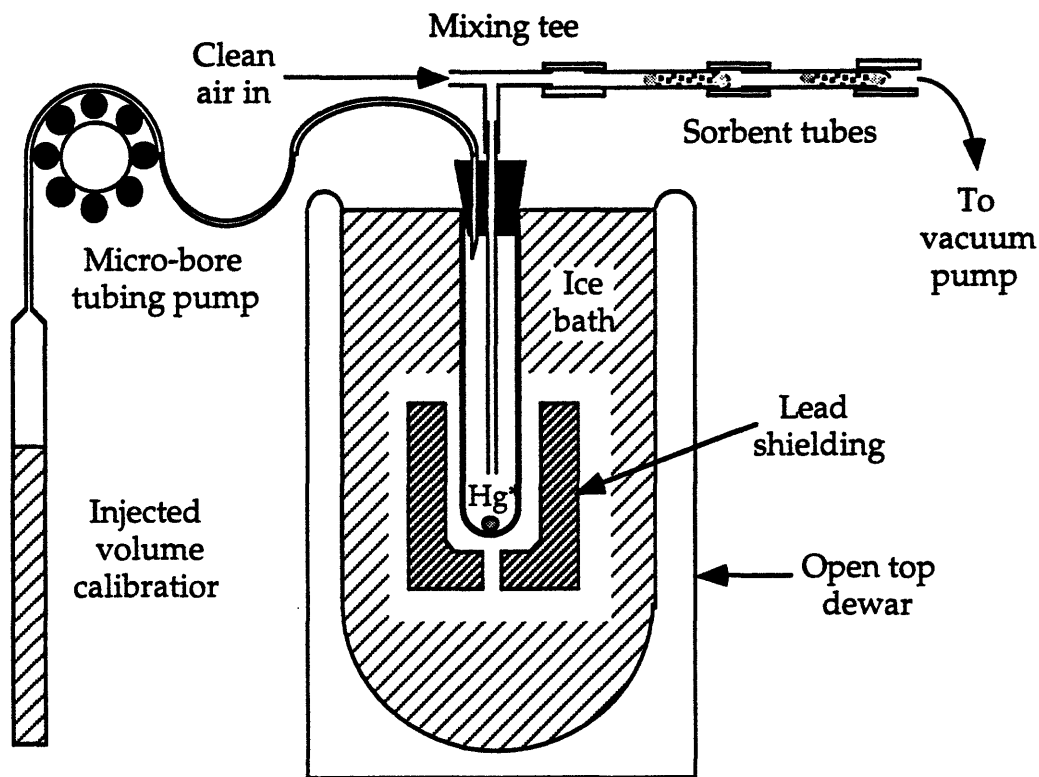


Figure 14. Radioactive mercury tracer experiment, type 4. The micro-bore tubing pump could produce a source flow rate of down to 1 µL/min, which at a source temperature of 0°C and a total flow of 1 L/min resulted in a final mercury concentration of as low as 2.5 ng/m<sup>3</sup>. The suspended lead shielding was necessary because of the high activity of the mercury tracer. The injected volume calibrator was an upside down 25 mL pipette tube used to measure the flow over several hours, and was only needed to calibrate and check the flow rate. As before the main flow was measured by a variable area flow meter.

Because this radioactive tracer setup can produce vaporphase mercury concentrations in the same range as those found in ambient air (ng/m<sup>3</sup>), it is the final one used for this work and hopefully will be used in the future to

check the efficiency of various sorbents and systems (see Chapter VI). A full description of it is thus somewhat in order before the results of the tracer and sampling tests are given. On the front end of the system is a Cole-Parmer® tubing pump comprised of a 1 - 100 RPM variable speed motor (# 7553-80), a 5:1 speed reducing 8 roller pump head (# 7519-25), and a small size tubing cartridge (#7519-65). The lowest flow rates (0.6  $\mu\text{L}/\text{min}$ ) were achieved using 0.19 mm inner diameter microbore Tygon® tubing (#95609-10), though flow rates of up to 2.9 mL/min were also used by running 1/16" inner diameter tubing. A tubing or peristaltic pump operates by successively occluding a small section of the tubing and rolling the occlusion from the inlet to the outlet side of the cartridge. It is a particularly useful pump type for metering small amounts of fluid or for handling high purity or corrosive materials, since the pumped fluid only contacts the tubing. Connections to the micro-bore tubing were made by inserting the needle of a hypodermic syringe into the tube and using the attached luer fitting or pushing the needle through a rubber stopper as shown at the top of the source section in the figure. In order to measure the flow rate of air through this pump, two types of flow meters were used. At higher flow rates (above 1 mL/min) a Gilian® optically timed bubble flow cell was used (called the Gilibrator™, it is a primary standard airflow calibrator discussed in section 3.8 "Field Operations"). Lower flow rates were measured by timing the rise of water in an inverted 25 mL pipette tube.

The radioactive mercury tracer section is a 6 mg drop of mercury which was irradiated for 12 hours (from 18:00 on 11-22-'94 to 6:00 on 11-23-'94) in the bottom of a 15 mm x 125 mm test tube. The stopper has two needles pushed through for a metered inlet, and a micro-bore outlet tube which goes down almost to the bottom. It also has a 1/8" hole for a Teflon® thermowell made from tubing sealed at the bottom, which held a K-type thermocouple. The micro-bore tubing was used for the outlet to reduce molecular diffusion of mercury up to the mixing tee. The fluence of mercury through larger tubing by diffusion (~25 ng/day) would have been larger than the lower injection rates (down to 2 ng/day). The temperature of the mercury was kept at 0°C ( $\pm 0.3$  roughly) by immersing the test tube in an ice bath in an open topped dewar. Replacing the ice daily was sufficient to hold the temperature constant. Because of the high specific activity of the mercury, a 1/2" thick lead



shield was suspended around the source which reduced the measured dose rate near the set-up to background levels.

To create a low concentration mercury flow the outlet of the source was directly connected to the middle arm of a mixing tee which had a clean air stream passing through the run of the tee. Sorbents to be tested were attached to this tee using silicone tubing. Total air flow through the sorbents was measured at the clean air inlet by a variable area flow meter, and was controlled by a needle valve on the inlet to the vacuum pump. The predicted maximum amount of mercury sampled in a run could be calculated by multiplying the source flow rate, the sampling time, and the equilibrium concentration of mercury in air at 0°C of 2.2 mg/m<sup>3</sup>. Multiplying this concentration by the ratio of the source flow to the total flow would give the expected maximum mercury concentration in the sample stream. The actual collected mercury could be estimated by dividing the measured activity of the sample by the specific measured activity of initial mercury present in the test tube.

This initial activity, and all the sorbent activities were measured using a +1000V bias high-purity germanium (HPGe) detector connected to a Canberra Series 35 multi-channel analyzer (MCA). Because the initial activity of the 6 mg source mercury was so high it was counted at 23 cm from the detector to avoid excessive dead time in the detector's electronics. At this distance the two gamma ray peaks were 1900 counts per second (c/s) @ 77keV, and 170 c/s @ 279keV. In order to estimate the count rate at 0 cm where the sorbants would be counted a Ba-133 source was counted a 23 cm and 0 cm. The barium source has gamma ray peaks at 81, 276, and 302 keV, so the change in detection efficiency between the two distances for the mercury peaks could be easily calculated. Thus the specific measured activity at 0 cm for the mercury source was  $31 \times 10^6$  c/s per gram @77keV and  $1.7 \times 10^6$  c/s per gram @279keV (on 11-28-'94). Though the 77keV peak was stronger, its low energy tail coincided with the high end of the 68keV X-ray peak also emitted by the mercury, and this tended to make background subtraction more difficult on the MCA. Also this peak is the result of the Hg-197 decay which has a half-life of only 64 hours and so its use in the tracer experiments would require half-life corrections for all the measurements, and after 12 days it would be the same strength as the 279keV peak anyway.

The first efficiency tests in this new round of experiments using a radioactive tracer however were performed at high mercury concentrations using the setup shown in Figure 13. A selected set of results for these tests are given in Table 3. The most important feature of this table is the increase in

Source temp. (°C)	Source flow (mL/min)	Total flow (L/min)	Calc. Hg conc. ( $\mu\text{g}/\text{m}^3$ )	Total run time (min)	Meas. Hg conc. ( $\mu\text{g}/\text{m}^3$ )	Sorbent efficiency (%)
35.4	27	2.6	520	1090	440±47	3±2
35.4	27	2.5	540	600	450±33	4±2
24.1	11	1.0	220	1040	140±12	11±5
24.1	9.5	1.0	190	2320	95±9	12±4
0	9.7	1.0	21	1260	21±5	15±6
0	9.5	1.0	21	2530	17±3	16±4
0	10	1.0	22	3850	16±2	15±4

Table 3. Selected efficiency tests of Calgon Carbon sorbents using the radio-tracer set-up from Figure 12 and MSA iodated charcoal as a backup. The calculated mercury concentration was determined from the vapor pressure at the source temperature, and the ratio of the flow rates. The measured concentration was determined from the measured activity on the sorbants compared to the specific activity of the source. The errors quoted in the rightmost two columns are all a result of the counting statistics, as the other variables in these figures could be measured with much better precision than the counting.

the charcoal's collection efficiency with decreasing mercury concentration. Also it should be noted that the measured mercury concentration is close to, but lower than the calculated concentration probably because of the kinetics of the mercury vaporization, and that the total amount of mercury collected

continued to increase with time though the efficiency did not change, confirming that saturation was not a problem. The front sorbent used in these tests was the Calgon Carbon charcoal which had been used for almost all of the field samples, while the back-up was the MSA iodated charcoal. The efficiency of the MSA was also checked using two of these sorbents, and a variety of other tests were run with some of the previously considered or otherwise interesting sorbents and at other flow rates and temperatures. The increasing efficiency seen in the table and mentioned previously led to more tests at lower concentrations using the fully described configuration from Figure 14, producing the results shown in Table 4.

Source flow (mL/min)	Total time (min)	Calculated Hg concentration ( $\mu\text{g}/\text{m}^3$ )	Measured Hg concentration ( $\mu\text{g}/\text{m}^3$ )	Sorbent efficiency (%)
3.0	1090	6.6	$3.7 \pm 0.1$	$14 \pm 1$
0.5	1350	1.1	$0.62 \pm 0.03$	$15 \pm 1$
*	1100	*	$0.55 \pm 0.03$	$13 \pm 1$
0.08	1295	0.18	$0.08 \pm 0.01$	$15 \pm 2$

Table 4. Selected efficiency tests of Calgon Carbon sorbents using the radio-tracer set-up from Figure 14 and Cameron-Yakima iodated charcoal as a backup. The source temperature for all of these tests was  $0^\circ\text{C}$ , and the total flow was 1 liter per minute. The asterisk (\*) indicates that the source flow was uncertain due to a leak in the thermowell, so the mercury concentration was not calculated though the efficiency determination is still valid. The errors quoted in the rightmost two columns are all a result of the counting statistics, as the other variables in these figures could be measured with much better precision than the counting.

These tests used the new iodated charcoal from Cameron-Yakima as a back-up, because MSA had discontinued its iodated charcoal in favor of a hopcalite sorbing. Before its use for these tests it was run in the Figure 15 test

set-up and found to be completely efficient at these flow rates. The very promising result of these tests was that the efficiency of the Calgon charcoals remained at 15% down to mercury concentrations of 80 ng/m<sup>3</sup>. The final confirmation of this figure for use in correcting the field measurements came from tests involving actual samples taken in our lab (NW13-269) and on the roof of NW13 with Calgon charcoals being run in parallel with the two iodated charcoals. Results of these measurements which were performed in parallel with the tracer tests, are given in Table 5.

Location	Iodated Charcoal	Flow rate (LPM)	Time (hours)	Hg (ng) by INAA	Hg conc. (ng/m <sup>3</sup> )	Calgon eff. (%)
Lab	Cam-Yak.	2.95	24	53.2±1.4	12.1±0.3	13±1
Lab	MSA	2.10	24	57.2±1.0	18.5±0.3	16±1
Lab	Cam-Yak.	1.00	24	16.6±0.8	10.2±0.5	13±3
Lab	MSA	2.10	12	31.6±0.6	20.6±0.3	14±1
Roof	Cam-Yak.	2.95	24	14.0±1.4	2.8±0.3	15±3
Roof	MSA	3.00	24	81.6±1.2	18.5±0.3	17±2
Roof	Cam-Yak.	1.00	24	5.1±0.7	3.2±0.4	*
Roof	MSA	3.00	12	8.7±0.3	3.3±0.2	17±2

Table 5. Efficiency test of Calgon Carbon charcoal using parallel samples taken with iodated charcoals. Lab samples were taken in NW13-269 and roof samples are from the roof of NW13. The measured Hg and Hg concentration numbers refer to the iodated charcoals, which were completely efficient. The asterisk (\*) indicates that the Calgon charcoal did not collect enough mercury to be detected above its blank level so no efficiency was determined for that test. The errors quoted in the rightmost three columns are all a result of the counting statistics, as the other variables in these figures could be measured with much better precision than the counting.

When the results of the roof and lab test samples were combined with the low mercury concentration ( $<25 \mu\text{g}/\text{m}^3$ ) tracer tests, the efficiency of the charcoal used for ambient measurements was determined as  $14.5 \pm 0.35\%$ . This figure was calculated by weighting each efficiency measurement by inverse of the square of its own error, and the final error was calculated as the square root of the sum of the squares of each measurement's individual error. This value was then used to correct the calculated concentrations from the field.

Another important result of this efficiency study was that it became obvious that the initial assumption that plain coconut charcoal was a suitable collector for vapor-phase mercury should have been examined more carefully. The degree to which this assumption was held as true and hindered the uncovering of the actual problem can be seen from the fact that every other possible explanation for the low field measurements was examined before the collection efficiency of the charcoal was checked (and this occurred almost by accident). In hindsight, this was a rather serious mistake. The solution for the present work has been to use the measured charcoal efficiency to determine the ambient mercury concentrations from the INAA results. Also, finding a more efficient charcoal and an easy way to test the efficiency will help in making future uses of this methodology easier. A scientific explanation as to what determines the efficiency of activated charcoal in general is not available and so it is only possible to empirically test the effects of various conditions. Though this may not provide enough insight to completely prevent further difficulties, the experiments described above can now be used in a routine fashion as a quality assurance (QA) check for future sampling programs.

### **3.7 Sampler Equipment Design**

The design of the mechanical and electrical system which was needed to take automated samples at the Upstate New York sites began in the early spring of 1992. In November of 1991, before the author became involved with this project, an SKC Automatic Trace Sampler was purchased. This would have been an ideal system as it was easily programmable, recorded the times that the different channels turned on and off, and could handle up to ten

samples a week. However, because the different sampling channels each had their own pumps, the pumps were small piston pumps which could only produce 4" Hg of vacuum ( $\approx 100$  torr) for any extended period. After running these samplers at full flow for a few hours with the charcoal sorbent tubes, the overload protection would shut the pumps off. It was then obvious that what was needed was a system with one large vacuum pump that would switch channels through the use of electrically controlled solenoid valves. Though this does not seem to be too unusual a set of requirements, no commercially available equipment was found.

Rather than construct a sampler from scratch however, an Andersen volatile organics toxic air (VOTA) sampler was purchased to see whether it could be modified for our purposes. The VOTA sampler is designed to take up to four simultaneous (parallel) samples using a large (1/4 hp) carbon vane rotary vacuum pump and special sorbent tubes for extracting specific volatile organics. The basis for the sampler is an aluminum housing which Andersen modifies for several different types of air sampling. The changes needed for four channel sampling were incorporated following a request by the New York State DEC for such a unit. Though the sampler was not exactly what was required for the mercury sampling, it provided a well built and tested platform which was easy to adapt to our purposes. The housing for the pump, controller, and other equipment is made of 15" wide x 0.080" thick gray anodized aluminum sheets attached to 44" tall x 2" square L-shaped legs at the corners. The roof which is made of the same sheet is pitched at 45° in front and back, is 13" deep from peak to edge, and is 32" wide. Two fittings for the sorbents are under the eaves on either side of the roof. The roof is hinged at the back to make changing the sorbents easier and has a latch in the front so that the roof can be secured from blowing open in high winds or locked shut. A pivoting 1/4" rod was added to the underside of the roof to allow it to be propped open. The main section of the sampler has a locking door in front. Figure 15 shows the layout of the larger components within the sampler after its modifications were completed, and the drawing is roughly to scale. A full description of the sampler follows in the text.

This base structure, the vacuum pump, and some of the fittings were left in place, but the rest of the system was rebuilt for mercury sampling. The first change was that the single channel, one week mechanical timer/relay controller was removed so that the four sampling channels could be

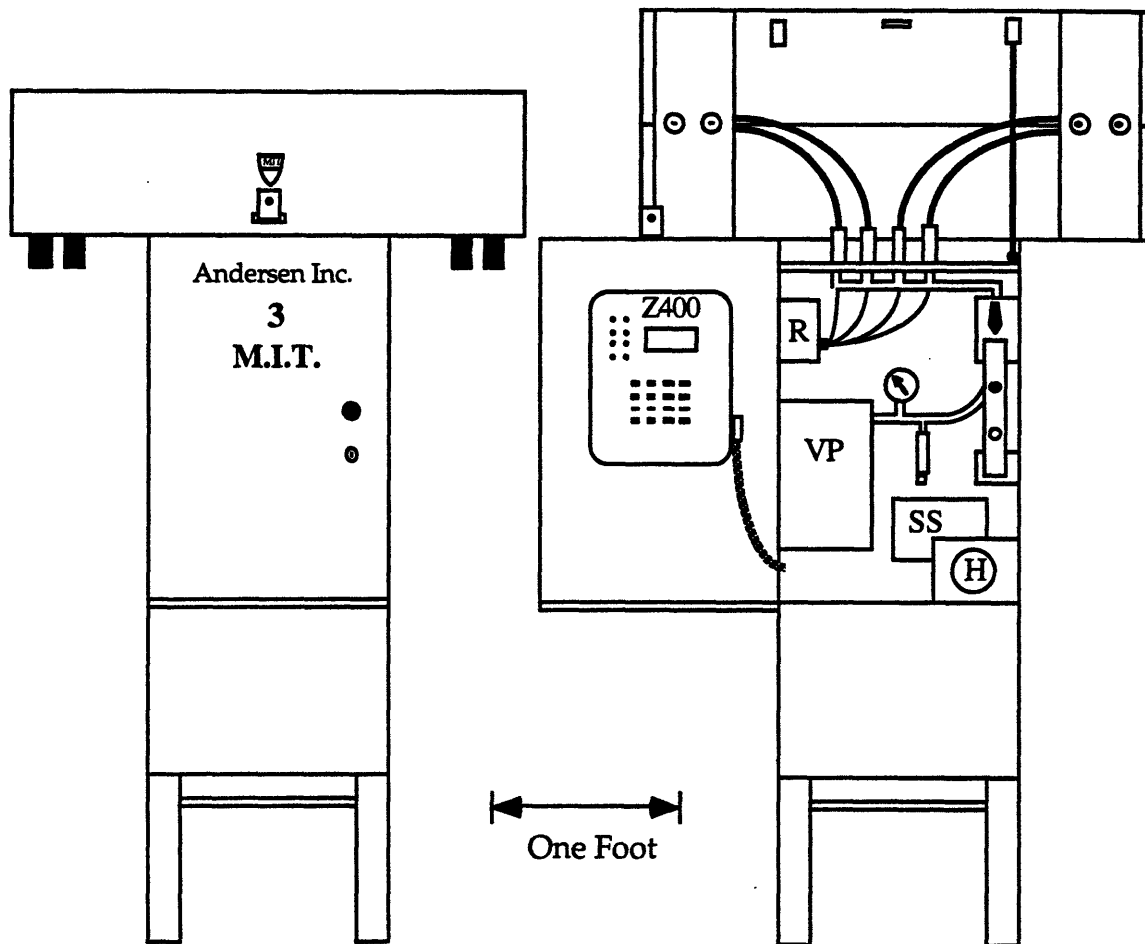


Figure 15. A front view of the complete vapor-phase mercury sampling system. At left, with the door and roof shut, the ends of four sampling assemblies can be seen hanging from under the roof ends. At right it is shown with the roof and door open. Labeled parts include: the Z400 controller on the inside of the door; R, the relay box; VP, the vacuum pump; SS, the electrical surge suppresser; and H, the elapsed hour meter. Also visible in the middle from left to right are the vacuum gauge, the vacuum relief valve, and the rotameter. The four channel vacuum manifold can be seen at the top of the main housing, and the four quick-connects for the sample assemblies are shown under the ends of the roof.

controlled independently. It was replaced by a four channel Tork Z400 electronically programmable controller. This device has four single-pole, double-throw (SPDT) relays, a battery back-up for the clock and program, and was ordered in the optional low temperature version (operation down to -30° F/ -35° C). Each of the controller's relays were connected to a PrecisionDynamics A2017 normally closed 120 VAC brass solenoid valve and a Potter & Bromfield T-91 panel mount 120 VAC SPST normally open (NO) relay. The solenoids were inserted in the place of an elbow in the flow path for each sampling channel, and the relays were connected in parallel with each other and in series with the vacuum pump's line voltage. In this configuration, when the programmer closed one of its relays the solenoid for the corresponding sampling channel would open and the vacuum pump would switch on. Because the electronic controller is sensitive to disturbances in its line voltage, an ISOBAR 4 surge suppresser was installed which has four AC outlets using two separate filter banks so that any surges caused by the starting and stopping of the vacuum pump should not affect the electronic controller. So that the actual time the sampler ran during the week could be checked using a Cramer type 636 resettable hour meter with 0.1 hour resolution was installed in parallel with the vacuum pump's electric line.

In its original configuration the VOTA sampler was used with sorbents for specific organic compounds which required very low flow rates and so a fine needle valve was present in each channel. Because the activated carbon sorbents could be used at a higher flow rate slightly larger needle valves (Nupro B-4MA, 1/4", brass, angle-pattern) were used instead. The flow rate was originally determined by measuring the pressure drop across the needle valves using a manometer with a range of up to eight inches of water. Because the flow rate was to be increased, and because a more robust device was desired, this was replaced by a Matheson E700 Tube Cube rotameter in an aluminum body FM-1050A-NV holder. This type of flow meter operates by having an upward flow of air 'float' a small ball within a tapered glass tube. The faster the flow of air, the higher the ball will float. These particular meters have 150 mm of active length and contain both a steel and a glass ball for greater range. One problem with rotameters is that the height of the ball is significantly affected by the pressure of the air within the tube even when the flow at atmospheric pressure is unchanged. Because the best location for the flow meter in the mercury sampling system was just ahead of the vacuum



pump, a vacuum gauge was necessary at this point, and the flow meters had to be calibrated over a range of pressures. The initial calibration of the flow meters was carried out using a two liter bubble flow cell at the NYSDEC Air Quality Lab in Albany NY where the VOTA samplers were first developed. So that the flow meter could be bypassed during normal operation, a three-way ball valve was installed at the meter's outlet. The inlet to the flow meter was connected to a vacuum manifold constructed of 1/4" brass Swagelok® tees, elbows, and port connectors, with four Swagelok® B-QC4-B1-400 brass, quick-connect, bulkhead bodies with automatic shut-off as inlets.

To maintain the vacuum (and thus the pressure drop through the sorbents) at a level of 20" Hg ( $\approx$ 500 torr) a Nupro® B-4CA-3-VI brass, in-line, adjustable, pressure relief valve with a viton O-ring was put on the branch of a tee fitting right at the inlet to the vacuum pump. Though this is a pressure relief valve, by connecting its outlet to the flow line it was able to be used as a vacuum regulator. The viton O-ring was needed for extended outdoor operation over a wide range, and the inlet to the valve was covered by a screen in a brass pipe plug, a device referred to as a mud dobber, to prevent insects from being sucked into the valve. After a period of operation from about one to six months, the internal parts of the valve would become partially clogged with dust which generally caused the vacuum level to increase (though a few times the valve stuck partly open and the level decreased) which would require the valve to be replaced, cleaned, and re-adjusted. The vacuum level was measured weekly using a gauge calibrated at the Air Quality Lab, and the sites initially had three spare valves which were adjusted and labeled at this lab. The valves were replaced when the vacuum level was outside a  $\pm$  10% limit from the set point. They were then sent to the MIT ER&R lab for refurbishing and returned to the field. This design and maintenance procedure for the vacuum regulation was carried over from the VOTA because the operators in New York were familiar with it, and it was recommended by the Air Quality Lab.

As mentioned above, each sampling channel had its own needle and solenoid valves. Between these two there was also a Nupro® B-4F-7 Compact, in-line 7 $\mu$ m brass sintered filter unit. This also carried over from the original VOTA design and was included to prevent small particles from clogging the needle valve. Because the mercury sampling included a particulate filter at the inlet, this in-line filter may not have been necessary,

and none of them ever became even partially full but, on the early recommendation of the Air Quality Lab they were left in the system. The needle and solenoid valves and a filter were mounted as a unit on a removable aluminum panel, four of these were then mounted using thumb screws to the top of the sampler's main structure but under the roof. A Swagelok® B-QC4-S-400 brass quick-connect stem attached this valve assembly to the vacuum manifold, and the inlet to the assembly was fitted with a 1/4" hose barb fitting to connect to the Tygon® tubing coming from the sample assemblies on the roof. The solenoid valves were connected individually to the relay box using 2 contact Conxall weather tight mini-con-x cable connections (6282-2SG-3XX). Again, this arrangement which allowed the easy removal of the valve assembly was prompted by the Air Quality Lab and the original design of the VOTA which, when used for organic sampling, required periodic replacement of the filter and needle valve. When used for mercury sampling this turned out not to be necessary, and over the entire program only one assembly needed replacement due to charcoal entering the solenoid valve and causing it to jam open.

Connections to the sampling assemblies in place on the original VOTA sampler were Swagelok® 1/4" nylon bulkhead unions (NY-400-61) with brass 1/4" hose to tube adapters (B-4-HC-A-401). These were replaced by 1/4" Delrin® panel mount to hose barb CPC quick-connect bodies which mated to matching quick connect inserts used in the sample assemblies. The two advantages of these parts over the originals were that they are very easy to use and that both of the quick connect parts automatically shut off when disconnected. The ease of use was immediately noted by the site operators who sometimes need to change the samples in very adverse weather conditions and who also appreciated the absence of small loose parts which had caused problems with the previous design. The automatic shut off feature on the sample assemblies sealed this end of the assembly for shipping of the samples and the shut off of the body connector made it easier to diagnose leakage problems when they occurred.

A complete sample assembly consisted of the quick-connect fitting, an activated carbon sorbent tube which has already been described, and a particulate filter and holder. Figure 16 shows the full assembly; the sorbent tube and filter were replaced with entirely new ones for each sample, while the quick-connect fitting and the filter holder were reused. The filter

prevented particulate mercury from entering the sorbent tube and provided a uniform air intake for all the samples. Twenty-five mm diameter x 0.8  $\mu\text{m}$  pore size Gelman mixed cellulose ester (MCE) filters (GN-4 Metricel®) were used initially because of their low cost and because they were not going to be analyzed. Later, these were replaced by 2 or 3  $\mu\text{m}$  pore size Teflo® filters which could be analyzed by INAA and were identical to those used in the dichotomous samplers except for their smaller diameter. Though the pore size of these later filters was larger, they both retain at least 99.8% of aerosols larger than 0.3  $\mu\text{m}$ , and because the particulate associated mercury concentrations are  $\approx$  1-2% of the gas phase levels, any change in the particulate retention would be very small. The filter holder is a Millipore threaded closure, carbon-filled polypropylene, aerosol monitor with a 50 mm extension cowl, an inlet cap, and a hose barb outlet (MAWP 025 AC). After repeated reuse, there was a problem with some of the filter holders leaking where they screwed together. This was solved by adding a 1" wide rubber seal band cut from 1" diameter Gooch tubing around the holder at the joint.

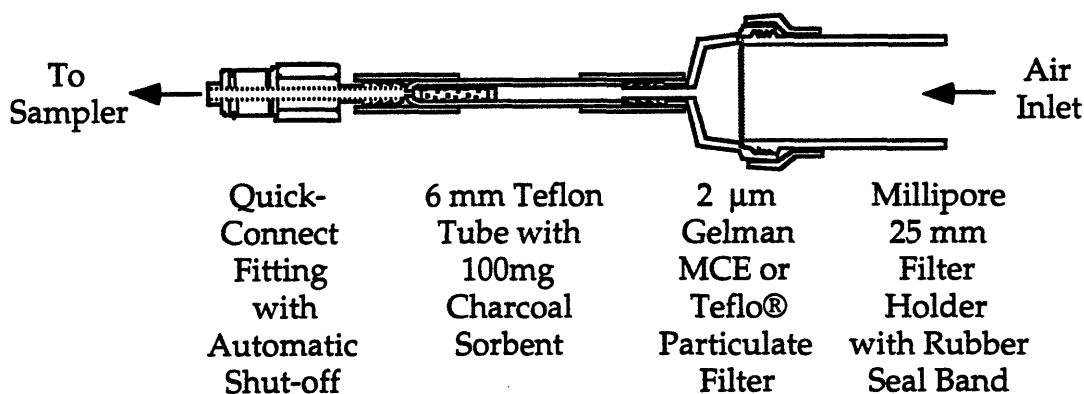


Figure 16. Sample assembly. The charcoal and the Teflo filter can be analyzed by INAA for vapor-phase and particulate mercury respectively. The filter holder and the quick-connect fitting were reused after the assemblies were returned from the sites, the entire sorbent tube and the filter and backing were replaced for each sample. A cap for the filter holder which was used for leak checking and for shipping is not shown.

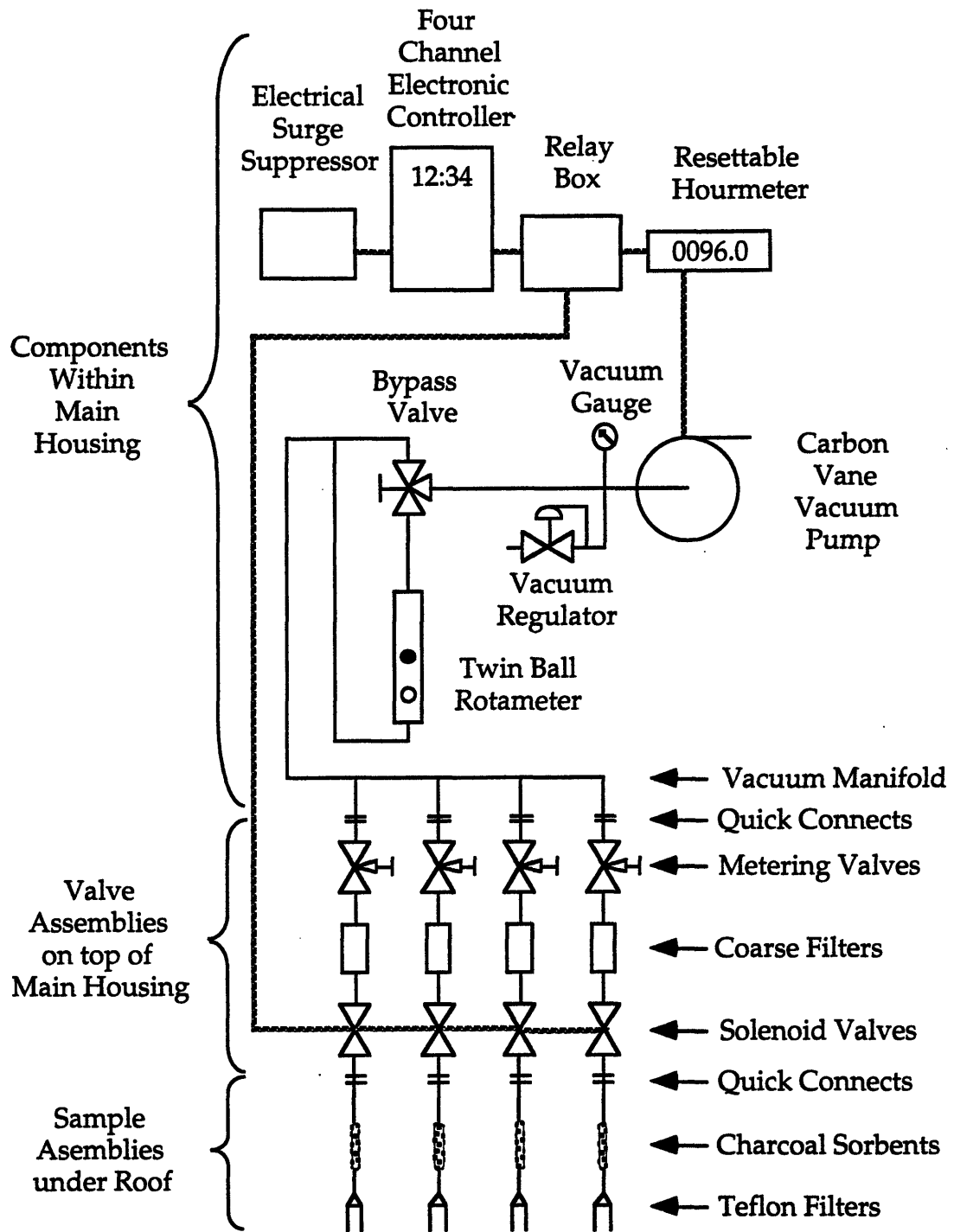


Figure 17. Schematic flow diagram of the vapor-phase mercury sampling system. The solid lines indicate 1/4" vacuum parts of either nylon or Tygon® tubing, or brass fittings. The dashed lines are electrical connections (the solenoid valves are actually each connected separately to the relay box). The valve and sample assemblies are designed for easy removal from the sampler.

All of the components for the sampling system were first built into a single prototype unit in April 1992, and when this was shown to work seven identical models were assembled in parallel in May and June of that year. The vacuum connections within the main housing were made using 1/4" outside diameter nylon tubing and brass Swagelok® fittings, because this combination is very strong, and not prone to leakage. Because the connections from the valve assemblies to quick-connect bodies in the roof needed to be somewhat flexible but also hold up under vacuum, they were made with 3/16" inside diameter x 1/16" wall Tygon® tubing and hose barb fittings. The sample assemblies themselves required a small amount of flex as well but over a very small distance. They also had to withstand more handling in possibly extremely cold conditions but did not need to hold up under vacuum because they were well supported, so the tubing used here was 3/16" inside diameter x 1/16" wall silicone tubing, which is very soft, and does not become brittle down to -80°F (-62°C). A schematic of the vacuum and electrical lines and the main components for the sampler are shown in Figure 17.

### **3.8 Field Operations**

In late June 1992 six samplers were taken to the NYSDEC Air Quality Lab in Albany NY so that their flow meters could be calibrated. They were then delivered to the five sampling locations across Upstate New York which are shown in Figure 18. A complete spare sampler was brought to Westfield because the distance to that site from Cambridge made unplanned site visits for repairs difficult. The sites were selected by the NYSDEC for the atmospheric trace elements program. Dichotomous samplers had been collecting airborne particulates at the five sites since October 1991, and two sites (Moss Lake and Willsboro) had been set up with wet deposition collectors as well. Westfield, Belleayre, and Willsboro are part of the NYSDEC's network of environmental sampling stations, and the samplers there were serviced by state environmental workers. Moss Lake was already being used as a sampling location by the Adirondack Lakes Survey Corporation (ALSC), and the Perch River site was set up for the dichotomous sampler by this group, which maintained these two sites. The three NYSDEC sites had the samplers on the roofs of permanently placed trailers. The

Westfield and Belleayre trailers were very modern with plumbing, heating,, and air conditioning, and were equipped with instrumentation for measuring, among other things, atmospheric SO<sub>2</sub> and O<sub>3</sub>, wind velocity and direction, and rainfall. These trailers were surrounded by chain link fencing, and had stairs to the samplers on their roofs. Willsboro's trailer was considerably older, with much less instrumentation (though it did house a variety of wildlife including a snake), and its roof was accessed by an extension ladder which was kept underneath the trailer. The Moss Lake and Perch River sites were merely elevated wooden platforms with the sampler bolted to the top. Moss Lake had several levels which were from about five to seven feet off the ground, and Perch River had only one small platform, about five feet square and about two feet high.



Figure 18. Atmospheric sampling locations in Upstate New York. Vapor-phase mercury and atmospheric particulates were collected at all five sites, and wet deposition was collected only at Moss Lake and Willsboro.

From west to east: the site at Westfield is surrounded by grape orchards and was within sight of Lake Erie. Perch River is in a remote, somewhat flat and not forested area about twelve miles northwest of Watertown, New York, and fifteen miles from Lake Ontario and the entrance to the St. Lawrence River. Moss Lake is about in the center of the Adirondack State Park which is sparsely populated, mountainous, and mostly forest land; Willsboro is located on a peninsula on the western shore of Lake Champlain about half

way along its length Belleayre is just north of the Catskill State Park at the base of the Belleayre Ski Center. It is also in sparsely populated, and somewhat mountainous, mostly forested area. This selection of remote sites gave full coverage of the state without the influence of strong local sources.

At the sites, the operation of the samplers was explained to the field operators, the electronic controllers were programmed, and a set of test sample assemblies were installed. A manual for the samplers was given to each operator which included copies of the manufacturers' manuals for the electronic controller and the flow meter, normal operating procedures for weekly sample changing, and set of trouble-shooting tips for unusual conditions. With each weekly set of sample assemblies a "Sampler Data Sheet" was included so that the flow rate for each channel, the total sampling time, and any unusual events could be recorded. The full operating procedures and a data sheet are in Appendix B. Following a run of about two weeks using the test sample assemblies during which no problems were reported the first actual samples were taken beginning in August 1992. The sample assemblies were prepared and sent to the sites in one month batches, with each week's assemblies packed in a pre-addressed and postage paid shipping canister. The canisters were cardboard tubes with a crimped on steel bottom and a screw on steel top and were either 3-1/2" diameter by 7-3/4" long for mercury samples only or 4-1/2" diameter by 10-1/4" long when the mercury and particulate samples were sent together. They were returned to MIT weekly by U.S. Priority Mail (for \$2.90 each).

Four 24 hour samples were taken each week beginning at 12:00 noon on Wednesday until 12:00 noon Sunday, except at Perch River where samples changed over at 3:00 P.M. The operators changed the samples on Tuesdays, except for Perch River which was visited on Wednesdays (this being the reason for the 3:00 sampling change), because Moss Lake and Perch River were maintained by the same operators from ALSC and the distance between the sites made it impractical for both to be visited on the same day. The basic procedures for weekly changing of the samples were as follows:

- Open and prop up the sampler's roof and open the door.
- Record the total hours indicated by the hour meter on the data sheet for the previous week and reset the meter.

- If the total hours are less than 96 (four days sampling) indicate any probable cause in the comments section on the data sheet.
- Cap the four sample assemblies and remove them from the sampler.
- Re-wrap the assemblies in the bubble pack in which they were shipped, and place them with their data sheet into their shipping canister.
- Remove and unwrap the new sample assemblies and data sheet from their shipping canister, and insert the assemblies into the sampler in order (#'s 1-4 increasing from left to right).
- Turn the valve over the flow meter so that it points down so that the sample flows can be measured.
- Turn channel one on manually using the round switch on the upper left of the Z400 controller.
- With the sample assembly still capped check for leaks by noting the position of the black ball in the flow meter. If it is resting at the bottom of the tube put a check in the channel 1 leak check box, or if it is not record the ball height there.
- Remove the cap from the channel one sample assembly and record the height of the black ball and the reading of the vacuum gauge. If the black ball is at the top of the flow tube record the height of the silver ball and make a note of this in the comments section.
- Repeat the leak check and flow measurement for channels 2-4.
- Be sure that the round switches on the Z400 are in the AUTO position so the controller will function correctly during the week.
- Bypass the flow by returning the valve above it to the up position.
- Close the door and secure the roof to the sampler.
- Return the week's sample assemblies to MIT by U.S. Priority Mail.

Sampling continued until the end of July 1994 at Westfield, Willsboro, and Belleayre, and until January 1995 at Perch River and Moss Lake, for a total of 2,288 samples sent to the field. Of course, not all of the sample assemblies sent out were used successfully for a variety of reasons. General site problems were mostly related to weather problems and power outages. During the winter of 1993-1994 severe snow storms, mostly at Perch River and Moss Lake, caused several of the sites to be inaccessible on the day the samples were



to be changed which resulted in the #1 channel or Wednesday sample being run twice. Power outages could be confirmed by noting any shortage of hours sampled compared to the usual 96. The day of the outage was checked when possible using the flow chart recorder mounted in the dichotomous particulate sampler. Some of the sites had unusual but recurring problems. Perch River seemed to experience more site power outages than the other sites, and Belleayre had problems with water entering the electrical outlet which the sampler was plugged into and causing the outlet's ground fault sensor to trip (this was eventually fixed by re-routing the electrical line). The site operator at Westfield was ill for several weeks in the winter of 1993-1994, and the NYSDEC office there could not always find a replacement operator, so some of the sample changes were missed entirely during this period.

A few samples were missed due to problems with the samplers themselves. The electronic controller at Belleayre had a problem with its internal battery's connections shortly after it was installed; this was fixed easily but resulted in the loss of a full week's samples. The controller at Perch River had a problem with the relay for channel four which resulted in only three samples being collected for about four weeks while the problem was diagnosed and the complete sampler replaced (the relay was replaced by Tork under warranty). In July of 1993 some of the sample assemblies were sent out to the sites with the sorbent tube inserted upside-down (the author made all of the assemblies except for these due to a conference, a scheduled vacation, and a family illness that month). Though the operators were notified and instructed to reverse the sorbents, some of the upside-down ones were run. Of these a few had their charcoal blown out of the large open end of the tube (which is supposed to be the inlet), and some of this charcoal became stuck in the solenoid valves which prevented them from closing fully. This problem repaired itself as the charcoal became unstuck, but one of the valve assemblies in Westfield was replaced in the field by the site operator using a spare assembly because of a persistent leak of the solenoid valve.

Originally, audits of the flow meters were performed by personnel from the NYSDEC Air Quality Lab who routinely monitor the performance of all the NYSDEC sampling equipment. In the fall of 1992 it was decided that the ER&R lab should perform these audits instead, and so beginning in January of 1993 this was the case. The ER&R lab used the above mentioned Gilian Gilibrator™ airflow calibrator. This device is a primary standard,

optically timed bubble flow meter with three interchangeable flow cells enabling it to measure flows from 1 mL/min. up to 30 L/min. To be a primary standard measuring device, all values must be absolute, and measured as absolute (i.e. not derived). Volume is measured as the space within the flow chamber which is between the infra-red sensors, and time is measured as the elapsed duration for the bubble to pass between the sensors. Measurements using the Gilibrator are NIST traceable, and are accurate to within 0.5%. A dedicated thermal printer was connected to the calibrator to provide an immediate hard copy of the flow audits, showing the individual and average measurements. Generally ten flow measurements were performed on two different channels of the sampler by inserting a rubber stopper into the sample assembly's filter holder inlet, and connecting this to the outlet of the calibrator's flow chamber. The readings from the vacuum gauge and rotameter were noted for each channel tested, and the flow measurement determined by these was compared to that from the calibrator. In all cases the agreement was better than  $\pm 5\%$ , which was the initial accuracy quoted for the rotameters.

Site visits for flow audits were performed on a roughly quarterly basis, with visits to the Westfield site being less regular due to the travel distance involved. The time it took to perform the flow checks themselves was negligible; measurements for two mercury channels and the coarse and total flow of the dichotomous sampler could be finished in half an hour. Travel to, and between the sites however, often required the audits to be performed over a few days. Though this was a major effort relative to the added sampling quality assurance benefit, it was generally useful to visit the sites to check for other problems, perform minor preventive maintenance, and meet with the site operators. Among the minor operations which were performed during the visits were: checking the carbon rotor vanes in the vacuum pump for excessive wear (none was found); replacing the original vacuum gauges with calibrated units; and installing the elapsed hour meters (these were intentionally left out of the original design due to problems with the ones in the dichotomous samplers, but heavier duty meters were installed in the mercury samplers and these operated without any problems for the duration of the program).

#### 4. INSTRUMENTAL NEUTRON ACTIVATION ANALYSIS (INAA)

The use of neutron activation for elemental analysis relies on a few simple properties of neutrons, atomic nuclei, and gamma radiation. First, because neutrons are uncharged they are able to penetrate through both a considerable amount of bulk material, and the Coulombic field of the atom and the nucleus. Secondly, atomic nuclei have some probability of absorbing an extra neutron, especially when the neutrons are thermalized. In some of these cases the new nucleus is no longer stable and will undergo radioactive decay accompanied by the emission of characteristic gamma rays. Finally, because the energy of the gamma rays is rather large (from tens to a few thousand keV), they can be measured easily and, thanks to the high resolution of solid state detectors, the various energy gammas distinguished from one another. Because the production of activated nuclei is proportional to the amount of the parent nuclei in the sample so is the gamma emission rate. Thus, by measuring the various gamma rays emitted from a sample, its elemental composition can be determined.

As an analytical technique neutron activation has several very distinct advantages over other methods, though it also has a few very limiting disadvantages (Olmez, 1989). Among the advantages are:

- High sensitivity for a wide range of elements.
- Excellent selectivity among different elements.
- Virtually no matrix effects from self-absorption or enhancement.
- Fairly non-destructive nature of the analysis.
- Concentrations of many elements can be found from a single sample.
- Analysis is generally completely instrumental.
- Very few inter-element interferences.

The disadvantages are however significant:

- In general a major nuclear facility such as a research reactor is required.
- The initial cost for detection equipment is high (\$50,000-\$100,000).

- For most elements an analysis requires 2-3 weeks.
- Only elemental concentrations are obtained, not chemical composition.
- Elements lighter than Na (except F) as well as Si, Ni, and Pb can not be measured well.

It is probably the first of these limitations which restricts the use of neutron activation analysis to the nuclear reactor research centers at a few universities and national laboratories.

#### 4.1 Basic INAA Theory

The amount of activity of a given radio-isotope produced by neutron activation is a simple function of the properties of the isotope, its parent nuclide, and the spectrum and strength of the neutron irradiation. For a given parent nuclide the activity present in its activation product immediately after its irradiation is given by:

$$1. \quad A^\circ = \sigma\phi n\theta(1-\exp(-\lambda t_{\text{irr}}))$$

$A^\circ$  = activity at end of irradiation ( $s^{-1}$ )

$\sigma$  = neutron absorption cross section ( $cm^2$ )

$\phi$  = neutron flux ( $n \text{ cm}^{-2} \text{ s}^{-1}$ )

$\theta$  = isotopic abundance of given isotope

$n$  = number of atoms of parent element

$\lambda$  = decay constant of activation product ( $s^{-1}$ )

$t_{\text{irr}}$  = irradiation time (s)

Complicating matters somewhat is the fact that both the cross section and the neutron flux are functions of neutron energy, so that the proper expression

for their product is:  $\int_{E=0}^{\infty} \sigma(E)\phi(E)dE$ . Usually the number of atoms of the

parent element is more conveniently expressed as its weight  $w$ , in which case  $n$  should be replaced by  $wA/m$  where  $A$  is Avagadro's number,  $6.02 \times 10^{23}$ , and  $m$  is the element's atomic weight. The isotopic abundance of the

activable parent nuclide is included explicitly to show that not all isotopes of an element may activate, and because the isotope's abundance will influence the eventual activity produced. Because the gamma rays produced by the activation products are not typically counted immediately after irradiation, an additional factor of  $\exp(-\lambda t_{\text{cool}})$  is needed to account for the cooling time between the production and the detection of the products.

When one considers the order of magnitude of some of the parameters in equation 1, the need for a nuclear reactor to perform NAA becomes evident. Foremost among these is the neutron absorption cross section, which is routinely expressed in barns or  $10^{-24}$  cm<sup>2</sup>. In general the actual value for the cross section is on the order of a few or tens of barns, but even when it is a few thousand barns, a very small number of activations actually take place. To make up for the low probability of activation taking place the neutron flux needs to be as high as possible. However because the cross section is a function of neutron energy (with a typically inverse proportionality to the neutron velocity), it is not enough to simply have a lot of neutrons, they should also be low energy neutrons. Specifically for mercury (in its natural isotopic composition), the total cross section for thermal energy neutrons (those in thermal equilibrium at room temperature, 0.025 eV) is 380 barns, while above 10 eV it is on the order of 10 barns. Also, at low energy the cross section is largely due to capture, while at higher energies various scattering events predominate (Garber, 1976).

Further, nuclear reactions produced by fast neutrons produce activation products which can interfere with those produced by thermal neutrons. An example of this is the production of <sup>28</sup>Al from <sup>28</sup>Si when a fast neutron is captured and a proton emitted (standard notation for this is <sup>28</sup>Al (n,p) <sup>28</sup>Si). The product of this reaction is indistinguishable from the product of the thermal capture of a neutron by <sup>27</sup>Al, and complicates the determination of aluminum concentrations in a sample with silicon also present if the irradiation includes a large number of fast neutrons. Operationally, the ratio of thermal to higher energy neutrons in the spectrum of an irradiation facility is defined by the 'cadmium cutoff ratio'. Cadmium has an absorption cross section that drops off from 7500 barns at 0.5 eV to essentially zero at higher energies (Henry, 1986). The cadmium ratio is thus the neutron flux measured outside a cadmium foil over the flux measured within a such a foil.

These requirements are largely why reactors are much better neutron sources for NAA than accelerators which produce a small beam of high energy neutrons. Reactors generally produce and require a large number of thermal neutrons distributed over a fairly large space because the usual fission reaction's neutron cross section is also greatest at low energies, and reactor cores are usually at least a few feet in size. In this respect, the M. I. T. research reactor MITR-II is well suited for neutron activation due to its high available neutron flux and cadmium ratio. The irradiation facilities used for the elemental determinations in this work have a thermal flux of  $\approx 8 \times 10^{12}$  n/cm<sup>2</sup>s, with a cadmium ratio of 220.

Following irradiation, a gamma ray spectroscopic detector is needed to measure the induced activity of the sample. When gamma rays interact with matter there are three main processes which occur, and these are used to detect the radiation. At low energies (up to about 150 keV in a germanium crystal) photoelectric absorption is the primary type of interaction. This results in all of the gamma's energy being transferred to an electron which then comes to rest within the detector. The signal derived from this event has a narrow peak, the photopeak, at the full energy of the gamma ray, and at the energy of the X-rays which arise from the filling of the space left by the photoelectron. At intermediate gamma energies (between about 150 keV and 8 MeV in germanium), Compton scattering is the most likely mechanism for gamma ray absorption. This is an inelastic scattering of the gamma ray from an electron. Because not all of the gamma's energy is transferred to the electron, and because the scattered gamma ray may exit the detector without interacting again, the signal produced by Compton scattering covers a broad range of energies, from about 250 keV for 180° scattering of high energy gammas up to energies about 200 keV below the photoelectric peak (if the scattered gamma is absorbed within the detector then the signal is identical to the photopeak's). This broad Compton scattering signal is useless for spectroscopy, and the background it produces under low energy photopeaks is a major problem when samples containing high concentrations of high energy activation products (<sup>24</sup>Na being the most common) need to be analyzed for low energy peaks. The final type of interaction between gamma rays and matter is the production of an electron and a positron by the gamma ray and is called pair production. This requires a gamma energy of greater than  $2m_e c^2$  or 1,022 keV, and it becomes more likely than Compton scattering

in germanium at about 8 MeV. The positron will annihilate an electron in the detector immediately producing two 511 keV gamma rays, one or both of which may then escape the detector. If one escapes a peak at 511 keV below the photopeak will result, and if both escape a peak 1,022 keV below results. Figure 19 shows a schematic of a spectrum produced by the interaction of a fairly high energy gamma ray and a germanium detector.

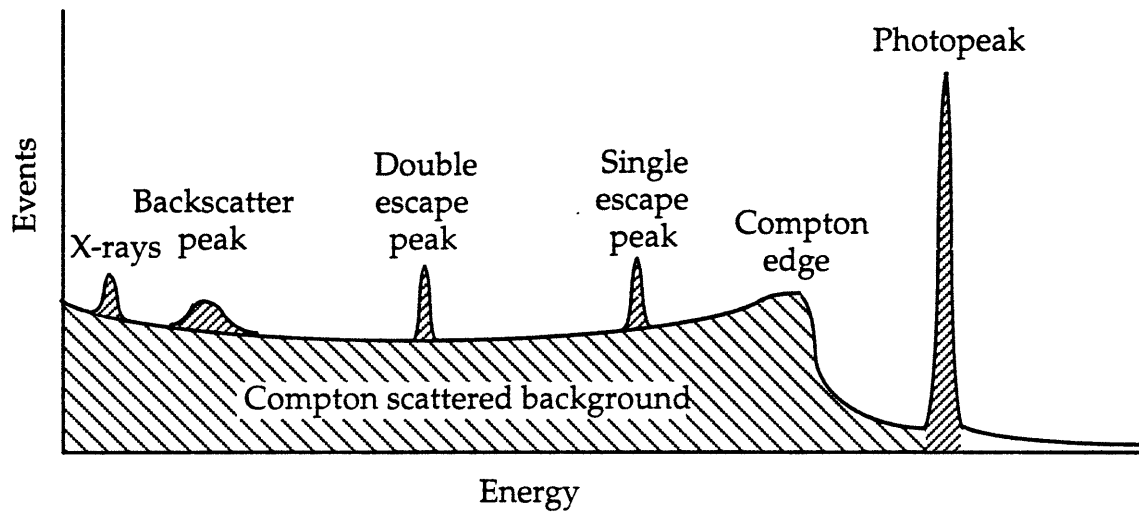


Figure 19. Schematic spectrum of single, high energy gamma ray source obtained using a germanium detector. The Compton scattered background is shown larger than it would actually be, the backscatter peak is due to 180° gamma backscatter, and the portion of the background between the Compton edge and the photopeak is due to multiple scattering. Also the narrow peaks are shown considerably wider than normal.

Currently NAA spectroscopy relies on the use of semi-conductor detectors, primarily made of high purity germanium (HPGe) or lithium doped germanium (GeLi). Electron-hole pairs are produced in these crystals in a number proportional to the absorbed gamma ray energy, with the pairs requiring about 3 electron volts to be formed. By applying a bias of a few thousand volts across the crystal the pairs can be collected and subsequently amplified to produce a measurable electronic pulse. The height of the pulse is proportional to the number of electron-hole pairs and thus to the original gamma ray energy. An energy spectrum is derived from these pulses by using an analog to digital converter (ADC), and a multi-channel analyzer (MCA)

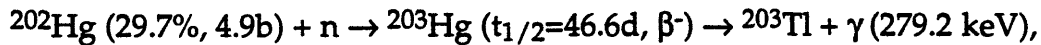
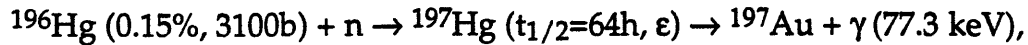
which totals all the gamma ray events which occur in specific energy bands over a period of time. More specifics concerning gamma ray spectroscopy as applied in this work will be discussed in section 4.2.

Semiconductor detectors however, were only first developed in the 1960's; they were initially both expensive and rare and were not commonly used for spectroscopy. In the 1980's methods for producing high purity germanium became available, and these rapidly became the standard detector for gamma spectroscopy. The most common detectors used before this time were scintillators made of sodium iodide crystals with a small amount of thallium added (NaI(Tl)). The scintillator was connected to a photomultiplier tube (PMT) which converted the light from the scintillator into an amplified electronic pulse which, again, had a height proportional to the original gamma energy absorbed. Scintillation events within the NaI(Tl) crystal require about 20 electron volts, and the number which are efficiently coupled to the PMT is typically from 20% - 30% (Knoll, 1989). Because the statistical nature of the signals from scintillator/PMT's or semiconductor detectors determines the width of the resulting spectral peaks, the lower number of signal events from a scintillation system means that it has much less energy resolution than a semiconductor device. For scintillation systems the peak width and thus the energy resolution is about 5% - 10% of the peak energy, while for semiconductor systems this value is usually about 1% or less. The lack of energy resolution from older NaI(Tl) detectors is not of direct consequence in this work, but it is relevant to how mercury was determined in the past using NAA.

#### **4.2 The Past Use of NAA for Mercury Determination**

Mercury measurements have been performed over the years in a wide variety of samples by neutron activation analysis using both scintillation (Kim, 1973; Olmez, 1975; and van der Sloot, 1976) and semiconductor gamma detectors (Germani, 1988; Milley, 1987; Olmez, 1989 and 1993b). Also two of mercury's seven naturally occurring isotopes,  $^{196}\text{Hg}$  and  $^{202}\text{Hg}$ , are suitable for NAA and depending on the circumstance both have been used. The relevant nuclear reactions are respectively:





The parent nuclides are shown with their isotopic abundance and thermal neutron capture cross section; the activated products show their half lives and decay type ( $\epsilon$  indicates electron capture and  $\beta^-$ , beta decay); the decay products are listed with the energy of the primary gamma ray. Though  $^{196}\text{Hg}$  is the least common of mercury's stable isotopes and  $^{202}\text{Hg}$  the most common, the difference in their cross sections results in  $^{197}\text{Hg}$  being produced 21.3 times more rapidly than  $^{203}\text{Hg}$ . Furthermore, the difference in their decay rates (which are equal to  $\ln 2/t_{1/2}$ ) means that immediately following irradiation there will be 372 times the activity from  $^{197}\text{Hg}$  compared to  $^{203}\text{Hg}$  (activity being equal to the number of atoms times the decay rate). Though it would seem that the use of  $^{197}\text{Hg}$  is obviously the better choice from these basic considerations, the use of  $^{203}\text{Hg}$  has some practical advantages in certain situations.

When the only available gamma detectors were NaI(Tl) crystals, the low energy resolution of these devices usually required that the activated mercury be separated from the sample matrix either chemically or by heating. The gamma peak from  $^{197}\text{Hg}$  at 77 keV was far more prominent than the  $^{203}\text{Hg}$  peak at 279 keV, but it was indistinguishable from the X-rays also produced near this energy. Some of these X-rays are produced when K electron shells of the  $^{197}\text{Hg}$  decay product  $^{197}\text{Au}$  are filled (these are at 65 and 68 keV), but some are from the decay of other heavy elements. Also, if any high energy gamma rays are present in the sample they may produce 75 keV X-rays in lead shielding surrounding the detectors due to the filling of holes left by photoelectrons. In these cases the peak at 279 keV can be used for corrections after the ratio of the two peaks has been determined from the irradiation and counting of pure mercury.

With the change from scintillators to semiconductor detectors, mercury analysis by neutron activation no longer required the chemical or physical separation of the mercury from the sample matrix. The far superior energy resolution of the newer detectors meant that the activated mercury's gamma peaks could be identified among the peaks from various other elements in the sample. This distinction is what allows current methods to

be called *Instrumental* NAA; all of the variables in the analysis are measured either absolutely or more often relatively. Without separating the mercury from the sample however, it is easier to use the 279 keV peak of  $^{203}\text{Hg}$  for analysis than the 77 keV peak of  $^{197}\text{Hg}$ . The reason for this can be seen in Figures 20-22, which are the actual spectrum of an atmospheric mercury sample on 100 mg of activated carbon. The sample is from Willsboro, taken on July 27, 1994, it was irradiated for six hours and counted for 17.4 hours (longer than the more usual six) one week after irradiation; the amount of mercury including the charcoal blank is  $5.39 \pm 0.26$  ng.

Figure 20 is the complete spectrum up to an energy of about 1850 keV, with some of the larger and more important peaks identified. The 77 keV peak of  $^{197}\text{Hg}$  is located right at the top of the Compton scattered background nestled among several other peaks, while the 279 keV peak of  $^{203}\text{Hg}$  is further down on the background hump and more isolated from other peaks.

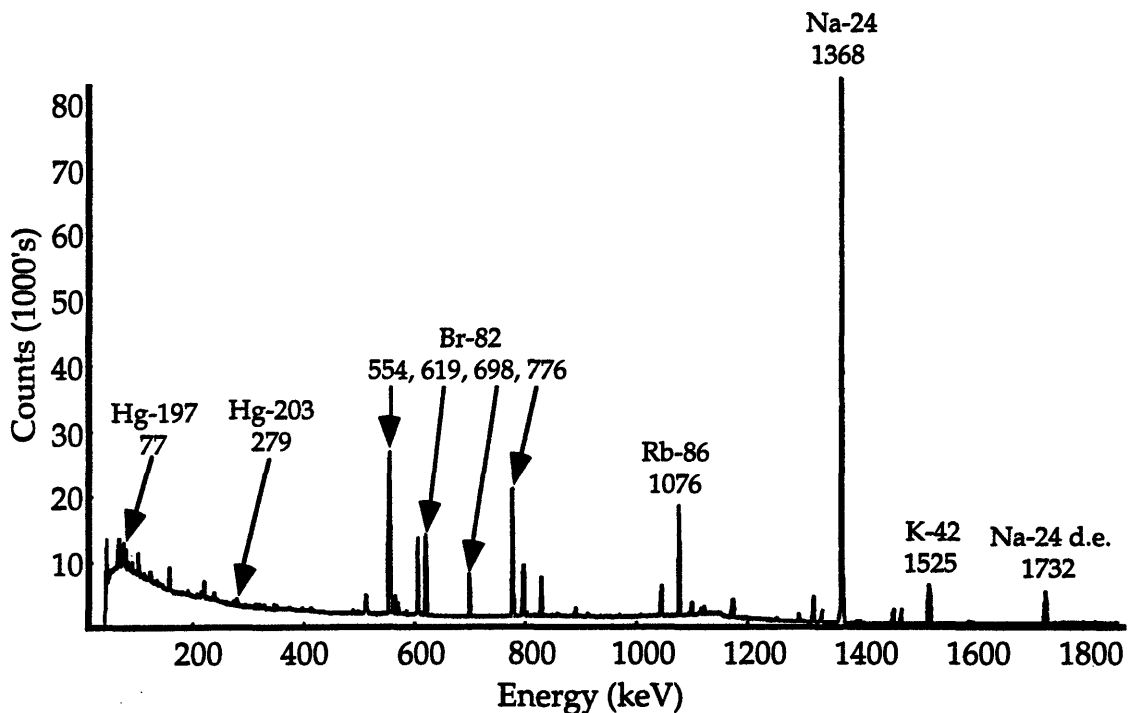


Figure 20. The full collected INAA spectrum of an atmospheric mercury sample on 100 mg of activated carbon with the mercury and other major peaks identified by nuclide and energy. The sample was irradiated for six hours and counted for 17.4 hours one week later.

Expanded views of these two regions are shown in the Figures 21 and 22 so the differences between the two can be seen more clearly. The first thing to note is that the background is 2.7 times higher in the 77 keV region compared to the 279 keV region. Because of the statistical nature of the counting, and the way in which the peak area is calculated, this gives rise to an increased error in the determination (this will be covered more fully below). The background is due to the presence of higher energy gamma rays emitted by  $^{24}\text{Na}$  and  $^{82}\text{Br}$ , among other isotopes. These two have half lives of 15 hours and 35 hours respectively, so it is possible to decrease the background by waiting for the decay of these before counting the sample. This is very useful when  $^{203}\text{Hg}$  is employed for mercury determination because its half life is 47 days, but the half life of  $^{197}\text{Hg}$  is only 65 hours so this technique, while helpful, can not be applied fully (the specifics of this delay in counting will be covered shortly).

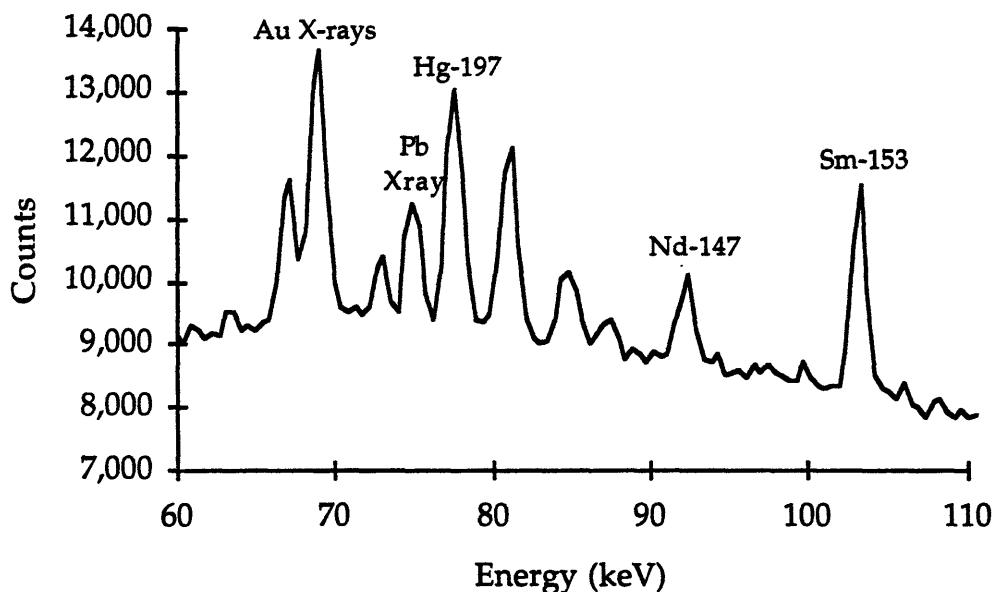


Figure 21. INAA spectrum of an atmospheric mercury sample on 100 mg charcoal, expanded around the 77 keV peak of  $^{197}\text{Hg}$ . Note the level of the background, and the proximity of the 75 keV X-ray due to the photoelectric effect in the lead shielding.

The second obvious difference between the two peak areas is the presence of several other peaks around 77 keV. The 75 keV Pb X-ray in particular, can cause the mercury signal to be obscured if care is not taken to reduce its presence, as was done here (this too will be discussed further). If the resolution of the detector is close to the 2.5 keV difference between these two peaks it may be necessary to 'strip' the X-ray from the collected spectrum in order to determine the area of the mercury peak. In Figure 21 the detector resolution as measured by the full-width at half-maximum (FWHM) of the mercury peak is 1.2 keV, and the two peaks are just separated at their bases. Older detectors with poorer resolution, or a larger X-ray peak would cause considerable difficulty in analysis. Because of the advantages in detection and counting of the peak at 279 keV, it has generally been used in the past as the primary peak for mercury analysis despite the fact that there is initially far more activity at 77 keV.

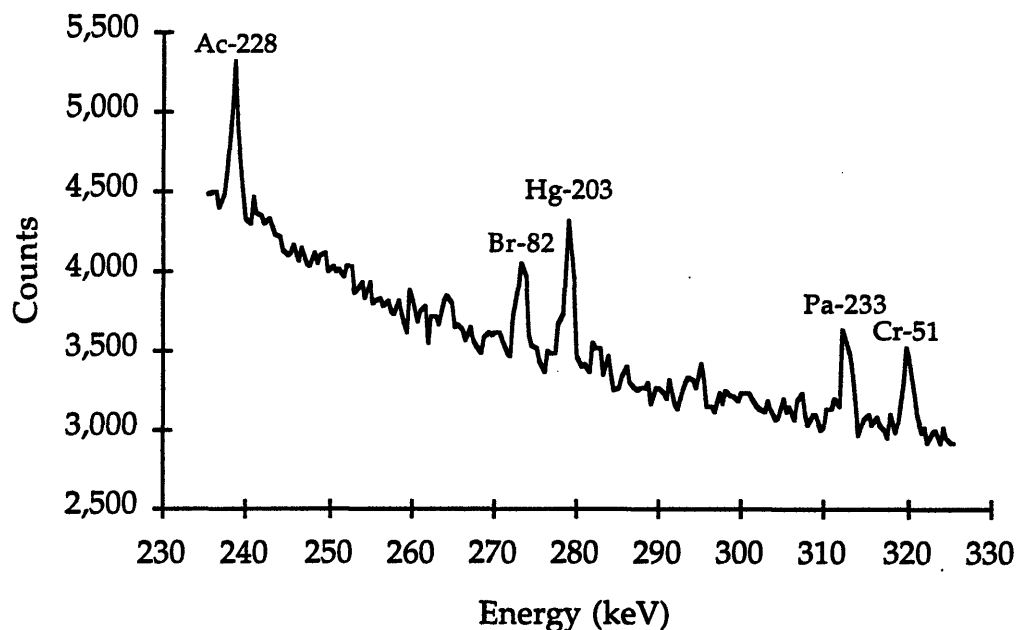


Figure 22. INAA spectrum of an atmospheric mercury sample on 100 mg charcoal, expanded around the 279 keV peak of  $^{203}\text{Hg}$ . Note the lower background compared to Figure 22.

Unfortunately, there is a further complication in performing mercury analysis by using the 279 keV peak, and this is the problem of spectral interference from the decay of  $^{75}\text{Se}$  which also emits a gamma ray at this energy. Such interferences are not uncommon in INAA and the method for correcting for them is rather straightforward. In the case of  $^{75}\text{Se}$ , a second gamma ray emitted at 264 keV allows the contribution of  $^{75}\text{Se}$  to the peak at 279 keV be separated from  $^{203}\text{Hg}$ 's contribution because the emission ratio of the two gamma rays is constant and well known. However, this is again complicated by spectral interference at 264 keV from  $^{182}\text{Ta}$ , so a second correction is required generally using another  $^{182}\text{Ta}$  peak at 1221 keV. To perform the correction explicitly requires the measurement of three peaks, the detector efficiency at those energies, and the knowledge of the branching ratios of the different gamma ray emissions from  $^{75}\text{Se}$  and  $^{182}\text{Ta}$ :

$$2. \quad 279(\text{Hg}) = 279(\text{tot}) - \left\{ 264(\text{tot}) - 1221(\text{tot}) \left( \frac{\% \text{Ta@264}}{\% \text{Ta@1221}} \right) \left( \frac{\text{eff@264}}{\text{eff@1221}} \right) \right\} \times \left( \frac{\% \text{Se@279}}{\% \text{Se@264}} \right) \left( \frac{\text{eff@279}}{\text{eff@264}} \right)$$

where:

$279(\text{Hg})$  = the area at 279 keV due to  $^{203}\text{Hg}$

$279(\text{tot})$  = the area at 279 keV due to  $^{203}\text{Hg}$  and  $^{75}\text{Se}$

$\% \text{Ta@264}$  = branching ratio of  $^{182}\text{Ta}$  at 264 keV

$\text{eff@264}$  = detector efficiency at 264 keV

Of course, actually performing this correction can be very problematic because when one calculates a figure using so many measurements, the cumulative error can get to be rather large. If  $\sigma(x)$ , the statistical error of the measurement is taken to be the square root of the number of counts, then:

$$3. \quad \sigma(279(\text{Hg})) = \left\{ \sigma^2(279(\text{tot})) + 264(\text{tot}) \left[ \left( \frac{\sigma(264(\text{tot}))}{264(\text{tot})} \right)^2 + 1221(\text{tot}) \left[ \left( \frac{\sigma(1221(\text{tot}))}{1221(\text{tot})} \right)^2 + \left( \frac{\sigma(\% \text{Ta@264})}{\% \text{Ta@1221}} \right)^2 + \left( \frac{\sigma(\text{eff@264})}{\text{eff@1221}} \right)^2 \right] \right] + \left( \sigma \left( \frac{\% \text{Se@279}}{\% \text{Se@264}} \right) \right)^2 + \left( \sigma \left( \frac{\text{eff@279}}{\text{eff@264}} \right) \right)^2 \right\}^{1/2}$$

Taking the uncertainty in the branching ratios as 2%, the uncertainty in detector efficiency as 5%, and using the measured efficiency ratio between 264 keV and 1221 keV, the correction becomes:

$$4. \quad 279(\text{Hg}) = 279(\text{tot}) - 0.42 \times 264(\text{tot}) + 0.24 \times 1221(\text{tot})$$

with a calculated counting error of:

$$5. \quad \sigma(279(\text{Hg})) = \left\{ \sigma^2(279(\text{tot})) + 264(\text{tot}) \left[ \left( \frac{\sigma(264(\text{tot}))}{264(\text{tot})} \right)^2 + 1221(\text{tot}) \left[ \left( \frac{\sigma(1221(\text{tot}))}{1221(\text{tot})} \right) + 0.029 \right]^2 + 0.0004 \right] \right\}^{1/2}$$

The actual magnitude of the correction and the associated cumulative error is of course dependent on the relative concentrations of mercury, selenium, and tantalum in the sample. By using the measured values for these from a small assortment of samples, the fact that negative concentrations and errors greater than 100% can result, is evident. This is shown in Table 6. When the 264 keV and 279 keV areas are comparable (part. sample 1 and soil) the correction compares well with the determination from 77 keV though the error is much larger. The other examples show determinations from 279 keV both under and over the 77 keV figures as well as negative values.

These spectroscopic difficulties in using INAA for mercury determinations are compounded somewhat by an operational difficulty at almost every reactor where INAA is performed. Because mercury is volatile and can exist as a permeable, elemental gas it can be easily lost from the sample especially if any heating occurs. Though this is a problem in some other analytical methods, it is difficult to avoid in INAA because most reactor's irradiation facilities operate at elevated temperatures. The solution employed at all the reactors used in the above referenced measurements (other than those from this lab) is to encapsulate the samples in quartz. This contains the mercury, while also adding negligibly to the blank value. Quartz is required instead of glass due to the excessive heating which would result from the high cross section for the (n, $\alpha$ ) reaction of the boron found in ordinary glass. While this solves the problem, quartz encapsulation is time consuming and expensive. The expense arises from the need to use large

	279 keV Area	264 keV Area	1221 keV Area	Hg Area in 279 keV	ppb Hg 279 keV uncor- rected	ppb Hg 279 keV cor- rected	ppb Hg by 77 keV
Vapor Sample	81,855 ±2100	183,741 ±36,870	7036 ±1575	4378 ±112	2020 ±52	157 ±785	29 ±5
Part. Sample 1	1094 ±182	1862 ±292	0	292 ±63	0.186 ±0.039	0.053 ±0.132	0.045 ±0.011
Part. Sample 2	1288 ±129	3120 ±160	0	-22 ±166	223 ±22	-127 ±958	0.014 ±0.003
Soil	8134 ±625	2646 ±1001	2094 ±509	7492 ±571	2090 ±160	1822 ±542	1610 ±64
Coal	2586 310	3498 ±350	657 ±139	1235 ±148	555 ±67	123 ±213	338 ±60

Table 6. Sample corrections for spectral interferences when using 279 keV for mercury determinations. Areas are in counts under peak, ppb figures include sample weight (the vapor sample weight is the charcoal weight) or volume (particulate samples are in m<sup>3</sup> of air on Teflon filters).

enough quartz tubes so that in the process of sealing them, the samples are not melted or burned (quartz's softening point is 1665°C and sealing it requires an oxygen torch). Because the containers used for irradiation are usually small in size, the irradiation of many quartz encapsulated samples could become prohibitively expensive.

#### 4.3 The Optimization of INAA for Mercury Determination

The above mentioned difficulties and limitations of mercury analysis by NAA were well known, and were partly the reason that mercury was not originally included in the "Atmospheric Particulates in Upstate New York" proposal as mentioned in section 1.2. However, each of these problems have been addressed and been eliminated or reduced. This has resulted in the

ability to routinely measure nanogram levels of mercury in charcoal sorbents, and sub-nanogram levels on Teflon filters. It was first decided to use the 77 keV gamma ray emitted by  $^{197}\text{Hg}$  which, despite its drawbacks, offers the possibility for more sensitive measurements. Then, several steps were taken to optimize the counting set up and procedures for the detection of this peak. Because the samples were only to be analyzed for mercury, fewer compromises were required than is normally the case when the analytical needs for several elements need to be taken into account.

Reduction of the 75 keV lead X-rays was done using the standard technique of lining the lead shielding with materials of lower atomic number. This works by absorbing the low energy X-rays from the lead in the liners which themselves produce much lower energy X-rays in their interaction with the high energy gammas (X-ray energy is proportional to  $Z^2$ ). A four inch outer diameter, 1/8 inch thick aluminum tube was slid over the detector, but inside the lead shielding. This reduced the X-ray peak by about 40%, so a second liner of 1/8 inch thick rolled copper sheet was added outside of the aluminum which resulted in a total reduction of about 80%. Figure 23 is a composite of several collected spectra showing this reduction. The X-ray peaks were produced using a one micro-Curie  $^{60}\text{Co}$  source (primary gamma rays at 1173 and 1332 keV) so that the liners could be tested in a short period of time. The 77 keV peak is from an activated charcoal sample which had a similar size X-ray peak to the one shown with no liner. A schematic of the shielding, liners, high energy gammas, X-rays, and the detector is shown in Figure 24. Copper is used as an outer liner because its high density ( $8.9 \text{ g/cm}^3$ ) provides good low Z X-ray shielding, and aluminum is used as an inner liner because of its very low Z and because it matches the material of the detector's housing so it does not present a new material in the system. The characteristic X-rays from these materials are in the range of a few keV so they do not even penetrate the detector's housing.

The other adjustment to the procedures needed to improve the counting sensitivity at 77 keV was to try to reduce the Compton scattering background. Because the majority of this background comes from activated sodium, a large effort was put into finding a low sodium charcoal as described in Section 3.3. After selecting a charcoal for collection (or when a source sample such as coal or oil are to be counted) the problem of the background can be dealt with by allowing the sodium to decay somewhat before counting



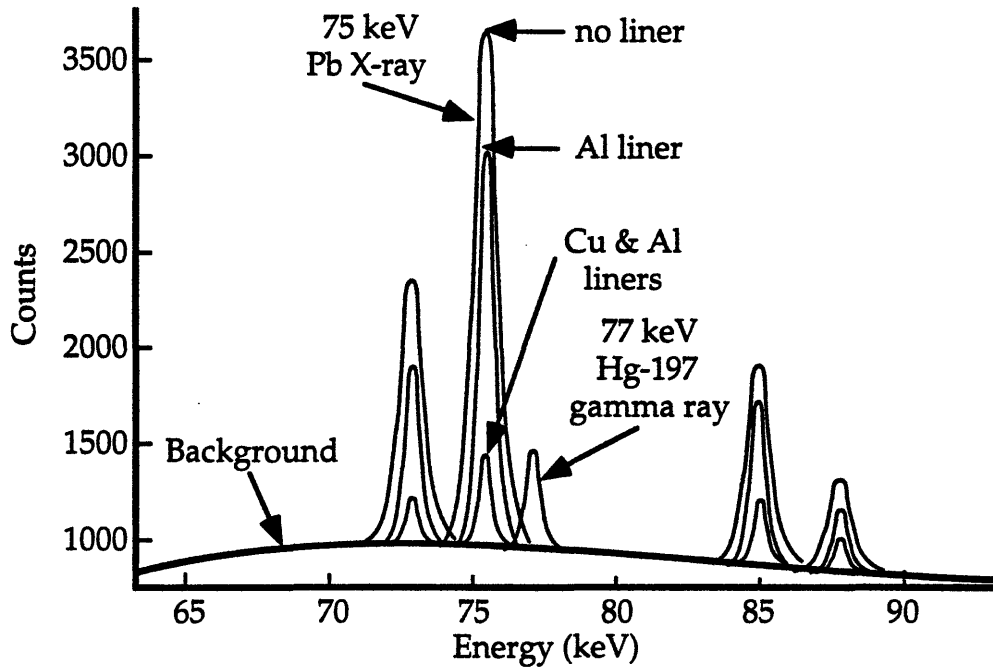


Figure 23. Composite spectrum showing reduction of lead X-rays by lining detector's shielding. The liners are each 1/8 inch thick, between the detector and shielding, with the aluminum inside the copper.

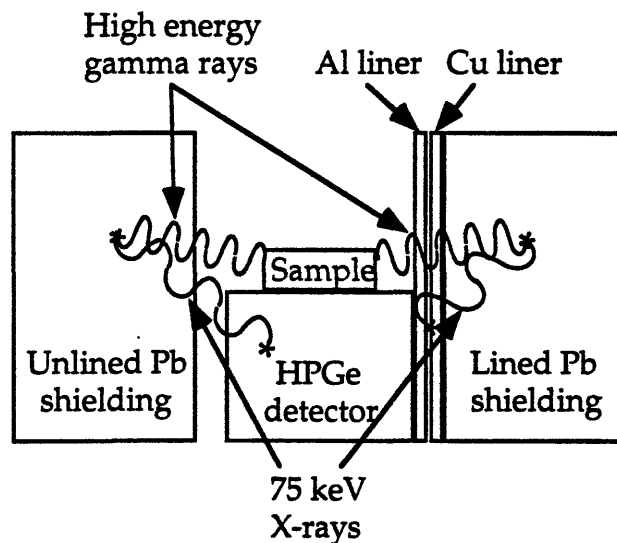


Figure 24. Schematic diagram of aluminum and copper shielding liners used to reduce lead X-rays at the detector. The liners are each 1/8 inch thick. On the left X-rays from unlined lead shielding reaches the detector, while on the right the lining is shown attenuating the X-rays.

the sample. This is also a standard technique to improve the counting of long-lived samples, but in the case of  $^{197}\text{Hg}$  it needs to be done with some care. Activated  $^{24}\text{Na}$  has a half life of 15 hours, and  $^{197}\text{Hg}$  has a half life of 64 hours, so a balance must necessarily be struck between waiting long enough to reduce the sodium background but not too long to affect the mercury peak. In order to determine the optimum decay time, typical mercury, sodium, bromine, and rubidium peak heights were inserted in a spread sheet and used to calculate the background height under the 77 keV mercury peak as a function of time. The calculation takes into account the half lives of the isotopes and the peak to Compton ratio, which is a measured property of how well a detector collects full energy peaks relative to partial energy scattered collection. The percent net error in the peak area determination is then calculated using Equation 6, the method employed by the Canberra analysis software (Canberra, 1991), the peak and background areas are shown schematically in Figure 25.

$$6. \quad \% \text{ error} = \frac{\sigma(A)}{A} = \frac{[A + Bk(1 + \frac{n}{2})]^{1/2}}{A}$$

$\sigma$  = the standard deviation of the peak area

$A$  = the peak area

$Bk$  = the background area under the peak

$n$  = the number of channels used in the two areas (nine in Figure 26)

By examining the equation for percent error it can be seen that without the background the error is inversely proportional to the square root of the peak area. However because the background is not Gaussian, its area is affected by the errors inherent in the number of counts at its endpoints, and so the size of the background to be subtracted from the total counts (background plus peak counts) greatly affects the accuracy of the peak determination. It should also be noted that the narrower the peak, the more accurately it can be measured. The results of the error calculation as a function of sample decay time are shown in Figure 26. From this figure it is clear that allowing the sample to cool between three and eight days is sufficient to reduce the background from  $^{24}\text{Na}$ , but after this time the decay of  $^{197}\text{Hg}$  causes an increase in the error due to a smaller peak size.

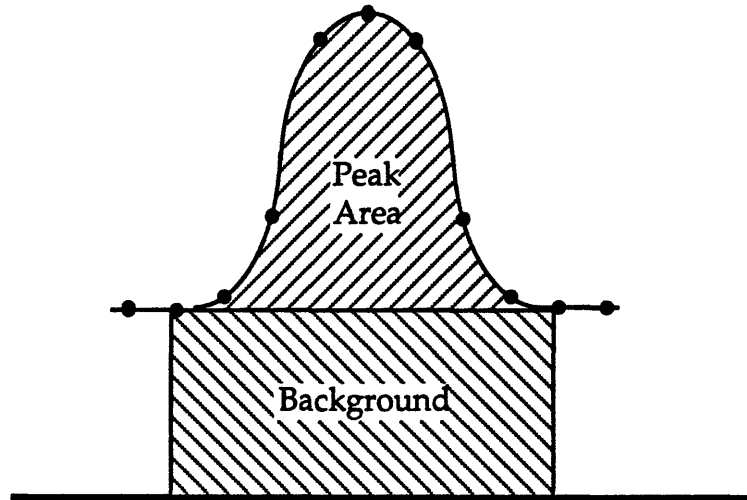


Figure 25. A schematic of the peak and background areas used in a gamma spectrum. The points do not generally fall exactly on a Gaussian curve as shown, and in calculating the background height the counts in three channels at the limits of the peak are averaged. Also if the counts at the limits are not equal the background will be trapezoid shaped.

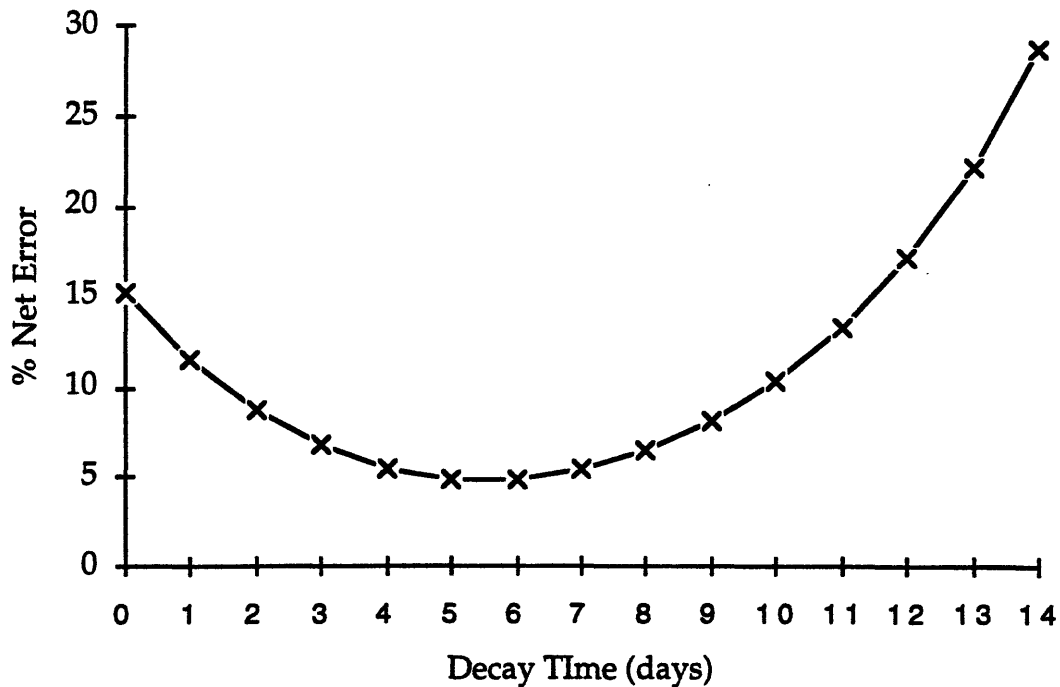


Figure 26. Calculated error of 77 keV peak determination as a function of cooling time of an atmospheric mercury sample on 100 mg charcoal.

#### 4.4 Analytical Difficulties

The improvements in detection of mercury by INAA mentioned above were sufficient to allow its routine use at levels down to 0.1 nanograms of mercury on Teflon filters and one nanogram in charcoal with a standard deviation of 5 - 10%. However, some of the particular procedures used in the early measurements of mercury in charcoals pointed out some rather unexpected and peculiar difficulties in performing the analysis.

Through 1992 and until March 1993, when charcoals were analyzed for mercury blank values by INAA in this lab the values obtained were considerably higher than those found in other labs using different procedures. Specifically, our results showed blank mercury levels in commercially available charcoal sorbent tubes to be in the range of a few hundred ppb by weight (nanograms per gram), while others reported values more on the order of a few to tens of ppb. This was thought to be evidence that the other techniques were losing the mercury which was tightly bound within the charcoal because they required the digestion or evolution by heating of the mercury from the charcoal, whereas INAA could detect all the mercury within the charcoal's volume. Because the blank values were subtracted from measurements of collected mercury, so long as the same techniques were applied this discrepancy had no effect on the final analyses other than the fact that a much larger blank had to be subtracted when using INAA.

In March of 1993, the National Institute of Standards and Technology (NIST) set up an inter-laboratory comparison for the determination of mercury in charcoal sorbents. NIST was going to do INAA determinations of their own using the National Bureau of Standards (NBS, NIST's former name) reactor which, because of the temperature in the irradiation facility, required them to quartz encapsulate the samples. They therefore requested that we also quartz encapsulate some of our samples in addition to using our standard procedures which was to simply seal the samples into polyethylene bags. The result of our analysis was that the samples which were quartz encapsulated showed an average of 10 ppb mercury while those packaged only in polyethylene bags showed an average of 180 ppb. Mercury contamination during sampling and handling in the lab has been a major concern in the analysis of environmental samples, and would normally be the suspected cause of this discrepancy. However, the quartz and plastic packaging and the

post-irradiation handling were performed completely in parallel; the low concentrations measured in the quartz encapsulated charcoals indicated that the charcoal was somehow absorbing mercury during the irradiation. The quartz encapsulation in these tests was in fact keeping mercury out of the sample rather than keeping it in as is its usual role during irradiation for INAA.

It was known that volatilized mercury could diffuse through the polyethylene bags which were used to package the samples; this had been tested in March 1992 using particulate samples to show that no mercury loss from the samples occurred. When no difference was found between the mercury measured in quartz and plastic packaged particulate samples it was decided that the mercury was sufficiently bound to the sampling matrix that quartz encapsulation was not necessary to prevent its loss. In light of these new findings tests were needed to show where the mercury might be coming from, and how to seal the samples to prevent contamination during the irradiation. Four rabbits were irradiated containing an assortment of charcoal, mercury standards, and empty polyethylene bags and vials, using inside containers of the same bags and vials, as well as quartz and aluminum foil and thin walled tubing which was crimped shut.

The results indicated that mercury was being lost from the standards and from the bags themselves, diffusing through the bags, and being absorbed by the charcoal. The clearest evidence for the first type of contamination came from sealing both some loose charcoal and a bagged mercury standard inside a quartz tube. The charcoal from this test contained 560 ppb mercury, well over any previous levels. Though the amount coming from individual bags was not nearly as much, the total mass of the bags in a typical rabbit was about six grams compared to about 15 milligrams of standard. The samples irradiated in polyethylene vials contained no more mercury than those encapsulated in quartz. Interestingly, the charcoal which was packaged directly in aluminum foil or tubing, showed higher levels still, indicating that some mercury was being released by the aluminum during irradiation.

The new method for packaging samples for mercury analysis was then established: heat sealing the samples into acid cleaned polyethylene vials. The reason the charcoal does not absorb mercury from these directly is perhaps because of a difference in the manufacturing processes between the bags and the vials. The difference in processes was confirmed in a phone

conversation with an engineer at du Pont who further mentioned that a coating is often applied to the inside of polyethylene bags to keep the inside surfaces from sticking together, but who was unsure whether either of these would cause a difference in the amount or properties of the mercury within the products. Mercury concentrations in the bags and vials as measured by INAA with quartz encapsulation are both about 5 ppb, so the difference must have to do with the location or the mobility of the mercury. Also there is no mechanical pressure between the charcoal and the vials, while the bags of charcoal are usually pressed together inside the rabbit, so the charcoal may be abrading the bag. Other workers in the field have reported that snow samples packed into zip-lock bags were often contaminated with mercury (snow crystals are rather sharp on a small scale). Finally, the vials are thick enough that any mercury volatilized from the standards or from anything else in the rabbit will not diffuse through the plastic and be absorbed by the charcoal.

To further ensure that mercury from the standards would not contaminate the samples, the two weighed standards in single polyethylene bags were to be sealed into a quartz tube for irradiation. The mercury concentration in the standards is 106 ppm, and they typically weigh 5 mg each, so they contain a total of about one microgram of mercury or 200 times the amount in each sample. Even a small amount of mercury lost by the standards could easily contaminate the samples without measurably affecting the standard's own concentration. Though the Teflon® filters used for aerosol sampling never had this contamination problem, possibly because the Teflon does not absorb the volatilized mercury as the charcoal does, after these tests the Teflon samples were all packaged in polyethylene vials for irradiation.

One of the reasons contamination within the lab was not considered as a likely cause for the original problem (though it was seriously investigated anyway) was that the samples were showing very consistent concentrations. If the excess mercury was a result of improper handling the mercury values would vary widely. Instead the measured mercury concentrations varied very little because the irradiations were performed in a consistent manner, with the same number of samples and bags, and approximately the same amount of standard in each rabbit. For this reason, the results obtained during the period when the charcoal was packaged in bags are still valid. The same amount of mercury was absorbed by the atmospheric samples and the

blanks so that when the blank value was subtracted from the sample value the absolute error was zero.

#### **4.5 The Analytical Methodology for Mercury Determination by INAA**

Because the development of an analytical methodology has been a major part of this thesis' work, and because some of the specific procedures have been developed by trial and error, an explicit, annotated, step-by-step description of the methodology will be given here as documentation (it may be passed over without loss of continuity). This is not to imply that this is the final or optimum set of procedures; improvements have been considered and on occasion implemented. However, environmental monitoring in general, and mercury measurement in particular relies on the consistency of the procedures used. This ensures that the results obtained will be of a predictable quality, and that when problems arise that they can be identified and corrected (as can be seen in the past discussions of collection and analytical problems in this project). It is for these reasons that the analysis has been performed largely in the same way by the author with the help of one technician for two years, that the procedures have not been altered since the packaging changes described above were initiated, and that they are being described in such detail here. If a problem with the analysis becomes evident at some future date, then this account may enable a quicker and more complete solution.

##### **A. Sample receiving and storage**

The sample assemblies are received from the field sites once a week, packed in re-usable cardboard and steel shipping canisters. They include four particulate filters in their holders, four charcoal sorbent tubes with automatic shut-off quick connects, and a sampler data sheet for that week (shown in Appendix A). After receiving the samples from the field, they are unpacked from their canister and prepared for storage as follows:

1. The sampler data sheet is checked for any unusual occurrences, problems in the field, or requests from the site operators, and it is

then punched and placed in a three-ring binder for the sampling site.

2. A sampling label which matches the field label on the filter holder is attached to the sorbent tube to identify the sample's location and date (e.g. ML930727M indicates a sample from Moss Lake, taken on July 27, 1993, the M is to identify it as a vapor phase mercury sample).
3. The sorbent tube is removed from the assembly and capped on both ends using 7/32 inch end caps obtained from SKC Inc. These caps are slightly undersized but can be pushed onto the Teflon sorbent tubes to provide a very tight seal. They are made of polyethylene and conform to NIOSH standards for sorbent tube sealing (SKC, 1992).
4. All of the sorbent tubes from a particular week (twenty total) are placed into a labeled zip-lock bag and stored at room temperature.
5. The Teflon particulate filters are removed from their holders and put into sterile 50 mm Petri dishes which are labeled with the sample's date and location but with the suffix MP instead of M to identify them as particulate mercury samples (e.g. ML930727MP). These are also stored at room temperature.
6. The quick connect fittings, filter holders, and silicone connecting tubing are inspected, stored in zip-lock bags and then re-used for the next batch of sample assemblies to be shipped to the field sites.

This method of storing the charcoal sorbents has been shown to have no effect on the measured mercury concentrations. Samples which were analyzed shortly after being received and those obtained at the same site and the same week but analyzed two years later showed no significant difference in concentration. In fact, early tests to try to reduce the amount of mercury in the charcoals (when the blank values were being incorrectly measured as hundreds of ppb) indicated that even at 400°C mercury was not lost from the charcoal. Mercury absorption by the filter holder, filter backing, Teflon sorbent tube, and the foam and glass wool packings have been checked using radioactive mercury tracers, and found to be negligible.



## **B. Preparing the charcoal sorbent for irradiation**

1. Irradiation vials are made from Fisher Scientific 1 mL polyethylene sample vials (part number 03-338-1A). These are 1-1/4 inches long and 5/16 inch outside diameter with an attached snap in cap. The caps are cut off and the vials are cut down to 3/4 inch so that three layers can be stacked into a rabbit. The vials and caps are then washed in 20% nitric acid for two hours, rinsed four times with de-ionized water, and dried in a Class 100 laminar flow clean hood.
2. Fifteen charcoal samples (usually three from each site for a given week or one from each site for three weeks) are placed in the clean hood with cleaned vials and caps. The vials are labeled on two sides with the sample identification number (sometimes abbreviated on one side so that it is easier to read later) using a permanent extra fine point Sharpie® marker.
3. The end caps of one sorbent tube are removed and the front plug is picked out using a fine point stainless steel tweezers. The corresponding vial is then placed over the open end of the sorbent tube (these two parts fit together snugly).
4. Turning the vial and tube over and rapping sharply on the tube with the tweezers' handle (for example) causes most of the charcoal to fall into the vial. If further rapping does not make the last charcoal pieces fall, a 1/16 inch stainless steel rod can be inserted into the back end of the tube which pushes the charcoal out using the back plug.
5. Small amounts of the charcoal which stick to the inside of the tube are held by static cling so it does not take much to make them fall. The stainless steel tweezers and rod only need touch the tubes end plugs, not the charcoal itself.
6. The empty sample tube is removed from the vial, and the vial's cap is pressed in place.
7. After all the charcoal samples are in their labeled vials the caps are heat sealed shut using a 90 Watt soldering iron with a heavy inverted cone tip.

8. The vials are then individually sealed into 1 inch by 2 inch polyethylene bags to keep the vials labels from rubbing off and as a secondary containment.

The process of transferring the sample from the tubes to the vials in steps 3 and 4 above takes only about 30 seconds at most. This is an important consideration in evaluating the likelihood of mercury contamination when comparing this methodology with others for mercury determination. Not only do other methods usually require longer exposure of the sample to the laboratory's environment, but also require more direct handling of the sample for chemical or physical removal of the mercury. By irradiating only fifteen field samples at a time it is easier to keep track of them. Also because a total of eighteen vials can fit into a rabbit with along with two mercury standards sealed in a quartz tube, it allows the routine analysis of lab or sample blanks in parallel with actual samples.

Each rabbit sent for irradiation contains two mercury standards to comparatively calculate the amount of mercury in the charcoal samples. The reference material is the National Institute of Standards and Technology's RM 8408 "Mercury in Tennessee River Sediments". It is a fine sediment (smaller than 100 mesh or 0.15 mm) from the East Fork Poplar Creek which passes through the city of Oak Ridge Tennessee and most of the mercury present in it is due to mercury discharges from the Oak Ridge National Laboratory (namely the Y-12 plant) in the 1950's and 1960's. Reference material 8408 has a mercury concentration of  $107 \pm 2 \mu\text{g/g}$  as determined by NIST using CVAAS and INAA with SRM 2704 Buffalo River Sediment as a control. These are packaged for irradiation as follows:

### **C. Preparation of the standards and the rabbit for irradiation**

1. Small polyethylene bags (one inch by about 5/8 inch) are washed in 10% nitric acid for two hours, rinsed in de-ionized water four times and dried in a Class 100 laminar flow clean hood.
2. Between 5 mg and 10 mg of RM 8408 are placed in a bag and weighed using an electronic balance with 0.01 mg resolution. After recording the weight, the bag is then heat sealed shut and sealed into a second bag which is labeled with the standard's number. All

of the standard handling takes place in the above mentioned hood, and is generally done in batches of 20 to 40 standards well ahead of the time the samples are prepared, and are stored in a labeled zip-lock bag.

3. The weight and standard number is recorded in a notebook for future reference. The number identifies the type of standard, the year, and a sequential ID (e.g. HG94076).
4. After the samples are prepared as above two standards are taken out from storage to go into the rabbit.
5. Quartz tubing used for the encapsulation of the standards is 5 mm inside diameter by 7 mm outside, and is purchased in four foot lengths from Quartz Plus of Concord MA.
6. A six inch length of quartz is broken off after scoring with a file. Using a torch supplied with laboratory gas and oxygen the center of the tube is heated to white hot and then pulled apart to form two tubes with closed ends. The ends are then rounded by heating and allowing the sharp point to shorten and blunt.
7. After cooling, the tube is labeled on two sides at the closed end with the numbers of the two standards using a permanent marker.
8. The outer, labeled bag of the standards is cut open, and using a Teflon tweezers the standard removed, folded, and inserted into the open end of the quartz tube. It is then pushed down to the tube's bottom using an aluminum rod. The second standard is then also inserted but is only pushed down to about 1/2 inch from the first.
9. The open end of the tube is then heated over the torch and joined to another piece of quartz which has been pointed. This piece needs to join the one with the standards on two sides without closing off the end.
- 10 After cooling briefly the side with the standards in it is heated just below the joint and the two pieces are pulled apart sealing off the tube. The end is then rounded off as in step 6.
- 11 The identification numbers should be checked to be sure they have not rubbed off, and then after cooling the tube should be heat sealed into a polyethylene bag, also with the standards' numbers on it.

Working with the quartz is not difficult, though a bit of practice is advisable if one is not familiar with it. The sealed tube needs to be short enough to fit inside the rabbit which is 3-1/2 inches deep, but not so short that the polyethylene bags that the standards are in would melt during the work. Being able to perform the sealing quickly also helps prevent melting and by holding the tube at about the same place as the upper standard it is easy to tell if it is getting too hot. The ends need to be rounded to prevent them from breaking when the rabbit is shut or when it strikes the stops at the ends of the irradiation facility pneumatic system. Rounding the sealed end should not be done too fast to avoid local overheating which could cause a small bubble to form and pop open the tube. There needs to be some space between the standards in the tube to make it easier to remove them after irradiation.

The samples and standards are then packed into an irradiation rabbit by putting up to six samples in three layers around the standard which fits in the center of the rabbit. Thin pieces of closed cell polyethylene foam at the inside ends of the rabbit help keep the quartz from breaking (and if there are only a few samples in the rabbit for some reason, this keeps them in place). The end of the rabbit is then screwed shut and it is labeled to identify our lab group and the set of samples inside (e.g. OLMEZ HGJUL3). To irradiate a set of samples in a rabbit an MITR Irradiation Information for Approved Samples form (typically refereed to as a "Part I") must be completed which includes:

**D. Irradiation request form information**

1. Desired irradiation facility; the pneumatic tube for irradiations in the reactor's graphite reflector is referred to as 1PH1 but there are actually three equivalent locations in the reactor that can be used.
2. Sample material; usually just "charcoal" but other sample types in the rabbit must also be identified.
3. Sample weight; this is net weight, not including packaging.
4. Desired irradiation date and time; charcoal samples are irradiated for six hours, and the time is based on a reactor power of 4.9 MW so at lower power the actual time may be longer.
5. Radionuclides and calculated initial activities; because of the wide range of nuclides produced this is listed as various, with  $^{24}\text{Na}$  given

as the major source of activity. After six hours 1.5 g of charcoal has  $\approx 0.5$  mCi of sodium activity.

6. Decay time is given as anywhere from three to six days depending on the reactor and the counting schedules.

This form is given to Reactor Operations along with the rabbit. The information is transferred to a Part II Irradiation information Form and signed by the appropriate operations staff member. The rabbit is sent into the reactor from the hot cell in the reactor basement and is automatically ejected back to this cell after the set irradiation time. As mentioned above the thermal neutron flux received by the rabbit is about  $8 \times 10^{12}$  n/cm<sup>2</sup>s with a cadmium ratio of 220. Before the rabbit is delivered back to the lab it is measured for activity and contamination and then sent through the pneumatic system to the hot lab, or brought up in a small tin can.

The samples then need to be repackaged before they are counted so that the activated mercury present in the bags and vials does not contribute to the measurement. All the work with irradiated samples is performed in the hood in NW12-207 which is equipped with a two inch lead shield across its front and a one inch heavily leaded glass window for protection from the radiation. For transferring the samples the following steps are taken:

#### **E. Post-irradiation sample handling**

1. Inside bags are prepared by taking one by two inch polyethylene bags, cutting off the closed bottom, rolling them so that the side seams are on top of each other, and sealing the bottom shut again. This makes a bag which holds itself open to make the transfer easier.
2. Outside bags are made by labeling the same original bags with the sample numbers using a permanent marker. These are not rolled so that they will lie flat on the detectors.
3. The rabbit's cap is removed using a special set of tongs to hold the rabbit and a motorized socket wrench. The samples and the standard can then be taken out using a pair of twelve inch long tweezers and arranged in the hood.

4. Holding the vial with the long tweezers the outside bag is cut off and removed, then after tapping the vial downward to make sure the charcoal is in the bottom the vial's top can be cut off. Usually the cap can be made to pop open and then cut off by squeezing the vial with the scissors just below the top. This is gentler than actually cutting the whole top of the vial off and so is less likely to result in spilling any of the charcoal.
5. One of the inside bags is then placed over the open vial and held on by the long tweezers. By turning over the vial and the bag together with a rapid flip of the wrist the charcoal drops into the bag. If some of the charcoal is left in the vial a few sharp strikes with the tweezers will make it fall out.
6. The inside bag is then held just above the charcoal using a pair of tongs made from a bent piece of copper sheet 1/32 inch thick and one inch wide. These tongs squeeze the bag shut over most of its length so that when it is heat sealed there is not too much excess air in the bag and no charcoal falls out.
7. Heat sealing the bag shut is done outside the hood, so it is very important that the bag is closed firmly and that no charcoal is above the copper tongs.
8. The bag is then folded in half twice using the long tweezers so that it is about 1 by 1/2 inches with all of the charcoal in one of the outside quarter sections (i.e. all of the empty quarters of the bag should be behind the charcoal).
9. The inside bag is then heat sealed into the labeled outside bag with the charcoal on the side away from the label so that during counting, with the label on top, the charcoal is directly on top of the detector (the most easily reproducible arrangement).
10. The samples are put into four 1-1/2 inch diameter 1/2 inch thick pigs for transfer to the counting lab. The four pigs correspond to the four detectors to be used for easier sample changing.

These steps in the analysis are the only ones likely to cause any problem with radiation exposure or contamination and so care must be taken when handling and transferring the samples. A lab coat must be worn when working in the hot lab and gloves when working in the hood. For short

duration work which do not require any dexterity thin polyethylene gloves are recommended, but for transferring the samples latex gloves are preferred. The gloves should be disposed of in a special, lined trash can which is checked for contamination by the MIT Radiation Protection Office (RPO); other items which are disposed of such as the vials and rabbits which are older and may be radiation embrittled should be placed in the radioactive solid waste container in the hot lab. Film badges to measure radiation exposure should be worn on the breast pocket of the lab coat and either on the wrist or finger depending on the type available. At no time should the samples or the rabbit be handled directly with one's hands; a large part of the radiation from them at the time they are re-packaged is in the form of beta radiation which attenuates rapidly over distance. A Geiger-Mueller counter is always available at the hood, and should be used to check for unusually high activity levels. The normal dose rate from the full rabbit at four inches or ten centimeters is 0.5 to 1 millirem per hour (mr/hr) for beta and gammas (using the end window of the counter) and  $\approx 0.05$  mr/hr for gamma only (using the side of the counter), this is roughly 5 mr/hr beta and 0.3 mr/hr gamma dose when measured on contact.

Once the samples have been irradiated, contamination with non-activated mercury is not a real concern because this would not be measured. Sample loss is still a general concern though and as during pre-irradiation packaging, the short period of time that the samples are exposed greatly reduces the possibility that this will be a problem. The time between the opening of the vial and the sealing of the inner bag is only about one minute. Vials which have been emptied of charcoal have been measured for any residual mercury, and once the vial blank concentration was subtracted, no mercury was found. To avoid the possibility of activated mercury contamination however, mercury standards should not be packaged until all the samples are finished and removed from the hood. To package the standards:

#### **F. Post-irradiation standard handling**

1. Outside bags should be made as above with the numbers for each of the standard on them.

2. Again using the long tweezers cut the outer bag off and remove the quartz tubing.
3. Put the tubing into two 3/8 inch diameter copper tubes which are in the hood with the space between the tubes lined up with the space between the two mercury standards. The tubes provide shielding from the beta radiation coming from the quartz.
4. By holding the copper in one hand and angling the tubes slightly a gap will open in which a scoring mark on the quartz can be made using a triangular file.
5. The quartz can be snapped open after scoring by holding each copper tube in one hand and bending the gap open further.
6. Using a fine pointed Teflon coated tweezers, the standards can be removed from the quartz. They should be unfolded using blunt nosed Teflon tweezers so that they are of about the same size as the charcoal samples, and placed in the correct outside bags which are then heat sealed shut.
7. Following the re-packaging of the samples and then the standards, the paper on the bottom of the hood should be disposed of as radioactive waste to prevent the possibility of cross experiment contamination.

Measuring the amount of activated mercury in the samples and standards is done by counting the number of 77 keV gamma rays emitted by the sample over a period of time. The HPGe detectors and their operational principles have been described above. Procedures used to count a set of mercury samples will be covered here. The detectors are connected through an amplifier and an analog to digital converter (ADC) to a VAX 3100 workstation using the VMS operating system. The calibration, recording and analyzing of the gamma spectrum is handled by the Genie Display System (System ND9900, version 2.3) from Canberra Nuclear. A menu driven, interactive software package for spectrum collection and analysis is also installed (custom written for this lab by Canberra). The experimental and system files are backed up periodically on TK50 1/2" tapes. After setting up the files and directories for a given analysis, the custom menu can be used for counting and analysis:



## **G. Gamma spectrum counting**

1. Two elemental libraries (ELB's; two are required because of how the software functions) are created with the elements to be analyzed for, their half lives, concentration in the standards and the  $\pm$  error in this concentration, and the energy of the gamma peaks corresponding to the activated radionuclide. For mercury analysis the libraries are called STDHG.ELB and HG.ELB.
2. Four run descriptor files (RDF's) are created, one for each detector (D1 through D4) and grouped in a subdirectory with the experiment's name (e.g. [.HGJUL3]D1.RDF). The files contain the names of the element libraries, the names and weights of the samples and standards, and the irradiation date, time, and duration. The sample weights are given as one gram so that the output will be an actual weight of mercury present which is converted to a concentration later.
3. To acquire spectra, the experiment and run descriptor names, detector numbers, counting time, and sample number are input. The software erases the current spectra, starts the detector, and at the end of the counting time or when the detector is stopped manually, stores the spectra in configuration files (CNF's) in the experiment's subdirectory.
4. Charcoal samples are usually counted for six hours, and the mercury standards for fifteen minutes (because of the large amount of mercury in them this is all that is needed). Both standards are counted on all four detectors so that their specific activities can be compared as a quality control check.

Because the 77 keV peak is rather weak and is closely surrounded by others it is important to do the spectral analysis in a manual interactive mode. If the computer just performs the analysis automatically it sometimes incorrectly identifies the 75 keV X-ray as the mercury peak or inconsistently determines the background level. The low ratio between the peak height and the background level requires that the fitting be done carefully and most importantly consistently. The interactive peak fitting routine displays an expanded spectrum around the peak of interest with the counts in each

channel, fitted Gaussian curves through the peaks it has identified, the difference between the actual counts in each channel and the fitted curve, and a line showing the background level determined by the channel limits that have been set around the peaks. Setting the limits correctly is the main reason for manually fitting the peaks. If two peaks overlap at their bases, then the background's end points need to be set wider, but if the peak is in a part of the spectrum where the background is not very flat, the end points may need to be set close together. After adjusting the limits and possibly including other nearby peaks in the expanded spectrum it occasionally takes the software two tries to fit things correctly.

Once all the selected peaks in an experiment have been fitted, the printed output for the standard will give the peak areas, the 'standard constants' and a  $1\sigma$  error. The constant for a given radionuclide is its peak area divided by the counting time in seconds, the standard's weight, and its given elemental concentration; and it is back decay-corrected to the end of the irradiation (the units would be counts per second per gram). When two standards are used their constants are averaged for the sample calculations. The information given for the samples includes the peak areas and backgrounds and the calculated elemental concentration with a  $1\sigma$  error. The concentration is calculated by dividing the sample's area by its counting time, back decay-correcting to the end of the irradiation, and then dividing by the standard constant for that energy. The error for each peak is calculated as described above in Section 4.4; the fractional error in final sample concentrations is calculated as below:

$$7. \quad \frac{\sigma(\text{conc.})}{\text{conc.}} = \left( \left( \frac{\sigma(\text{area})}{\text{area}} \right)_{\text{sample}}^2 + \left( \frac{\sigma(\text{area})}{\text{area}} \right)_{\text{std.}}^2 + \left( \frac{\sigma(\text{conc.})}{\text{conc.}} \right)_{\text{std.}}^2 \right)^{1/2}$$

where  $\sigma(\text{conc.})$  is the reported accuracy of the NIST standard concentration. The error in the time measurements is negligible compared with the few percent error in the sample peak area and in the standard concentration. The concentration and error calculated and reported by the software is expressed as  $x \text{ ppb} \pm \sigma \text{ ppb}$  or in the case of the mercury samples which are artificially given the weight of one gram the units are  $x \text{ nanograms} \pm \sigma \text{ nanograms}$ .

To calculate the concentration of mercury in the air which was sampled, the charcoal mercury blank is subtracted from the measurement and

the result is divided by the total amount of air collected in the sample. As mentioned in section 3.3 the blank mercury concentration for the charcoal used for the sampling is  $8 \pm 2$  nanograms per gram and the weight of the sorbents is  $100 \pm 5$  milligrams. The blank correction is thus  $0.8 \pm 0.2$  nanograms. Air volume is determined by multiplying the measured air flow rate which was described in Section 3.6 by the sample duration which is usually 24 hours (1440 minutes). The accuracy of the measurement is  $\pm 5\%$  as measured during flow calibrations described in Section 3.7; again error in the time measurement of the sample duration is negligible. The mercury measurement and its error from the Canberra analysis software, and the calculated sample flow rate are input to a spreadsheet in Microsoft Excel. This calculates the air concentration and the propagated error as nanograms per cubic meter ( $\text{ng}/\text{m}^3$ ). The equation used for the final concentration error expressed as nanograms per cubic meter is:

8.

$$\text{Final error} = \sqrt{\left(\frac{\sqrt{(\sigma(\text{Hg}))^2 + (\sigma(\text{blank}))^2}}{\text{Hg} - \text{blank}}\right)^2 + \left(\frac{\sigma(\text{flow})}{\text{flow}}\right)^2} \times \frac{\text{Hg} - \text{blank}}{\text{flow}}$$

Hg = the measured amount of mercury in the sample in nanograms

blank = the measured amount of mercury in the blank in nanograms

flow = the measured total flow in cubic meters

$\sigma(\text{Hg})$ ,  $\sigma(\text{blank})$ ,  $\sigma(\text{flow})$  = the error in these measurements

The expression in the large parentheses in the center of equation 8 is the fractional error of the mercury measurement minus the blank value, and next to it under the large square root is the fractional error in the flow measurement. The square root of the sum of the squares of these is the total fractional error which, when multiplied by the concentration, gives the final concentration error. This is tabulated along with the concentrations of each sample for reporting.

## 5 RESULTS AND DISCUSSION

Before the Upstate New York sampling program began it was not known specifically what the results might show. Reported atmospheric mercury concentrations in such locations were typically on the order of a few  $\text{ng}/\text{m}^3$  and showed little variation either spatially or temporally, but several features of this project are rather unique and as such might provide new information regarding mercury's sources and transport. First among these features is the large number of samples to be analyzed. The two year duration of the sampling would allow seasonal variations to be identified; the frequent collection would provide for the detection of episodic events and enable the better use of statistical analysis of the data; and the use of five different locations permits regional patterns to be distinguished from site specific variations and increases the likelihood of positive results from receptor modeling and analysis. In terms of source identification, the concurrent particulate elemental determinations are invaluable, and completely unique for a study of atmospheric mercury. Finally, the size of the data base should allow analysis of the results in initially un-anticipated ways by this lab and others. The results presented here bear out some of these hopes, and will likely be the foundation for future work in the area.

The complete data set is given in Appendix B. Here it will be shown graphically and as represented by a few statistical measures. The seasonal variation of the concentrations and the similarity of the measurements from site to site are easily seen. Source identification has been attempted using the receptor modeling technique of factor analysis. At four of the sites this method has been of limited use, perhaps due to the method's meteorological limitations and the properties of vapor phase atmospheric mercury. At Perch River however, the factor analysis has been more successful and so these results will be discussed further and matched with limited wind trajectory analysis. The atmospheric transformations of mercury are examined by a comparison of its particulate and vapor phases and by relating the vapor phase's seasonal variations to ozone concentrations measured at (or near) the same sites by the NYSDEC.

## 5.1 Mercury Concentrations and Initial Interpretations

In a little over two years (106 weeks) a total of 2120 sample assemblies were prepared, installed in the field and returned to our lab. Of these, 1380 charcoal sorbents were analyzed for mercury, three per week per site between July 15, 1992 and September 11, 1993, and two per week per site from September 15, 1993 through July 28, 1994. Due to the analytical difficulties discussed in Section 4.4 and startup problems with the samplers only 53% of the analyses for samples up to December 2, 1992 produced meaningful results (this will be discussed further below). After this date 90% of the analyses were used in the results; the typical reason for charcoals from this period not providing atmospheric results was that some problem had occurred in the field such as a power failure which caused no sample to be taken. These charcoals were analyzed along with those which had operated as a way of checking the field blank level, and they had no more mercury than the lab blanks ( $0.8 \pm 0.2$  ng/sorbent). A final total of 1149 atmospheric mercury measurements were obtained representing 83% of the analyzed samples and 54% of the sampling days. The 740 charcoals which have not been analyzed have been archived for possible future uses.

Calculated analytical and volume measurement errors were discussed in Section 4.5, and the uncertainty of the charcoal efficiency determination was determined in Section 3.4. These were both included in the  $\pm 1\sigma$  error listed in the full table of values in Appendix B. Averaged over all the measurements the calculated error is  $\pm 0.32$  ng/m<sup>3</sup>. By far the greatest portion of this is from the statistical error inherent in the nuclear counting, and of this a large portion is due to the background calculation, even though the charcoal used and the counting procedures were both chosen to minimize this effect. An operational lower detection limit of 0.6 ng/m<sup>3</sup> was set as twice the average measured error. This is below the usual range of vapor phase atmospheric mercury, and for samples taken after December 2, 1992 only a few were excluded because of this limit and those were mostly due to sampling problems such as unusually low flow or short sample duration.

This limit was mainly useful for the samples taken before December 2, 1992 when analytical problems caused both the sample and blank measurements to be artificially high. This did not affect the calculated measurement error significantly (the average for this period is 0.38 ng/m<sup>3</sup>)

because the mercury levels were very consistent as discussed in section 4.4, and because it resulted in clearer spectral peaks which had less statistical detection error. Nevertheless, when subtracting the higher blank value of  $2.9 \pm 0.3$  ng/sorbent from sample values which averaged  $4.4 \pm 0.8$  ng/sorbent some of the measurements resulted in calculated concentrations which were unrealistically low. Only about 50 samples were excluded from the data by this method, and this has not affected interpretation of the results because of the way missing values have been handled in the data analysis, as will be described later.

With these facts about the measurement error and missing values in mind, the concentrations of vapor phase mercury at the five sites are shown in Figures 27 - 31. The dashes are the individual daily measurements, and the broad line is a smoothed average value which was calculated by averaging the values over the two weeks before and after the date shown, and then taking a second average of these values for the same period as a method of smoothing the line. The smoothed averages from the five sites are then all shown in Figure 32. Two things are immediately obvious from the plots. The first is that there is a pronounced seasonal variation in the mercury concentrations, which are summarized below as summer and winter averages in Table 7.

Site/ End Date	Belleayre	Moss Lake	Perch River	Westfield	Willsboro
9/21/'92	1.4	1.8	1.9	1.3	1.4
3/21/'93	2.5	2.3	3.2	2.9	2.5
9/21/'93	1.7	1.9	1.9	2.2	1.9
3/21/'94	2.7	3.7	3.0	3.5	3.0
7/29/'94	2.1	2.0	2.0	1.8	1.7
All Dates	2.2	2.4	2.5	2.6	2.2

Table 7. Seasonal and overall averages of vapor phase mercury concentrations in  $\text{ng}/\text{m}^3$  at the five New York sampling sites. The six month periods over which the averages are taken end on the date shown (the first period began on 7/15/'92).

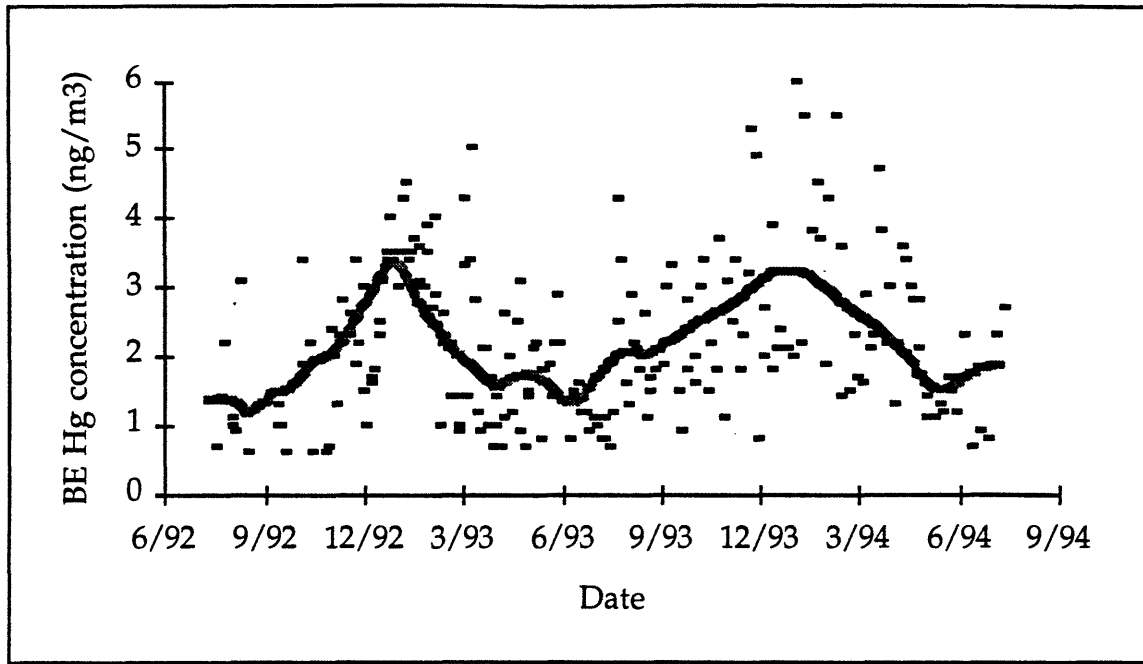


Figure 27. Vapor phase mercury measurements at Belleayre NY from July 15, 1992 to July 28, 1994 with a smoothed average shown.

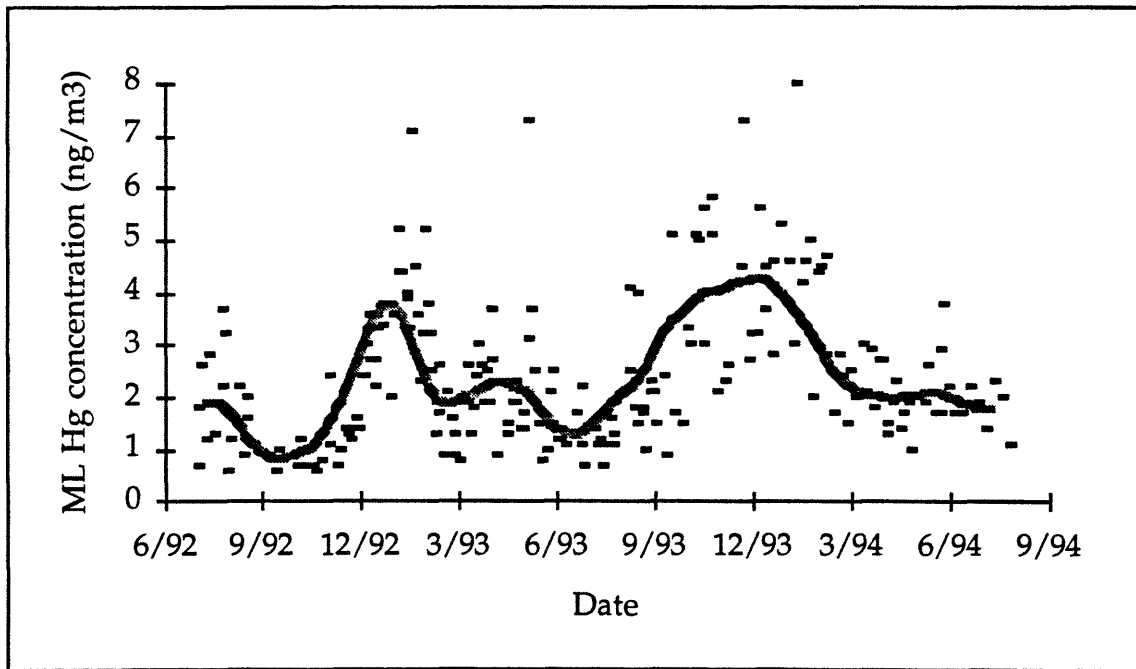


Figure 28. Vapor phase mercury measurements at Moss Lake NY from July 15, 1992 to July 28, 1994 with a smoothed average shown.

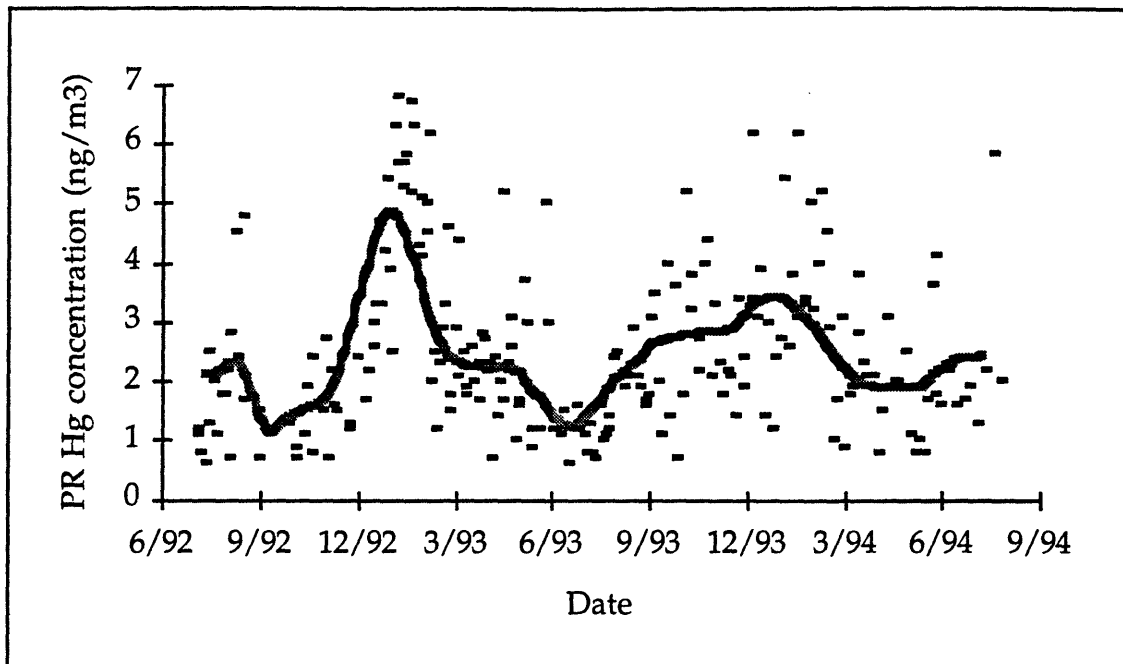


Figure 29. Vapor phase mercury measurements at Perch River NY from July 15, 1992 to July 28, 1994 with a smoothed average shown.

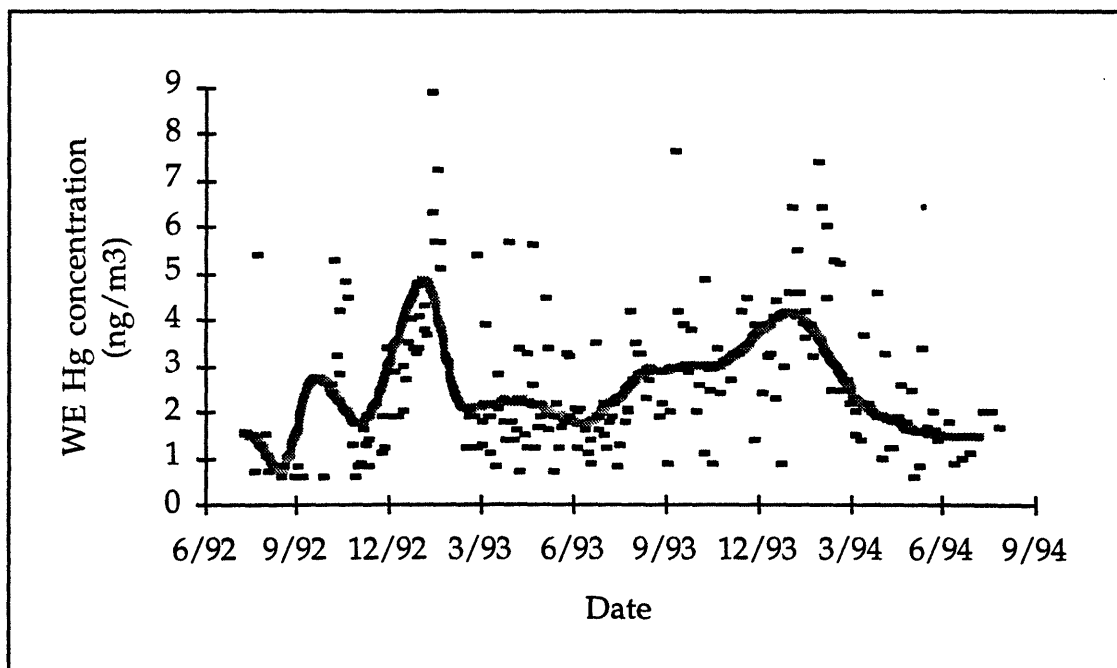


Figure 30. Vapor phase mercury measurements at Westfield NY from July 15, 1992 to July 28, 1994 with a smoothed average shown.



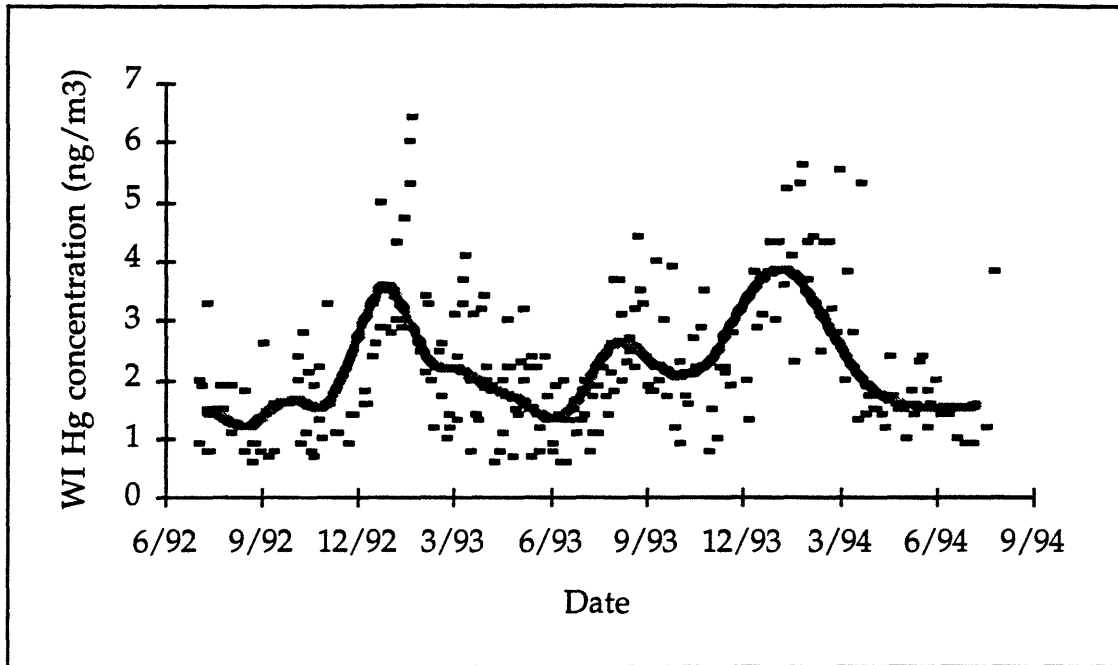


Figure 31. Vapor phase mercury measurements at Willsboro NY from July 15, 1992 to July 28, 1994 with a smoothed average shown.

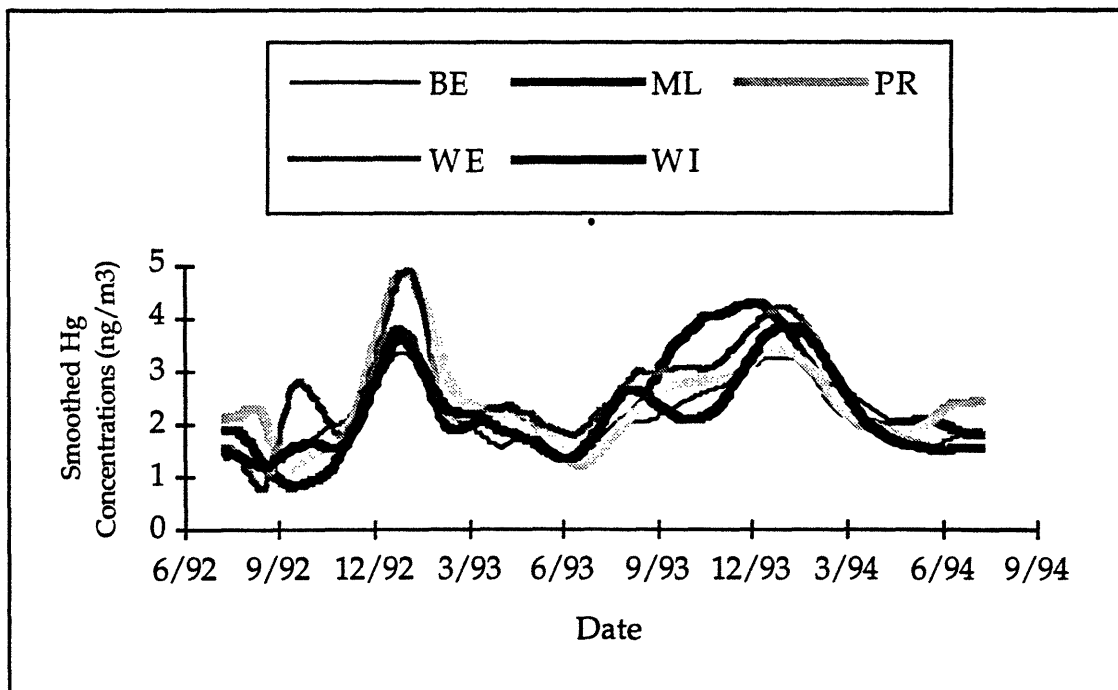


Figure 32. Smoothed mercury measurements at Belleayre, Moss Lake, Perch River, Westfield, and Willsboro NY from July 15, 1992 to July 28, 1994.

Seasonal variations such as these have been reported at remote locations in southern Sweden and Italy (Lindqvist, 1985), but were not seen in Michigan or Vermont (Expert Panel, 1994). Possible reasons for the variation will be discussed later.

On top of these seasonal changes there is a day to day variation which is likely due to local weather, regional wind patterns, or source effects. At Perch River some of this variation can be explained from the results of the factor analysis as will be shown later (along with the less successful factor analysis results of the other four site's data). As a matter of practical importance, the difference between the time scales of these two patterns will affect the sampling duration needed for future monitoring programs. If source identification is an important goal, then daily or more frequent sampling is necessary, but if larger scale phenomena are being studied weekly integrated sampling may be sufficient (the advantage of longer sampling periods being increased measurement accuracy). In order to characterize and compare the magnitudes of the seasonal and daily changes in the concentrations, the standard deviation of the smoothed average, and the standard deviation of the measurements from this average have been calculated for all five sites. These are given in Table 8 along with the total standard deviation of the individual measurements.

	Bellayre	Moss Lake	Perch River	Westfield	Willsboro
Seasonal Variation	0.6	0.9	0.8	0.9	0.7
Daily Variation	1.1	1.3	1.3	1.5	1.1
Actual Standard Deviation	1.1	1.4	1.4	1.5	1.2

Table 8. Seasonal and daily variations, and overall standard deviation in the mercury concentrations for two years at the five New York sites. The seasonal and daily variations are defined in the text, and the standard deviation has the usual meaning

Because the smoothing method is not an actual average the separated components of the variation are not true standard deviations and can not be combined to give the total. These values should only be taken in a comparative way and not used for calculation. For this reason they are identified simply as the seasonal and daily variations in the data. Recall that the uncertainty in the measurements is about  $0.3 \text{ ng/m}^3$ , so the daily variations are not the result of measurement errors.

The second important feature of these plots is the overall similarity among the sites as seen in Figure 32. This indicates that they are generally affected by the same sources and sinks and is the most significant result to be derived from these figures. While the day to day changes may be due to local and relatively nearby sources or other small scale factors, the environmental impact of atmospheric vapor phase mercury over the entire region is governed by larger scale phenomena. Among these may be seasonal changes in the natural and anthropogenic sources themselves, large scale changes in the wind patterns which would cause different sources to impact the region, seasonal differences in the atmospheric properties which govern the transformations and deposition rates of mercury from the air, and terrestrial changes which alter the retention of mercury which has reached the ground. Information currently available to this lab enables some of these mechanisms to be examined presently, namely the change in the relevant sources and in the atmospheric transformations. The availability of this large data set may allow the other mechanisms to be explored in the future.

Before entering into a more detailed discussion of the above subjects the problems and possibilities of the other two need to be mentioned. Measuring mercury emissions from large point sources over a full year is certainly possible, though the number of sources which would need to be covered may be prohibitive. Also, using standard methods, the collection and analysis of mercury from a smokestack is sometimes difficult due to the interference of other species. This may be a future application for the methodology developed here. As the sources get smaller and more numerous the problem of identifying candidates for analysis becomes more difficult. Area sources and natural emissions which need to be characterized more in terms of their mercury flux (e.g. in units of  $\text{pg m}^{-2} \text{ s}^{-1}$ ) are extremely difficult to measure. At the other end of the atmospheric pathway is the measurement of mercury uptake and retention by soil, water and vegetation.

If mercury deposited to these surfaces by wet or dry deposition is re-emitted by volatilization then there will be no net removal. This process is also difficult to measure, but it is an obvious speculation that some of the decrease in vapor phase mercury in the spring is due to an increase in retention of dry and wet deposition by vegetation. Both of these mechanisms may need to be evaluated and with the data and methods presented here this may be possible.

## **5.2 Factor Analysis and Source Identification**

Factor analysis is a standard statistical tool which enables the underlying structure of large data sets to be more easily examined (Hopke, 1985). It is particularly useful for the sort of data sets generated by this lab which contain 30 to 40 elemental measurements for each of hundreds of samples. In mathematical terms the goal of factor analysis is to reduce the dimensionality of the data set from the number of different measured variables to the number of actual factors influencing the system. When applied to the receptor modeling of environmental samples it allows the various sources influencing each sample and site to be separated and identified. As an example, atmospheric particulate samples almost always contain some amount of crustal material which contains among other things large relative concentrations of aluminum, scandium, iron, and rare earth elements. Rather than simply reporting the concentrations of these elements, it is much more useful to present the amount of crustal material in the sample from which the concentrations arose.

The difficulty in performing the analysis is due to the fact that the concentrations of most elements found in a sample are the result of the combined influences of several sources. In order to separate the effects of different sources the method relies on observing the commonalities of the variation of the variables. Simply put, if two variables rise and fall together they may be combined into one factor, but the variations due to one factor need to be differentiated from the variations due to a different factor. As another example high chlorine levels may be the result of the influence of ocean spray or a municipal incinerator. The chlorine from the ocean will be associated with sodium and the chlorine from the incinerator will likely be associated with cadmium. What is needed is to match the correct amount of the variations in the chlorine with each of the other two elements. This is

the reason why a large set of measurements is necessary for the separation to be successful. There needs to be enough change in the measurements, and enough combinations of change for the differences in the relationships to be observed.

A large data set, however, is not always sufficient for separation of the sources. Because the use of factor analysis to identify sources from receptor samples is entirely dependent on the transport of the species, it is very difficult to distinguish between two sources which are located close to each other even if they have very different types of emissions. Thus sources which are far from the sampling site tend to get smeared together, and local wind patterns can greatly affect the results by mixing air from different directions. Sampling durations which are longer than the temporal changes in the wind patterns can also result in the smearing of different sources into one factor. Since prevailing winds are often a function of season it is important and beneficial to have samples covering at least one year before performing the analysis. Also if there is a force which is not measured but which affects two or more of the elements equally (e.g. some atmospheric transformation dependent on humidity) then this might cause the elements to be linked as if they were from a common source.

There are several practical and investigatory reasons why factor analysis results are useful. First it produces a representation of the data as a summation of influences rather than effects, which is often more useful. From this representation the relative impact of the causal factors or sources can be determined. This is important in environmental work where several different sources may be partially responsible for some unwanted effect. The unknown source of a measured element can be found by its inclusion in a factor of known origin. Finally a source may be found which had not been previously identified. This is a result of the fact that no a priori knowledge of the sources is needed for factor analysis, the only input is the sample data. These last two uses are the ones to be explored here in relation to vapor phase mercury.

When factor analysis is applied to a data set, the first result is a factor matrix which relates each of the factors to each of the elements or variables. The numbers in the matrix are referred to as the factor loadings and indicate how much of the variance of the given element can be explained by the given factor. Though the complete square matrix would exactly transform the data

points between the two representations, the factors in the matrix are given in order of decreasing ability to describe the variance of the whole system. Usually only the higher order factors are retained for further analysis. The physical meaning of the factors must be interpreted by observing which elements or variables display high ( $>0.25$ ) loading within the factor. Recalling the simplest atmospheric example from above, a factor containing very high sodium and chlorine would be identified with marine aerosols.

The next step is to plot the data using the factors as the dependent variables instead of the concentrations. The magnitude of a factor's influence on given sample is given by a factor score for that sample. The factor scores are the number of standard deviations from the mean of that factor as averaged over all the samples; an average contribution from the factor gives a score of zero, a greater than average contribution gives a positive score, a less than average contribution gives a negative score. Factor scores greater than one indicate a strong influence of that source or factor on that individual sample. In order to identify individual sources in atmospheric receptor modeling, sampling dates with high factor scores are identified and the back projected wind trajectory for that day is examined. If a known source of the type indicated by the factor loading exists in the wind trajectory, then a fairly positive identification has been made.

For this study the vapor phase mercury data was combined with data from the elemental particulate samples which were collected on the same days and included particulate phase mercury determinations. Two additional variables were added, the ratio of arsenic to selenium concentrations and the ratio of the lanthanum to samarium concentrations. High loading of the former is indicative of the influence of smelters, and the latter indicates the burning of oil. Because factor analysis is very sensitive to missing data points these were replaced by the most expected value for each variable (the value corresponding to the highest point in a frequency distribution plot). The analysis was performed using Statgraphics Plus version 7.0 for Windows.

The factor loadings which resulted from three of the site's data placed the majority vapor phase mercury variance into a single factor. At Belleayre this factor also contained sodium, chlorine, manganese, cobalt, zinc, bromine, and cadmium. This factor has been identified as a signature for the influence of regional Canadian sources which together influence all of the sites when the wind is coming from the north and northwest. At Moss Lake the

mercury was within a factor containing sodium, magnesium, chlorine, vanadium, bromine, cadmium, and gold which matches the Canadian regional sources with the additional influences of oil (vanadium) and precious metals works (gold). A second factor paired mercury with cobalt and indium which is likely a particular but unidentified source, possibly a smelter. For the samples from Westfield mercury showed only a small commonality with chromium, cobalt, cadmium, and gold, which might arise from a smeared effect of various metal works. The results from Willsboro separated the mercury into two factors. One of these contains arsenic, indium, and a high arsenic to selenium ratio which has been identified as a signature for copper smelting. The other factor had a high loading of gold and correlated with northerly winds which signifies the influence of the various precious metal works located in Quebec to the north of Willsboro. The factor score plots for the first three sites and the first factor identified at Willsboro show a common seasonal pattern of high scores in the winter and low scores in the summer (though at Westfield the pattern is less distinct). This obviously matches the seasonal variation in the mercury measurements, but also is associated with winter wind trajectories from the north and northwest. The four plots are shown below in Figure 33.

The factor analysis results from the Perch River data were much more successful at separating the various sources of vapor phase mercury within the samples. This is perhaps due to Perch River's location near the northeastern end of Lake Ontario which is less likely to suffer from upwind local effects, as the prevailing winds tend to come across the lake, and which is closer to identified major sources in Ontario and Quebec. The elements of the factor matrix containing mercury loadings are shown in Table 8. The first factor containing vapor phase mercury is the same Canadian regional influence identified above, and the factor scores for this followed the same seasonal pattern shown in Figure 33. A second factor containing a distinct mercury source emitting chlorine and particulate mercury is combined with a high arsenic to selenium ratio indicating smelting. Factor three includes sodium, cobalt, cadmium, gold, and arsenic to selenium ratio which is the result of precious metals works and smelter signatures. The last factor contains a very high loading for aluminum along with lesser amounts of magnesium and chromium and it is proposed that this factor is due to aluminum plants.

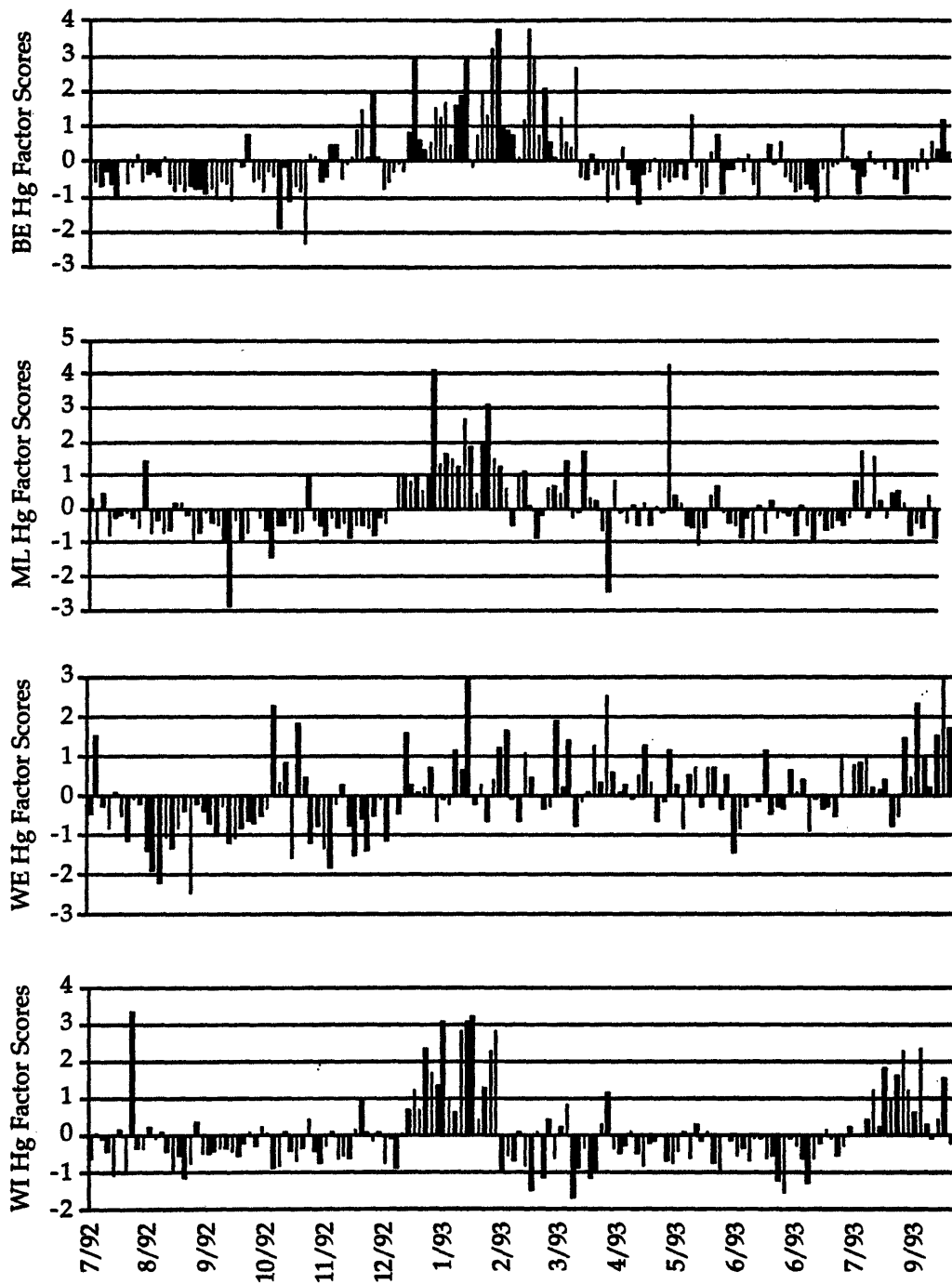


Figure 33. Vapor phase mercury factor score plots for Belleayre, Moss Lake, Westfield, and Willsboro. The high scores in the winter months correspond to the seasonal mercury concentration pattern and prevailing winds from the north and northwest.



Factor/ Element	Canadian Regional	Smelters	Precious Metals	Aluminum Plant
Na	0.81		0.31	
Mg	0.74			0.32
Al				0.73
Cl	0.36	0.73		
Mn	0.46			
Cr				0.30
Co			0.26	
As		0.36		
Br	0.34			
Cd	0.51		0.32	
In	0.61			
Au			0.81	
Hg vapor	0.26	0.25	0.33	0.41
Hg part.		0.80		
As/Se	0.24	0.37	0.38	

Table 8. Factor loadings containing vapor phase mercury for Perch River samples. Loadings indicate the variation of the elements' concentrations among the sample set which can be derived from the indicated factor; loadings under 0.25 have been omitted.

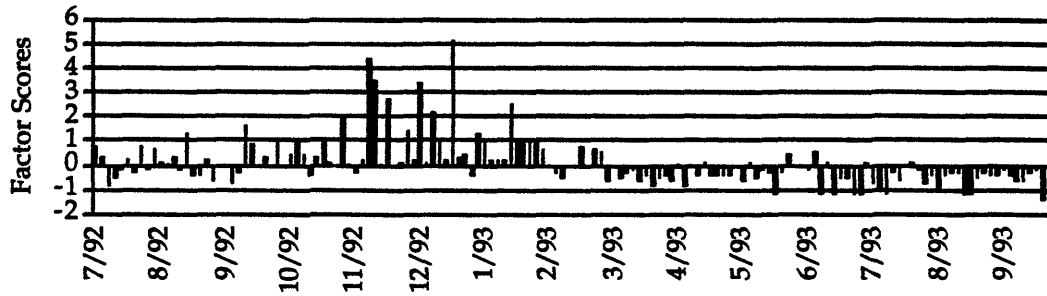
Apart from the source identifications themselves, an interesting point is that only in one factor do vapor phase and particulate mercury appear together. Whether this is due to actual differences in their sources or due to their different atmospheric transport properties is not certain. Support for the former mechanism comes from the completeness with which they have been separated by the factor analysis at all of the sites, and that there is one factor (smelters at Perch River) where they clearly appear together. This factor was previously identified in this lab's analysis of the particulate data alone. From the factor loadings the mercury source appears to be due to a process emitting high concentrations of chlorine, which from the wind trajectory analysis and the factor's absence from the other sites might be local to Perch River.

However, no specific facility which matches these criteria has been found in the area. A factor score plot for the Perch River Canadian regional factor follows the same seasonal trend as those for the other sites, but the other three factors' scores show less overall structure. These three factor scores are plotted in Figure 34.

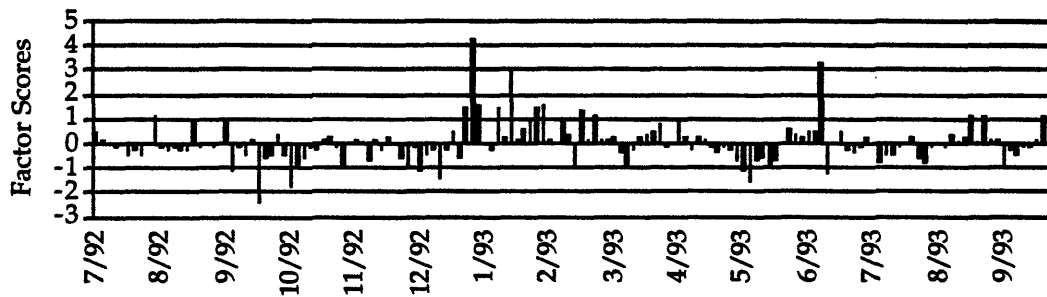
The source identifications for these factors have been further investigated by examining the back projected, mixed layer wind trajectories associated with the samples having the highest factor loadings. A representative set of these trajectories are shown in Figure 35. Trajectories for all of the sites and most of the sampling dates were calculated and tabulated by Professor G. J. Keeler of the University of Michigan, using the Branching Atmospheric Trajectory (BAT) model developed by Heffter (Billman Stunder, 1986). One might expect that it would be possible to identify specific facilities responsible for the major portion of a given factor by overlaying trajectories from different sites to 'triangulate' the sources location. However there is a great uncertainty associated with the wind patterns and as was described above there are difficulties with the use of factor analysis for receptor modeling, both of which preclude this approach.

The presence of a large number and variety of metal works industries in southern Ontario, and along Lake Erie and the Saint Lawrence River are what causes the distinctive factors seen at Perch River, but this also makes identification of specific emitters difficult. As a note, the large number of American factories and utilities located in the Midwest and the Ohio River Valley are too distant to be distinguished from one another, and the smearing of their effects produces a regional factor characterized by southwesterly winds at the sites. An additional problem in identifying specific sources is that the emission characteristics of some may not be constant over time, resulting in a variation in the factor scores which would be impossible to explain by changes in wind patterns alone. This might be the case for the aluminum plant scores in the third part of Figure 34 which show high values spaced one week apart in August 1992 and from June to August 1993. Without confirmation it can only be speculated that this pattern has to do with actual changes at the source.

### Perch River Smelters



### Perch River Precious Metals Works



### Perch River Aluminum Plants

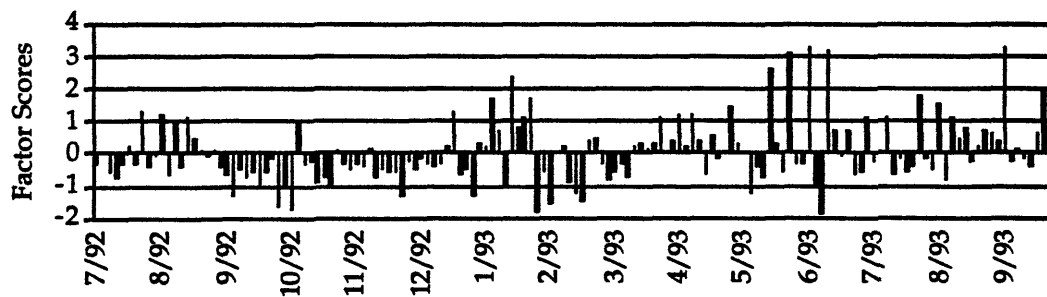
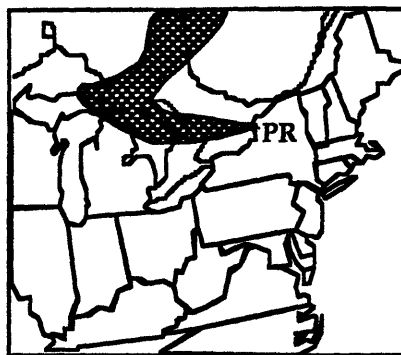
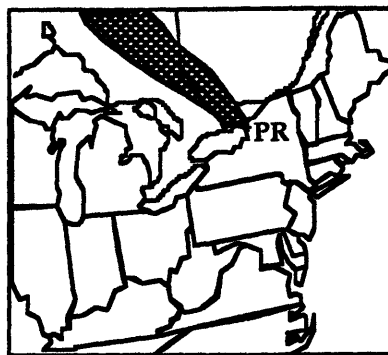


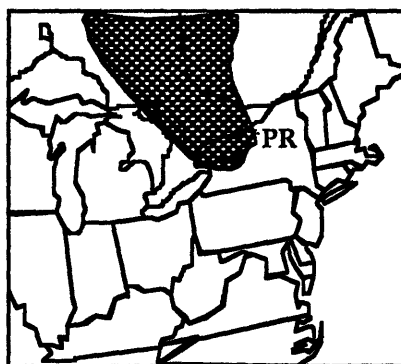
Figure 34. Perch River factor score plots for three identified source types. Sources corresponding to the highest scores are further checked using wind trajectory analysis.



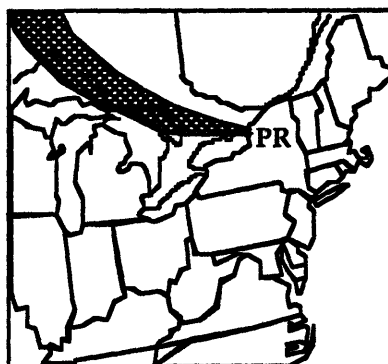
Smelters 11/28/92



Aluminum Plant 5/29/93



Typical Canadian Regional



Precious Metals Works 2/15/93

Figure 35. Wind trajectories ending at Perch River and associated with high factor scores for vapor phase mercury related sources. These trajectories have been used to try to identify the location or region of significant sources though no individual facilities have been determined.

Chemical mass balance is an additional method for identifying and apportioning source contributions which is often applied following the use of factor analysis. It has been applied to the atmospheric particulates data set produced in this lab but with little success. The major obstacle to the further use of this technique is that it requires a good a priori knowledge of the emission profiles of the sources. Because this is not available for most of the measured elements, the results for chemical mass balance as used in this lab have been subject to wide variations with small changes in input data and provided no new information beyond that obtained by factor analysis.

### 5.3 Atmospheric Transformations and Fate

The other part of the atmospheric mercury cycle which this work might help to understand is the chemical and physical transformations which cause vapor phase mercury to be deposited to the earth. This discussion here is somewhat more speculative than in the previous section because, unlike the elemental particulate concentrations which were measured by this lab and used for source identification, the supporting data for these interpretations is not as complete or available. Nevertheless, in addition to the vapor phase mercury measured under this project, particulate mercury was measured at the same sites by this lab, and ozone was measured by the NYSDEC. It has already been seen using factor analysis that the vapor and particulate phase mercury do not correlate in the simple statistical sense, but it is helpful to look at the data itself to see if there is any other relationship between the two. Aqueous oxidation of elemental mercury by ozone has been identified as the most important mechanism for mercury's removal from the atmosphere based on laboratory measurements of the reaction rate (Section 2.2 and Iverfeld, 1991). An observed relationship between the two in the atmosphere would substantiate this fact and lead to the better establishment of the reaction rate.

To examine both of these issues the smoothed values of vapor and particulate phase mercury and tropospheric ozone have been plotted for the five collection sites in Figures 36 through 40. Coarse fraction ( $2.5\mu\text{m} < \text{diameter} < 10\mu\text{m}$ ) particulates were collected at all of the sites for the entire sampling period but were only analyzed at Perch River and only up to December 1992, so this data does not overlap the vapor phase mercury data by very much. The coarse particulates represent more local sources because they do not travel as far as the fine particulates. They are also more likely to be of natural origin than the fine fraction. Ozone data was only available at three of the sites and only for the duration of the particulate sampling program. The seasonal variation in the ozone concentration is well known and is the result of a combination of tropospheric chemistry and downward transport from the stratosphere (Seinfeld, 1986). Ozone measurements for the end of the vapor phase sampling period have been made and when the data is available it will be incorporated, but is expected to show similar trends to the earlier values.

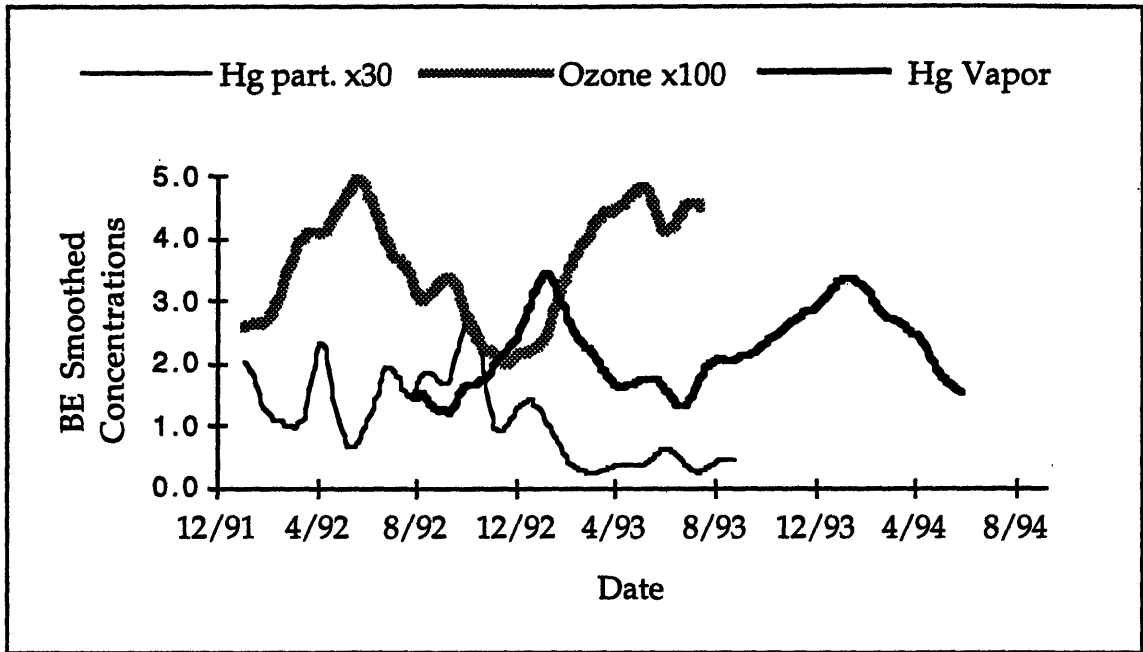


Figure 36. Smoothed concentrations of vapor phase mercury ( $\text{ng}/\text{m}^3$ ), ozone ( $\text{ppmv} \times 100$ ), and particulate mercury ( $\text{ng}/\text{m}^3 \times 30$ ) at Belleayre NY.

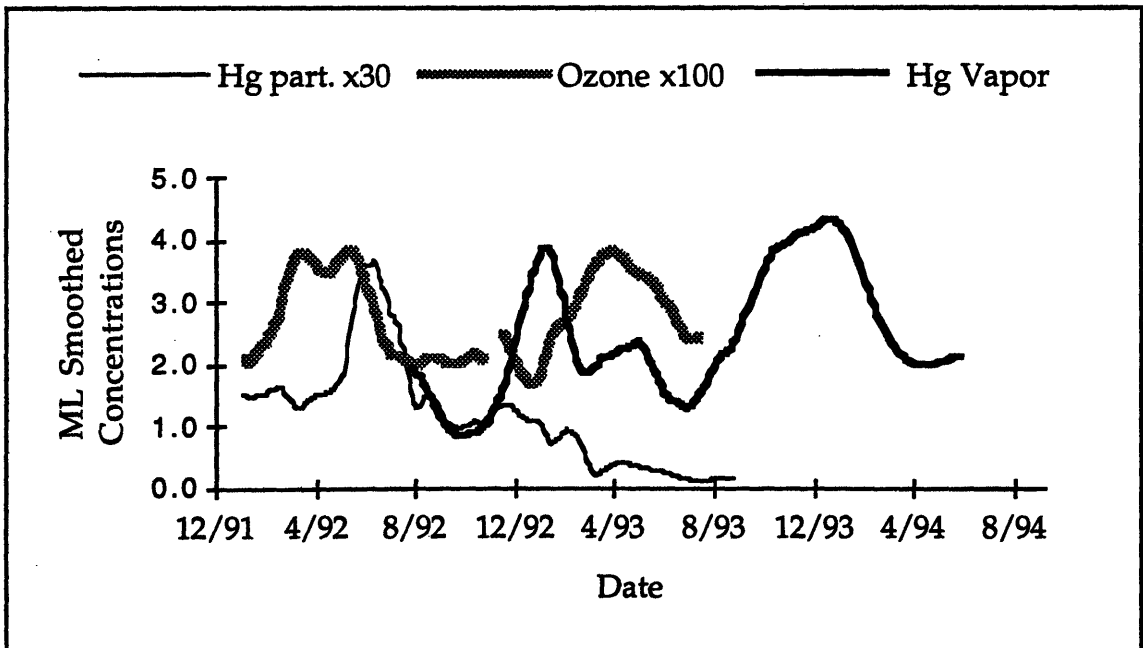


Figure 37. Smoothed concentrations of vapor phase mercury ( $\text{ng}/\text{m}^3$ ), ozone ( $\text{ppmv} \times 100$ ), and particulate mercury ( $\text{ng}/\text{m}^3 \times 30$ ) at Moss Lake NY.

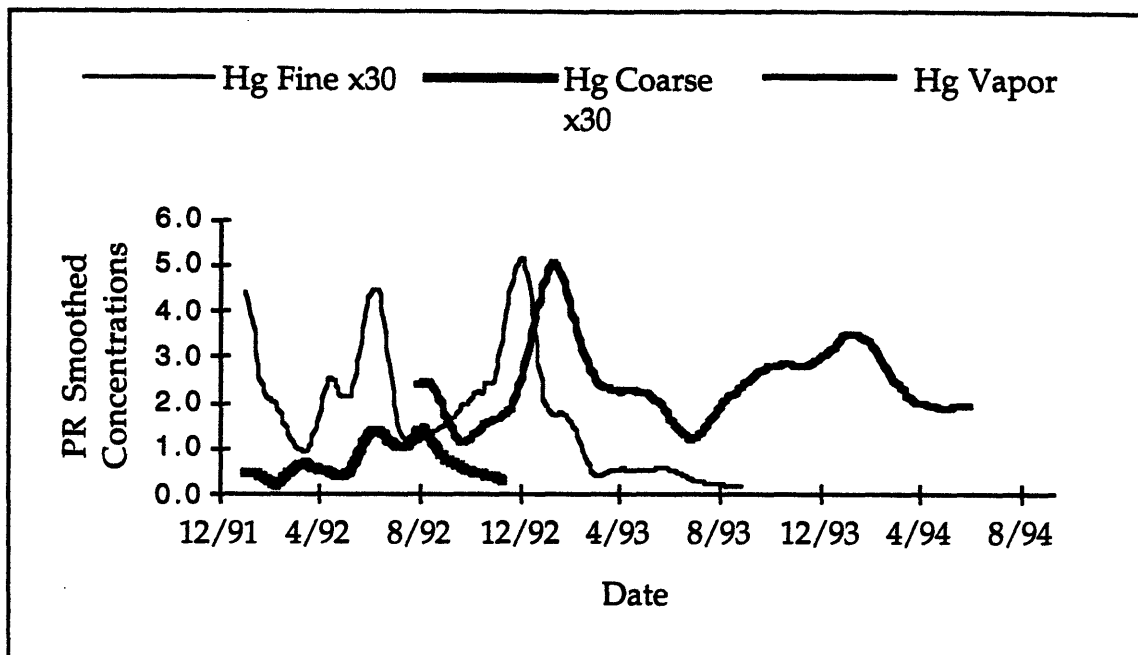


Figure 38. Smoothed concentrations of vapor phase mercury ( $\text{ng}/\text{m}^3$ ), coarse particulate mercury ( $2.5\mu\text{m} < \text{diameter} < 10\mu\text{m}$ ,  $\text{ng}/\text{m}^3 \times 30$ ), and fine particulate mercury (diameter  $< 2.5\mu\text{m}$ ,  $\text{ng}/\text{m}^3 \times 30$ ) at Perch River NY.

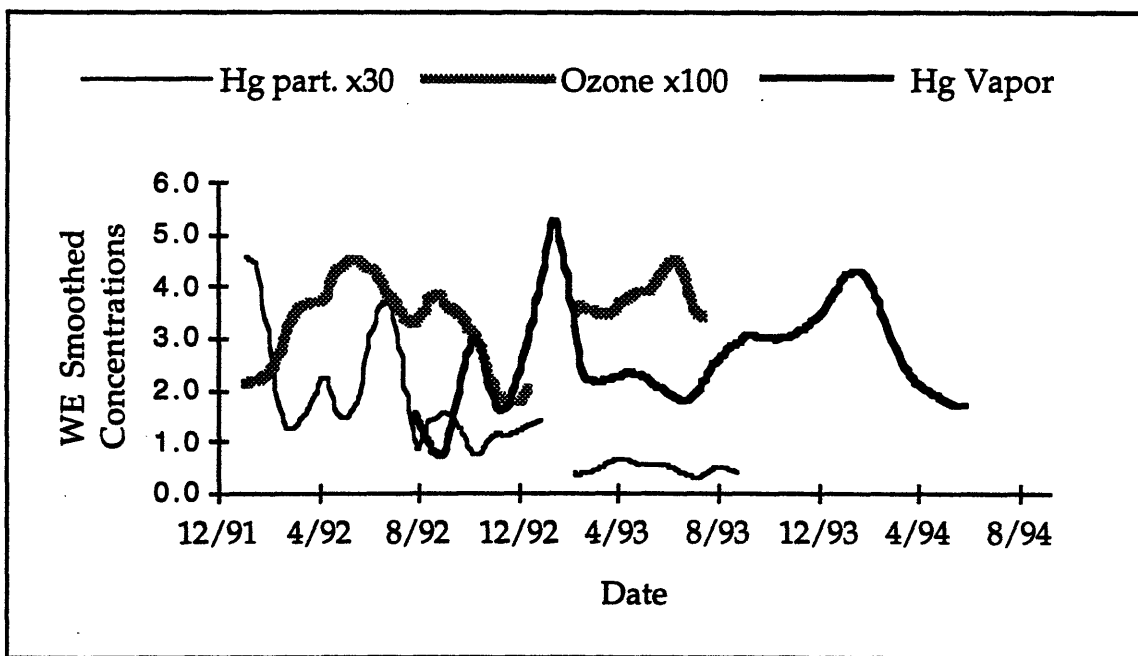


Figure 39. Smoothed concentrations of vapor phase mercury ( $\text{ng}/\text{m}^3$ ), ozone (ppmv  $\times 100$ ), and particulate mercury ( $\text{ng}/\text{m}^3 \times 30$ ) at Westfield NY.

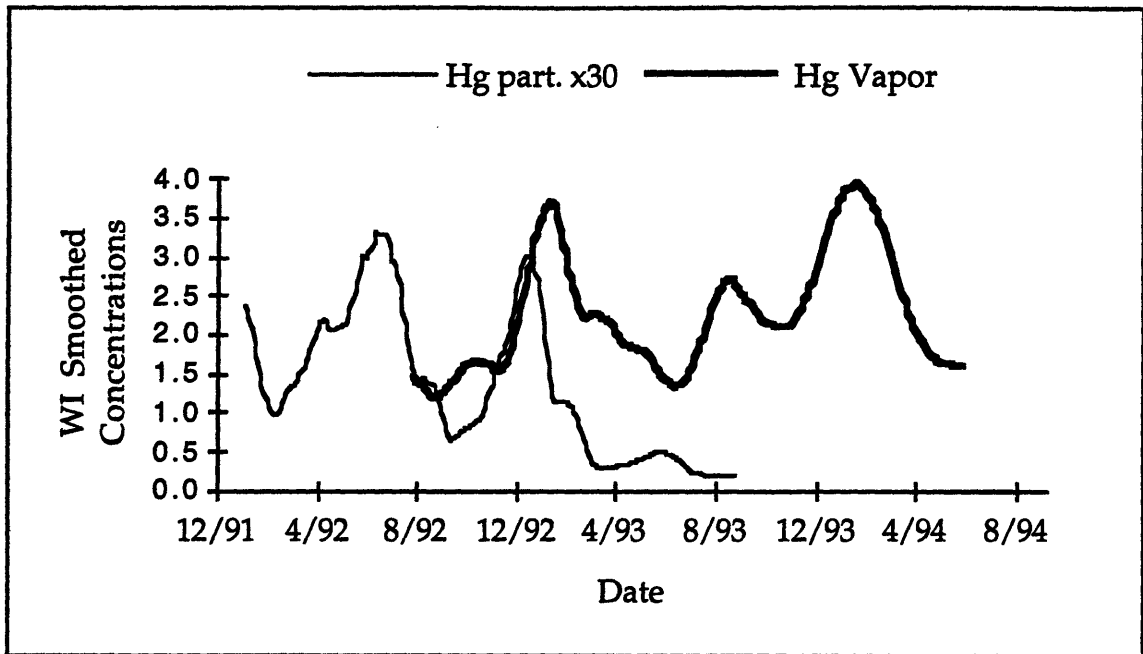


Figure 40. Smoothed concentrations of vapor phase mercury ( $\text{ng}/\text{m}^3$ ), and particulate mercury ( $\text{ng}/\text{m}^3 \times 30$ ) at Willsboro NY.

The particulate mercury concentrations show some distinct seasonal variations, but the patterns are not identical for all of the sites. This would tend to indicate that the variation is due to either changes in which sources are affecting the sites over different periods of time or in the sources themselves. The northern sites (from west to east: Westfield, Perch River, Moss Lake, and Willsboro) all show a high level of particulate mercury around June 1992. Perch River and Willsboro also have high levels in January of both 1992 and 1993; high mercury concentrations were seen in January 1992 at Westfield but unfortunately the particulate sampler was not operating in January 1993. These peak particulate mercury concentrations in January are similar to the vapor phase peaks, but do not correspond precisely to them. Therefore, while it may be said that particulate mercury's temporal variations are source influenced because several but not all of the sites show common patterns, this is not evidence for vapor phase mercury's seasonality being such. From these figures it may be seen that either particulate and vapor phase mercury arise from different sources (which is supported by the factor analysis), or that the vapor phase mercury is not affected by source

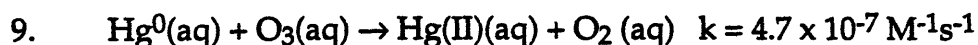


variations in the same way (the common vapor phase patterns among all of the sites may indicate a larger scale source effect).

The dropping off of the concentrations after February 1993 which is seen at all the sites has been examined from many angles but as yet, no explanation for this phenomenon has been found. It may be due to the large scale installation of some control technology or process change which affects particulate but not vapor phase emissions, but this has not been confirmed. This unfortunately makes direct comparisons with the vapor phase concentrations for the same sampling periods difficult, but as with the results from factor analysis there is no evidence for any commonality between the two from these figures.

In contrast, there does seem to be an inverse relationship between vapor phase mercury and ozone concentrations. Though this does not explicitly show a cause and effect, the mechanism exists for elevated ozone levels producing lower vapor phase mercury concentrations. Further, seasonal variations in wet deposition mercury concentrations have been observed, with the highest concentrations occurring in the summer months when ozone levels are highest (Sorensen, 1990; and Expert Panel, 1994). Other explanations for this may be the differences in gas absorption rates between snow and rain droplets, and that precipitation patterns are often different in winter and summer. In order to see whether the ozone could be the cause of mercury's seasonal changes two simple calculations can be made.

The concentration of mercury in wet deposition is usually on the order of 10 pg/gm. If the total annual precipitation is equivalent to one meter of rainfall, then the flux of mercury in wet deposition is  $10 \mu\text{g m}^{-2} \text{ yr}^{-1}$ . Using a mercury concentration of  $1 \text{ ng/m}^3$  and a mixed tropospheric height of 10 km gives a mercury burden of  $10 \mu\text{g m}^{-2}$ , and a lifetime of one year. Secondly, referring back to Section 2.2 and equation 8 the aqueous phase oxidation reaction:



can also be used to estimate the removal rate and lifetime. Using the above reaction rate; concentrations for mercury of  $1 \text{ ng/m}^3$  and for ozone 30 ppbv; and Henry's law constants of 0.1 M/atm for mercury and 0.01 M/atm for ozone the oxidation rate for mercury is  $3 \times 10^{-16} \text{ M/s}$  or  $10^{-6} \text{ g L}^{-1} \text{ yr}^{-1}$ .

Assuming an atmospheric concentration of water of  $1 \text{ gm/m}^3$ , this results in an atmospheric removal rate of  $1 \text{ ng m}^{-3} \text{ yr}^{-1}$  which also would give a lifetime of one year.

Though these calculations are neither exact nor new, they indicate the possibility that the ozone reaction could account for the removal of mercury from the atmosphere by wet deposition. If this is in fact the case then a doubling of the ozone concentration could account for the drop in vapor phase mercury in the summer months. In order to explore the correctness of this hypothesis from field data alone the concentration of soluble mercury in wet deposition would need to be measured along with vapor phase mercury and ozone. Because the reaction occurs in the aqueous phase the actual reaction rate is also affected by the moisture content of the air. With the current data only, there may not be much more that can be said, but some additional information may be available soon which will allow a better argument to be made one way or the other. If this hypothesis is found to be correct, it may help to explain the high concentration of deposited mercury in urban areas (Lindqvist, 1985) where ozone levels are much higher.

Whether the overall regional impact of atmospheric mercury on the terrestrial environment is determined by mercury's sources, its transformations, a combination of these, or by some other unidentified mechanism remains to be seen. The fact that atmospheric particulate mercury may originate from different sources and its fate influenced by different transport and deposition mechanisms must also be considered when attempting to make predictions or develop remedies. Some interesting possibilities have been explored here, and the data set generated by this project will hopefully be augmented and used to help understand the sources, transport and fate of atmospheric mercury.

## 6 SUMMARY AND SUGGESTIONS FOR FUTURE RESEARCH

The motivation for measuring atmospheric mercury does not come from any direct danger it poses; the concentrations are far too low for this to be the case. Rather, the concern is that by virtue of mercury's high vapor pressure and low solubility, it can travel over great distances through the air, deposit in remote areas and there accumulate to hazardous levels within the muscle tissue of fish. By being able to measure the amount of mercury in the air, it is hoped that a better understanding of its transport and fate will result. This in turn may lead to methods for reducing its hazardous impacts on a regional and global scale.

The work described within this thesis may be separated into its two goals. The first was to solve the well defined problem of developing a methodology for measuring ambient vapor phase mercury using instrumental neutron activation analysis, and then applying the methodology in a long term monitoring program in Upstate New York. The second goal, which is more closely linked to the work's motivation, was to use the data resulting from this monitoring program to better understand the sources and fate of atmospheric mercury. Specifically how the data was going to enable this goal to be attained was not known when the sampling began, and the issues involved are far more open ended than those relating to the first goal. As the initial data becomes joined with additional information and as new questions arise, the investigation both by this lab and by other researchers will continue.

Neutron activation has been used for decades as a method of elemental analysis, and indeed was applied to mercury in 1969 by this thesis' supervisor. Despite the method's sensitivity, selectivity, and the advantages it has over other methods for measuring mercury, problems with mercury's volatility, and spectral interferences have kept the method from being commonly used. Likewise, the collection of mercury by activated charcoal has been applied before, but because the subsequent analysis required the re-volatilization of the mercury, contamination was a common problem. However, by combining these two techniques and by solving both well known and unexpected problems with both, a new operationally simple, versatile, and sensitive methodology has been developed.

The accomplishments and improvements in the various parts of the methodology, and some of the difficulties which were overcome are summarized below.

Sample Collection:

- An automated air sampling system was designed and constructed which reliably collected four atmospheric mercury samples each week for two years at five Upstate New York locations.
- Problems with the collection efficiency of the activated charcoal sorbent were identified and measured; a new, iodated charcoal found which does not exhibit this behavior.
- An efficiency calibration procedure has been developed using a low concentration mercury source so that the efficiency of sorbents used in future collection programs may be checked routinely.

Sample Analysis:

- The sensitivity of mercury determinations by neutron activation was increased through the analysis of the 77 keV gamma ray emitted by  $^{197}\text{Hg}$  rather than the more commonly used 279 keV gamma ray emitted by  $^{203}\text{Hg}$ .
- Spectral interferences previously encountered when applying INAA to mercury determinations were also solved by employing the 77 keV gamma emission.
- The gamma ray counting procedures were optimized and the detector's shielding were modified to increase the analytical sensitivity.
- Loss of volatile mercury from the samples during irradiation was not encountered because the irradiation facility employed at the MITR-II is cooled to room temperature.
- Mercury contamination of the samples during irradiation was identified and prevented by heat sealing the samples in polyethylene vials and the mercury standards in quartz.

The entire methodology can now be used to routinely measure vapor phase mercury at levels found in ambient air with an accuracy of 5% - 15% (depending on concentrations and sample duration). The sensitivity and

accuracy of this methodology are comparable to others (Fitzgerald, 1979; Keeler, 1992; and Slemr, 1979) but, due to its non-destructive nature, is less prone to contamination and/or loss affected by other chemical species. It will continue to be applied by this lab at other locations and as of this writing is being used by other investigators in Budapest Hungary and Ankara Turkey. The complete methodology as well as the analytical techniques can also be used to study other environmental samples and media in order to understand the complete mercury cycle from source to sink. Future applications are listed below, some of which have already been employed by this lab.

- The direct analysis of mercury in raw source materials including coal, fuel oil, and motor oil, which are difficult to analyze by standard methods.
- Emission's measurements of atmospheric sources themselves such as electric utility, incinerator, and industrial smokestacks, and motor vehicle exhaust.
- The study of urban air which contains higher levels of mercury than air in remote locations, and is possibly influence by more local sources.
- Wet deposition measurements for both soluble and insoluble mercury; the former may be extracted through the use of ion exchange resins which can be analyzed directly by INAA. This will enable three phase atmospheric sampling and analysis by INAA.
- Mercury determinations of biological receptors obviously including aquatic animals but also unique cumulative receptors such as human hair and bird feathers.

The specific application which prompted this project was the measurement of ambient vapor phase mercury at five locations in Upstate New York for a two year period. Four 24-hour samples were taken each week at these sites from July 15, 1992 through July 29, 1994. The atmospheric mercury data set which resulted from this sampling program is among the largest in terms of both duration and the regional distribution covered by the collections. It is also unique in its inclusion of matching, detailed elemental aerosol analyses. It has provided the opportunity to pursue the second goal of

this research which is to better understand the sources and fate of atmospheric mercury. Several important features were found using this and other available data.

#### Overall Mercury Patterns

- There was a common overall yearly pattern in the vapor phase mercury concentrations among all five sampling locations, indicating that the major influences are of a large regional and temporal scale.
- The particulate mercury concentrations were similar at some, but not all of the sites and they did not correlate with the vapor phase concentrations. Thus particulate mercury either originates from different sources than vapor phase mercury, or is subject to different transport phenomena.

#### Source Identification

- Factor analysis was used to find commonalities between vapor phase mercury and elemental particulate concentrations.
- Using characteristic elemental source profiles obtained from particulate data, four major source types were identified as affecting mercury concentrations at Perch River.
- Wind trajectories corresponding to the greatest influences of these source types originated from industrial centers in Canada and the U. S.

#### Atmospheric Transformations

- The high winter and low summer mercury levels showed an inverse relationship to tropospheric ozone which is the oxidant primarily responsible for the removal of vapor phase mercury from the atmosphere by wet deposition.
- This pattern and mechanism would also match the higher mercury concentrations found in summer wet deposition by other researchers.

Though the interpretation of this data provides useful information about mercury's atmospheric sources and transport, the analysis is by no

means complete. Further information and resources will be need to be incorporated before a significantly more complete understanding of atmospheric mercury is reached. Some of these may be available to this laboratory in the near future, while more will be employed as the data from this study reaches other researchers. Recommended future analysis of the results should include the approaches given below.

#### Source Identification

- The use of better and more specific compositional profiles for source identification by receptor modeling. Some of these may require additional measurements of various types of emissions.
- The application of chemical mass balance techniques when the above source profiles become available.
- Apportioning the influence of the identified sources in terms of their impact on the Upstate New York region.

#### Atmospheric Transformations

- Ozone measurements for the remainder of the sampling period need to be tabulated to confirm the inverse relationship between ozone and vapor phase mercury.
- The inclusion of available wet deposition concentrations or the implementation of wet deposition sampling and analysis by INAA. This will provide closure in the atmospheric mercury measurements for study from source to sink.
- The application of atmospheric chemical and physical modeling through the inclusion of these and other measured values.

## 7. REFERENCES

- Alexandrov, S., Lead sulphide as a sorbent for the preconcentration of mercury from air and determination of mercury by atomic emission spectroscopy, *Fresenius' Zeitschrift für Analytische Chemie*, 321, 578-580, 1985.
- Billman Stunder, B. J., J. L. Heffter, and U. Dayan, Trajectory analysis of wet deposition at Whiteface Mountain: a sensitivity study, *Atmospheric Environment*, 20, 9, 1691-1695, 1986.
- BITC, (Bureau International Technique du Chlore) the mercury analysis working party of, *Analytica Chimica Acta*, 108, 1-11, 1979.
- Bloom, N. S., E. M. Prestbo, and V. L. Miklavcic, Fluegas mercury emissions and speciation from fossil fuel combustion, Presented at: *Conference on Managing Air Toxics: State of the Art*, Electric Power Research Institute, Washington DC, 1993.
- Bloom, N., and W. F. Fitzgerald, Determination of volatile mercury species at the picogram level by low-temperature gas chromatography with cold-vapour atomic fluorescence detection, *Analytica Chimica Acta*, 208, 151-161, 1988.
- BNA (The Bureau of National Affairs), *The Clean Air Act Amendments: BNA's Comprehensive Analysis of the New Law*, The Bureau of National Affairs, 1991.
- Bothner, M. H., R. A. Jahnke, M. L. Peterson, and R. Carpenter, Rate of mercury loss from contaminated estuarine sediments, *Geochimica et Cosmochimica Acta*, 44, 273-285, 1980.
- Brzezinska-Paudyn, A., J. C. Van Loon, and M. R. Balicki, Multielement analysis and mercury speciation in atmospheric samples from the Toronto area, *Water, Air, and Soil Pollution*, 27, 45-56, 1986.
- Canberra Nuclear, *Instruments Catalog, Edition 9*, Canberra Industries, Inc.-Nuclear Products Group, Meriden, CT, 34, 1991.
- D'Itri, F. M., *The Environmental Mercury Problem*, CRC Press, 1972.
- DeVito, M. S., and N. Bloom, Sampling and analysis of mercury in combustion flue gas, *Proceedings: Second International Conference of Managing Hazardous Air Pollutants*, 1993, Electric Power Research Institute, VII-39-68, 1993.



- Douglas, J., Mercury and the global environment, *EPRI Journal*, April/May, 1994, 14-21.
- Dumarey, R., R. Heindryckx, R. Dams, and J. Hoste, Determination of volatile mercury compounds in air with the coleman mercury analyzer system, *Analytica Chimica Acta*, 107, 159-167, 1979.
- Edner, H., G. W. Faris, A. Sunesson, and S. Svanberg, Atmospheric atomic mercury monitoring using differential absorption lidar techniques, *Applied Optics*, 28, 5, 921-929, 1989.
- Expert Panel on mercury atmospheric processes, *Mercury Atmospheric Processes: a Synthesis Report*, EPRI report TR-104214, Ed. R. H. Osa, 1994.
- Fitzgerald, W. F., and G. A. Gill, Subnanogram determination of mercury by two-stage gold amalgamation and gas phase detection applied to atmospheric analysis, *Analytical Chemistry*, 51, 11, 1714-1720, 1979.
- Fitzgerald, W. F., Mercury as a global pollutant, *The World & I, Natural Science*, October 1993, 192-199, 1993.
- Garber, D. I., and R. R. Kinsey, editors, *Neutron Cross Sections, Volume II, Curves*, Brookhaven National Laboratory, Associated Universities, Inc., 1976.
- Germani, M. S., And W. H. Zoller, Vapor phase concentrations of Arsenic, Selenium, bromine, iodine, and mercury in the stack of a coal-fired power plant, *Environmental Science and Technology*, 22, 9, 1079-1085, 1988.
- Henry, A. F., *Nuclear Reactor Analysis*, The MIT Press, 105, 1986.
- Hopke, P. K., *Receptor Modeling in Environmental Chemistry*, John Wiley & Sons, 1985.
- Iverfeldt, Å. and O. Linqvist, Atmospheric oxidation of elemental mercury by ozone in the aqueous phase, *Atmospheric Environment*, 20, 1567-1573, 1986.
- Iverfeldt, Å., Mercury in forest canopy throughfall water and its relation to artmospheric deposition, *Water, Air, and Soil Pollution*, 56, 553-564, 1991.
- Jepsen, A. F., Measurements of mercury vapor in the environment, *Trace Elements in the Environment*, 81-95, 1972.
- Keeler, G. J., M. E. Hoyer, and C. H. Lamborg, Measurements of Atmospheric mercury in the Great Lakes Basin, *Mercury as a Global Pollutant: Toward Integration and Synthesis*, Ed. J. Huckabee and C. Watras, Lewis Publishers, Boca Raton, FL, 1992.

- Kim, J. I., and S. R. Sunoko, Activation analysis of mercury in biological samples, *Journal of Radioanalytical Chemistry*, 16, 257-267, 1973.
- Kitto, M. E., D. L. Anderson, and W. H. Zoller, Simultaneous collection of particles and gases followed by multielement analysis using nuclear techniques, *Journal of Atmospheric Chemistry*, 7, 241-259, 1988.
- Knoll, G. F., *Radiation Detection and Measurement, second edition*, John Wiley & Sons, 1989.
- Kurland, L. T., S. N. Faro, and H. Seidler, Minamata Disease, *World Neurology*, 1, 370, 1960.
- Lindberg, S. E., Mercury partitioning in a power plant plume and its influence on atmospheric removal mechanisms, *Atmospheric Environment*, 14, 227-231, 1980.
- Lindberg, S. E., in *Toxic Metals in the Atmosphere*, John Wiley and Sons, 1986.
- Lindberg, S. E., T. P. Meyers, G. E. Taylor, Jr. R. R. Turner, and W. H. Schroeder, Atmosphere-surface exchange of mercury in a forest: Results of modeling and gradient approaches, *Journal of Geophysical Research*, 97, D2, 2519-2528, 1992.
- Lindqvist, O., Atmospheric mercury—a review, *Tellus*, 37B, 136-159, 1985.
- Mason, R. P., W. F. Fitzgerald, and G. M. Vandal, The sources and composition of mercury in Pacific Ocean rain, *Journal of Atmospheric Chemistry*, 14, 1-4, 489-500, 1992.
- Mason, R. P., W. F. Fitzgerald, and F. M. M. Morel, The biogeochemical cycling of elemental mercury: Anthropogenic influences, *Geochimica et Cosmochimica Acta*, 58, 15, 3191-3198, 1994.
- Milley, J. E., and A. Chatt, Preconcentration and instrumental neutron activation analysis of acid rain for trace elements, *Journal of Radioanalytical and Nuclear Chemistry*, 110, 2, 345-363, 1987.
- Moore, T., Hazardous air pollutants: measuring in micrograms, *EPRI Journal*, January/February, 1994, 6-15.
- Murphy, P. J., Determination of nanogram quantities of mercury in liquid matrices by a gold film mercury detector, *Analytical Chemistry*, 51, 9, 1599-1600, 1979.
- Nater, E. A., and D. F. Gringal, Regional trends in mercury distribution across the Great Lakes states, north central USA, *Nature*, 358, 139, 1992.

- Olmez, I., and N. K. Aras, Determination of mercury in selected fishes living in Turkish coast by neutron activation analysis, *Radiochemical and Radioanalytical Letters*, 22, 19-23, 1975.
- Olmez, I., Instrumental neutron activation analysis of atmospheric particulate matter, in *Methods of Air Sampling and Analysis*, 3rd edition, Lewis Publishers, Inc., 143-150, 1989.
- Olmez, I., M. Ames, J. Che, S. Meier, and P. Galvin, Elemental composition of charcoal sorbants, *Proceedings: Second International Conference of Managing Hazardous Air Pollutants*, 1993, Electric Power Research Institute, VII-145-162, 1993a.
- Olmez, I., M. Ames, and N. K. Aras, Mercury determination in environmental materials: methodology for instrumental neutron activation analysis, *Proceedings of the 1993 U.S. EPA/A&WMA International Symposium: Measurements of Toxic and Related Air Pollutants*, Air & Waste Management Association, 1993b.
- Olmez, I., X. Huang, and M. R. Ames, The role of instrumental neutron activation in environmental mercury analysis, to appear in: *Proceedings: AWMA 88th Annual Meeting & Exhibition*, San Antonio, TX, 1995.
- Peterson, G., B. Schneider, D. Eppel, H. Grassl, A. Iverfeldt, P. K. Misra, R. Bloxam, S. Wong, W. H. Schroeder, E. Voldner, and J. Pacyna, Numerical modelling of the atmospheric transport, chemical transformations and deposition of mercury, *18th International Technical Meeting on Air Pollution Modelling*, Vancouver, B.C., 1990.
- Pfeiffer, W. C., and L. Drude de Lacerda, Mercury inputs into the Amazon region, Brazil, *Environmental Technology Letters*, 9, 325-330, 1988.
- Raloff, J. (1), Mercurial airs: tallying who's to blame, *Science News*, 145, 8, 119, 1994a.
- Raloff, J. (2), More illuminating statistics on mercury, *Science News*, 145, 10, 142, 1994b.
- Schroeder, W. H., and R. A. Jackson, An instrumental analytical technique for speciation of atmospheric mercury, *International Journal of Environmental Analytical Chemistry*, 22, 1-18, 1985.
- Schierling, P., and K. H. Schaller, Quantitative determination of metallic mercury in air, *Atomic Spectroscopy*, 2, 3, 91-92, 1981.

- Seigner, C., J. Wrobel, and E. Constantinou, A chemical kinetic mechanism for atmospheric inorganic mercury, *Environmental Science and Technology*, 28, 1589-1597, 1994.
- Seinfeld, J. H., *Atmospheric Chemistry and Physics of Air Pollution*, John Wiley & Sons, 1986.
- SKC, *Comprehensive Catalog and Guide, Summer 1992*, SKC Inc., Eighty-four, PA, 1992.
- Slemr, F., W. Seiler, C. Eberling,, and, P. Roggendorf, The determination of total gaseous mercury in air at background levels, *Analytica Chimica Acta*, 110, 35-47, 1979.
- Slemr, F., G. Schuster, and W. Seiler, Distribution, speciation, and budget of atmospheric mercury, *Journal of Atmospheric Chemistry*, 3, 407-434, 1985.
- Slemr, F., and E. Langer, Increase in global atmospheric concentrations of mercury inferred from measurements over the Atlantic Ocean, *Nature*, 355, 434, 1992.
- Soldano, B. A., P. Bien, and P Kwan, Air-borne organo-mercury and elemental mercury emissions with emphasis on central sewage facilities, *Atmospheric Environment*, 9, 941-944, 1975.
- Sorensen, J. A., G. E. Glass, K. W. Schmidt, J. K. Huber, and G. R. Rapp Jr., Airborne mercury deposition and watershed characteristics in relation to mercury concentrations in water, sediments, plankton, and fish of eighty northern Minnesota lakes, *Environmental Science and Technology*, 24, 11, 1716-1727, 1990.
- Taylor, M., Re-usable sampling tubes for monitoring airborne mercury vapour concentrations: sample collection and analysis by cold vapor atomic-absorption spectrometry, *Analysit*, 108, 265-276, 1983.
- van der Sloot, H. A., *Neutron Activation Analysis of Trace Elements in Water Samples After Preconcentration on Activated Carbon*, Netherlands Energy Research Foundation, Petten, The Netherlands, 1976.

**APPENDIX A. ELEMENTAL COMPOSITION OF COMMERCIALY AVAILABLE CHARCOAL SORBENTS**

**CHARCOAL LABELS AND TYPES.**

LABEL	CHARCOAL	TYPE
SKC120	SKC for Organic Collection	Granular
SKCTRT	SKC Treated	Granular, Iodated
SKCPET	SKC Petroleum Derived	Granular
SKCCAR	SKC Carbide	Granular
SKCMER	SKC for Mercury Collection	Hopcalite (Cu-Mn oxide)
MSAOHC	Mine Safety Appliance for Organic Collection	Granular
AWCB1	SKC Anasorb 1	Spherical
ANACMS	SKC Anasorb CMS	Spherical
ANA747	SKC Anasorb	Spherical
1005-03	SKC Granular	Granular
EMBULK	EM Scientific Granular	Granular
SPECGRAN	Spectrum Scientific Granular	Granular
SPECCOC	Spectrum Scientific Coconut	Granular
AWCB2	SKC Anasorb 2	Spherical
SIGGRAN	Sigma Scientific Granular	Granular
SIGACID	Sigma Scientific Acid Washed	Powdered
CALG	Calgon Carbon Coconut	Granular, Steam Activated
CYAK	Cameron-Yakima	Granular, Steam Activated, Iodated

Elemental Concentrations of Activated Charcoal Sorbents (ppm). Blank +/- values indicate concentrations below the detection limit which is shown in the concentration column.

Element	SKC120	+/-	SKCTRT	+/-	SKCPET	+/-
Na	600	190	440	140	940	300
Sc	3.5	0.2	23	2	0.24	0.02
Cr	16	1	1.2	0.1	1.6	0.1
Fe	3490	140	180	10	1090	40
Co	11	1	0.26	0.01	0.53	0.03
Zn	0.41		1.3	0.2	1.3	0.3
As	9.5	1.7	0.57	0.11	0.26	0.08
Se	1.5	0.3	0.15	0.04	0.07	0.029
Br	0.55	0.34	1	0.6	1.7	1
Rb	3.9	0.5	64	7	37	4
Mo	3.6	0.9	0.61	0.16	0.29	0.09
Cd	0.056	0.035	0.0079	0.0067	4	4
Sb	1.5	0.1	0.52	0.05	0.079	0.008
Cs	0.25	0.03	0.65	0.07	0.35	0.04
Ba	110	10	8.8	1.1	11	1
La	9.1	0.6	0.099	0.007	0.54	0.04
Ce	18	1	0.2	0.02	1	0.1
Nd	9	1.1	0.05	0.02	0.36	0.05
Sm	1.8	0.2	0.013	0.001	0.068	0.006
Eu	0.34	0.04	0.0014	0.0007	0.02	0.004
Tb	0.3	0.06	0.0052	0.0018	0.012	0.003
Yb	0.76	0.13	0.0031	0.0023	0.034	0.006
Lu	0.13	0.03	0.0016	0.0004	0.0062	0.0014
Hf	0.44	0.04	0.011	0.003	0.04	0.005
Ta	0.071	0.03	0.0029	0.0029	0.011	0.01
Au*	0.33	0.06	0.019	0.007	0.022	0.015
Hg*	10	10	38	7	14	6
Th	1.5	0.1	0.023	0.003	0.19	0.01
U	1.1	0.1	0.01	0.009	0.037	0.012

\* ppb

Elemental Concentrations of Activated Charcoal Sorbents (ppm). Blank +/- values indicate concentrations below the detection limit which is shown in the concentration column.

Element	SKCCAR	+/-	SKCMER	+/-	MSAOHC	+/-
Na	1710	540	300	90	140	20
Sc	0.79	0.05	0.0011	0.0003	0.0071	0.0005
Cr	19	1	21	1	0.19	0.02
Fe	2250	90	280	10	73	3
Co	1.5	0.1	0.43	0.02	0.19	0.01
Zn	2.5	0.6	1.8	0.3	0.84	0.12
As	7.7	1.3	0.13	0.06	0.054	0.022
Se	0.7	0.18	0.077	0.051	0.072	0.023
Br	0.11	0.08	0.23	0.14	0.41	0.17
Rb	1.4	0.3	9.5	1.1	9.9	0.9
Mo	1.2	0.3	2.5	0.7	0.023	0.018
Cd	0.019	0.017	0.023	0.02	0.027	
Sb	0.28	0.03	1.7	0.2	0.051	0.004
Cs	0.08	0.013	46	5	0.54	0.05
Ba	0.021	0.002	4.8	1.4	5.5	0.8
La	1.9	0.1	2.5	0.2	0.023	0.003
Ce	3.7	0.2	430	20	0.052	0.01
Nd	1.5	0.2	1.2	0.2	0.057	
Sm	0.31	0.03	0.18	0.02	0.0033	0.0004
Eu	0.054	0.007	0.14	0.02	0.005	0.0012
Tb	0.051	0.01	0.0051	0.0023	0.0034	0.0028
Yb	0.24	0.04	0.014		0.0043	0.0013
Lu	0.039	0.009	0.011		0.00037	0.00019
Hf	0.3	0.02	0.014		0.0033	0.0019
Ta	0.073	0.03	0.02	0.013	0.011	
Au*	0.048	0.013	0.018	0.013	0.009	0.0008
Hg*	20	7	36	8	31	8
Th	0.83	0.05	0.012		0.0032	0.0002
U	0.32	0.03	0.043		0.0071	0.0071

\*ppb

Elemental Concentrations of Activated Charcoal Sorbents (ppm). Blank +/- values indicate concentrations below the detection limit which is shown in the concentration column.

Element	AWCB1	+/-	AMACMS	+/-	ANA747	+/-
Na	51	7	2.3	1.2	11	2
Sc	0.012	0.001	0.0042	0.0003	0.00017	0.00009
Cr	0.48	0.02	0.081	0.008	1.1	0.1
Fe	44	3	0.71	0.65	130	10
Co	3	0.2	0.0067	0.0027	0.052	0.004
Zn	0.48	0.12	0.14	0.04	0.06	0.029
As	0.7	0.09	0.03		0.031	0.015
Se	0.078	0.017	0.0082	0.0082	0.012	
Br	0.12	0.05	0.18	0.08	0.036	0.021
Rb	0.71	0.14	0.17	0.05	0.068	
Mo	0.25	0.06	0.05	0.01	0.017	
Cd	0.0074		0.0064		0.014	
Sb	0.043	0.004	0.0092	0.0013	0.0054	0.0009
Cs	0.013	0.005	0.022	0.004	0.0045	
Ba	3.8	0.6	0.58		0.29	0.18
La	0.29	0.02	0.34	0.02	0.074	0.005
Ce	0.58	0.03	0.78	0.04	0.21	0.01
Nd	0.15	0.02	0.2	0.02	0.063	0.009
Sm	0.0074	0.0007	0.0006	0.00012	0.00016	0.00009
Eu	0.0021	0.0009	0.002		0.0012	
Tb	0.0023	0.001	0.0014		0.00088	0.0008
Yb	0.013	0.003	0.00035	0.00024	0.00061	0.00041
Lu	0.002	0.0005	0.00009	0.000075	0.0001	0.00007
Hf	0.7	0.05	0.0028	0.0021	0.0017	
Ta	0.012	0.005	0.0052	0.0034	0.0037	0.0027
Au*	0.029	0.005	0.0047		0.0036	0.0015
Hg*	21	2	11	2	9.8	1.2
Th	0.025	0.003	0.0025	0.0008	0.0013	
U	0.18	0.01	0.0037	0.0023	0.0083	0.0037

\* ppb



Elemental Concentrations of Activated Charcoal Sorbents (ppm). Blank +/- values indicate concentrations below the detection limit which is shown in the concentration column.

Element	100503	+/-	EMBULK	+/-	SPECGRAN	+/-
Na	460	110	2260	540	2840	680
Sc	2.7	0.2	4	0.3	6.4	0.4
Cr	96	2	18	1	19	1
Fe	2220	90	2810	110	2160	90
Co	9.3	0.5	7.5	0.4	6	0.3
Zn	0.48		4.9	1.1	8.5	1.5
As	7.1	1.3	15	3	13	2
Se	1.4	0.3	12	2	10	2
Br	1.1	1.1	4.7	4.7	4.2	4.2
Rb	4.9	0.7	4.7	0.9	6.2	0.9
Mo	4.6	1.2	11	3	8.9	2.2
Cd	0.028	0.02	0.051	0.036	0.081	0.049
Sb	1.5	0.1	4.4	0.4	3.7	0.3
Cs	0.29	0.04	0.43	0.06	0.4	0.06
Ba	66	6	910	70	840	60
La	4.5	0.3	6	0.4	6.6	0.4
Ce	8.9	0.4	11	1	13	1
Nd	3.1	0.4	4.1	0.5	4.9	0.6
Sm	0.79	0.07	1	0.1	1.2	0.1
Eu	0.19	0.02	0.18	0.02	0.21	0.03
Tb	0.12	0.02	0.29	0.11	0.41	0.14
Yb	0.36	0.06	0.79	0.13	0.93	0.15
Lu	0.065	0.014	0.17	0.04	0.19	0.04
Hf	0.46	0.04	2.4	0.2	2.2	0.2
Ta	0.07	0.022	0.32	0.08	0.28	0.07
Au*	0.024	0.002	0.079	0.004	0.051	0.004
Hg*	99	9	36		24	
Th	1.8	0.1	7.2	0.4	6.2	0.4
U	1.6	0.2	8.2	0.9	6.6	0.8

\* ppb

Elemental Concentrations of Activated Charcoal Sorbents (ppm). Blank +/- values indicate concentrations below the detection limit which is shown in the concentration column.

Element	SPECCOC	+/-	AWCB2	+/-	SIGGRAN	+/-
Na	780	190	10	3	1560	220
Sc	0.0045	0.0004	0.014	0.001	0.37	0.02
Cr	50	12	0.41	0.01	2.9	0.1
Fe	31	2	53	3	3760	150
Co	0.17	0.01	2.5	0.1	0.98	0.05
Zn	1.2	0.2	0.23	0.05	1.2	0.3
As	0.036	0.022	0.66	0.12	5.8	0.7
Se	0.021	0.012	0.027	0.008	0.82	0.13
Br	2.6	2.6	0.11	0.11	28	13
Rb	30	3	0.15		2.1	0.3
Mo	0.015	0.015	0.24	0.06	0.48	0.13
Cd	0.0081		0.0062		0.027	0.022
Sb	0.019	0.002	0.033	0.003	0.32	0.03
Cs	0.43	0.05	0.0037	0.0025	0.11	0.02
Ba	3.2	0.6	2.2	0.4	79	5
La	0.022	0.002	0.04	0.003	1.3	0.1
Ce	0.06	0.009	0.075	0.005	2.4	0.1
Nd	0.034	0.016	0.058	0.01	1.2	0.1
Sm	0.0017	0.0003	0.008	0.0007	0.18	0.02
Eu	0.0021	0.0011	0.0012	0.0007	0.039	0.005
Tb	0.0055		0.00055	0.00022	0.024	0.009
Yb	0.0027	0.0009	0.01	0.002	0.093	0.015
Lu	0.00041	0.00017	0.0027	0.0006	0.017	0.004
Hf	0.0032		0.58	0.04	0.28	0.02
Ta	0.0054	0.0037	0.0044		0.04	0.017
Au*	0.0021	0.0006	0.0036	0.0005	0.0049	0.0016
Hg*	5.3	3.6	16	2	87	9
Th	0.0032		0.019	0.001	0.33	0.02
U	0.016	0.009	0.2	0.02	0.034	

\*ppb

Elemental Concentrations of Activated Charcoal Sorbents (ppm). Blank +/- values indicate concentrations below the detection limit which is shown in the concentration column.

Element	SIGACID	+/-	CALG	±	CYAK	±
Na	1480	200	330	45	1052	88
Sc	0.22	0.01	0.019	0.0013	0.026	0.002
Cr	17	1	0.315	0.02	335	7
Fe	670	30	123	7	273	18
Co	0.39	0.02	0.21	0.01	0.121	0.023
Zn	1.6	0.2	1.1	0.1	1.450	0.625
As	1.6	0.2	0.0775	0.022	0.109	0.014
Se	0.91	0.13	0.0555	0.02	0.078	0.073
Br	4.2	1.9	2.05	0.9	0.538	0.180
Rb	0.45	0.12	26.5	2	58	5.25
Mo	0.39	0.1	0.0485	0.0095	0.064	0.034
Cd	0.012	0.012	0.0195	0	0.014	0.014
Sb	0.23	0.02	0.0425	0.0035	0.033	0.003
Cs	0.02	0.007	0.675	0.065	0.775	0.073
Ba	0.036	0.002	3.5	0.6	6.73	1.53
La	1.1	0.1	0.0375	0.003	0.124	0.010
Ce	2.2	0.1	0.0765	0.0095	0.658	0.063
Nd	0.78	0.1	0.0745	0.0225	0.114	0.070
Sm	0.11	0.01	0.0038	0.0005	0.017	0.001
Eu	0.018	0.003	0.0045	0.0011	0.016	
Tb	0.0099	0.0045	0.0011	0	0.010	0.006
Yb	0.073	0.012	0.00255	0.0014	0.010	0.003
Lu	0.015	0.003	0.00052	0.00021	0.002	0.001
Hf	0.57	0.04	0.0038	0.0015	0.017	0.008
Ta	0.061	0.014	0.00855	0	0.091	
Au*	0.29	0.003	0.00725	0.0007	0.083	0.026
Hg*	2.3	2.3	9.6	4.35	11.53	3.28
Th	0.48	0.03	0.00345	0.00145	0.201	0.014
U	0.08	0.009	0.0145	0	0.012	0.005

\* ppb

## APPENDIX B. SITE OPERATING PROCEDURES AND SAMPLE DATA SHEETS

### M.I.T. ER&R Atmospheric Sampling Programs Vapor Phase Mercury Sampler Site Operating Procedures

#### A. Changing the Sorbant/Filter Sample Assemblies

Four sorbant/filter sample assemblies are provided for each week of sampling, these include a black filter holder with cap and site/date/channel label attached, a Teflon sorbant tube, and an automatic shut-off quick connect plug. To put the first assemblies into the sampler or to change the assemblies:

1. Remove the hold-down link from the front of the roof of the sampler, open the roof, and prop it up with the rod tucked under its front supports.
2. Press the filter holder caps with the red center buttons back onto the filter holders.
3. Push down on the metal tab on top of the quick-connect sockets and pull the sample assemblies straight out by holding the white quick-connect plug.
4. Insert the new sample assemblies by pushing the quick-connect plug into the socket until it clicks and locks in. If it can not be inserted push down on the metal tab on top of the socket until it clicks open. The sample assemblies are numbered from 1-4 and should be inserted so they are in order from left to right.

Next, operate each sampling channel manually to check for leaks, adjust the vacuum relief valve if necessary, and record each channel's flow rate:

5. Open the sampler's front door and turn the handle of the valve over the flow meter (in the upper-right front of the sampler) so that it points down at the flow meter.
6. Open the door of the TORK Z400 electronic controller and turn on the first sampling channel by moving the silver slide switch next to the channel one light (at the top left of the control panel) to the on (left) position.
7. Adjust the vacuum regulator so that the gauge indicates 20 inches of mercury vacuum. Turning the knob counter-clockwise will increase the vacuum (the gauge will also move counter-clockwise).
8. Check for leaks in the system by seeing if the balls in the flow meter are resting at the bottom of the tube. A small leak may be observed if the cap on the sample assembly's filter holder is loose. If this is the case press the cap on tightly. If the balls are resting at the bottom of the tube place a check mark on the mercury sampler data sheet next to leak test and under channel one. If there is a leak record the height of the black ball in this space (see step 9).
9. Remove the cap from the filter holder and record the height of the black ball in the flow meter; the reading should be taken at the center of the ball. If the black ball is higher than 150 mm. then record the height of the silver ball and note this on the sampler data sheet under "comments".
10. Return the silver slide switch to the auto (center) position. It is important that the switch is not in the off (right) position or no sample will be taken for that channel.
11. Repeat steps 6 through 10 for channels 2,3, and 4, recording the results of the leak check, the vacuum reading, and the flow reading for each channel on the data sheet.

12. Be sure that all four switches on the control panel are in the auto (center), and close the door of the electronic timer. Return the handle of the valve over the flow meter so that it points up to by-pass the flow meter during the sampling period. Close the main door of the sampler and turn the knob clockwise to hold it shut. Re-hang the prop for the roof on its hook on the front support, close the roof, and secure the hold-down link. If desired, the sampler can be secured using the lock installed in the door or by replacing the hold-down link with a small padlock.

## B. Programming the TORK Z400 Electronic Timer

The electronic timer will be programmed by MIT ER&R personnel either at MIT or when the sampler is installed at the site. If the timer's internal battery is left on and the unit does not malfunction during operation, there should be no need to reprogram the controller. If reprogramming becomes necessary the complete manual for the controller is included at the end of these procedures. The following hints may however be useful:

1. Do not switch off the battery, this keeps the date-time and program steps from being lost during a power outage.
2. The year-date setting may be checked by noting that the correct day of the week is indicated under the clock window.
3. Each channel's switching on and off requires one program step entered into the schedule. A normal program of four channels sampling in one week require eight program steps, four on steps and four off steps. If no off step is entered the channel will stay on all week.
4. When entering or reviewing any part of the program the advance key (ADV) moves the selected function downward through the cycle: CHANNEL, TIME, DAY, ON/OFF/DUTY CYCLE and then back to the top.
5. A program step is not entered and can be changed until the ENTER key is pressed.
6. The RUN/SET switch must be in the SET position to enter or change any program step, and must be returned to the RUN position when the changes are complete.
7. Be sure to check the AM/PM condition of each time entered in the program.

8. If there is a step in the program which is not correct, it must be deleted in the review mode, otherwise the schedule will not function correctly.
9. When setting or reviewing the program, the function which can be changed will have some part of it flashing (e.g. the colon in the time window).
10. An explicit procedure for programming the controller will be supplied by MIT for each sampling site and application.



Step-by-step program for the TORK Z400  
for the ESEERCO/ALSC sampling sites

Set the YEAR-DATE-TIME:

1. Clear all memory by gently inserting a small tool or pen tip into the hole above channel ON/AUTO/OFF switches or by temporarily turning off battery and main power.
2. Move RUN/SET switch to SET position.
3. Press the MODE SELECT button once so that the YEAR-DATE-TIME light is on and not flashing.
4. Enter the year (all four digits, e.g. 1992), press ADV (advance).
5. Enter the month and date as four digits (e.g. June 7 = 0607), press ADV, the correct day of the week should now be lit.
6. Enter the current time (twelve hour format) and press the AM-PM button once if it is after noon.
7. If there is some mistake in the program press ADV to go back to step 4, otherwise go to step 8.
8. If all steps are correct press ENTER, you will hear a double beep to indicate the YEAR-DATE-TIME has been set.

Set the Schedule:

1. Press the MODE SELECT button until the SCHEDULE light is on and not flashing.
2. Press 1 to select the channel being programmed, then press ADV.
3. Press 1200 (300 at Perch River) and the AM-PM button once to set the on time (noon), then press ADV.
4. Press WED and then MON to set the on day of the week, then press ADV.
5. The ON light will be flashing to indicate that this program step turns a channel on, if 2 - 5 were done correctly press ENTER to store this program step and go on to the next, if not press ADV to return to 2.
6. Press 1 to select the channel being programmed, then press ADV.
7. Press 1200 (300 at Perch River) and the AM-PM button once to set the off time (noon), then press ADV.

8. Press THU and then MON to set the off day of the week, then press ADV.
9. The ON light will be flashing, press ADV again so that the OFF light is flashing to indicate that this program step turns a channel off, if 6 - 9 were done correctly press ENTER to store this program step and go on to the next, if not press ADV to return to 6. Programming for channel 1 is now completed.
10. Repeat 2 - 9 except press 2 for the channel being programmed (#2 and #6), THU for the on day of the week (#4) and FRI for the off day of the week(#8).
11. Repeat 2 - 9 again except press 3 for the channel being programmed (#2 and #6), FRI for the on day of the week (#4) and SAT for the off day of the week(#8).
12. Repeat 2 - 9 again except press 4 for the channel being programmed (#2 and #6), SAT for the on day of the week (#4) and SUN for the off day of the week(#8).
13. If all the program steps are entered correctly return the RUN/SET switch to the RUN position to store the full program in the timer's memory.

MIT Nuclear Reactor Lab

VAPOR PHASE MERCURY SAMPLER DATA SHEET

SITE: \_\_\_\_\_

WEEK: \_\_\_\_\_ TO: \_\_\_\_\_

SYSTEM TESTS: (FIELD USE)

BEGINNING OF WEEK:

CHANNEL	1	2	3	4
LEAK TEST (put check if ok)				
VACUUM GAUGE READING (in. Hg)				
ROTAMETER READING (center of black ball)				

END OF WEEK: Please check yess or no.

TOTAL HOURS: \_\_\_\_\_

YES NO

System appears to have operated properly during the week. Record anything unusual in the COMMENTS section.

COMMENTS: \_\_\_\_\_

OBSERVER:

Signature: \_\_\_\_\_ Date: \_\_\_\_\_

In case of emergency, contact Dr. Ilhan Olmez or Mike Ames at the MIT Nuclear Reactor Lab: (617) 253-2995, or (617) 253-1743.

SAMPLES: (LABORATORY USE)

DATE \_\_\_\_\_ SAMPLE# \_\_\_\_\_

DATE \_\_\_\_\_ SAMPLE# \_\_\_\_\_

PUMP# \_\_\_\_\_ FLOW \_\_\_\_\_

PUMP# \_\_\_\_\_ FLOW \_\_\_\_\_

DATE \_\_\_\_\_ SAMPLE# \_\_\_\_\_

DATE \_\_\_\_\_ SAMPLE# \_\_\_\_\_

PUMP# \_\_\_\_\_ FLOW \_\_\_\_\_

PUMP# \_\_\_\_\_ FLOW \_\_\_\_\_

**APPENDIX C. VAPOR PHASE MERCURY CONCENTRATIONS IN  
UPSTATE NEW YORK (ng/m<sup>3</sup>, ± 1σ).**

Date/Site	BE	±	ML	±	PR	±	WE	±	WI	±
7/15/92			0.7	0.5	1.1	0.3			0.9	0.2
7/16/92			1.8	0.7	1.2	0.4			2.0	0.3
7/18/92			2.6	1.2	0.8	0.4			1.9	0.3
7/22/92			1.2	0.6	0.6	0.4			0.8	0.2
7/24/92			2.8	0.7	1.3	0.6			3.3	0.4
7/25/92					2.5	0.3			0.8	0.2
7/29/92	0.7	0.4	1.3	0.6	2.0	0.5			1.5	0.2
7/30/92									1.4	0.3
8/1/92			1.9	0.7	1.1	0.4	0.7	0.3		
8/5/92	2.2	0.3	2.2	0.2			5.4	0.4	1.9	0.2
8/7/92			3.7	0.3	1.8	0.6	1.3	0.2	1.9	0.2
8/8/92			3.2	0.3	1.8	0.4			1.5	0.2
8/12/92	1.0	0.2	0.6	0.2	2.2	0.3	1.5	0.3		
8/13/92	1.1	0.4	1.2	0.3	0.7	0.3			1.1	0.2
8/15/92	0.9	0.5			2.8	0.4	0.7	0.2	1.9	0.3
8/19/92					4.5	0.3				
8/20/92	3.1	0.2	2.2	0.2						
8/22/92					2.4	0.2				
8/26/92			0.9	0.4	1.7	0.6			1.8	0.5
8/27/92	0.6	0.5	2.0	0.5	4.8	0.5	0.6	0.2	0.8	0.3
8/29/92			1.6	1.5			0.8	0.2		
9/2/92									0.6	0.6
9/3/92									0.9	0.5
9/5/92									0.9	0.5
9/9/92					1.5	0.8	0.6	0.4		
9/10/92					0.7	0.6			0.8	0.5
9/12/92							0.8	0.4	2.6	0.9
9/16/92									1.4	0.5
9/17/92			0.9	0.8			0.6	0.4	0.7	0.4
9/23/92	1.3	0.5	0.6	0.6					1.6	0.7
9/24/92	1.0	0.3							0.8	0.4
9/26/92	1.0	0.7	1.0	0.9						
9/30/92	0.6	0.3								
10/7/92					1.3	0.5	0.6	0.3		
10/14/92	3.4	0.3	0.7	0.4	0.7	0.4	2.6	0.4	2.0	0.3
10/15/92	1.9	0.5	1.2	0.2	0.9	0.5	2.4	0.3	2.4	0.3
10/17/92							5.3	0.5	0.9	0.3
10/21/92							3.2	0.4	2.8	0.3

Vapor Phase Mercury Concentrations In Upstate New York (ng/m<sup>3</sup>, ± 1σ).

Date/Site	BE	±	ML	±	PR	±	WE	±	WI	±
10/22/92	2.2	0.4	0.7	0.3	1.1	0.6	4.2	0.3	1.1	0.3
10/24/92	0.6	0.4			1.9	0.5	2.8	0.6	2.1	0.3
10/28/92			0.7	0.5	0.8	0.8			0.8	0.2
10/29/92			0.6	0.3	2.4	0.5	4.8	0.4	0.7	0.2
10/30/92							4.5	0.3	1.9	0.3
11/4/92			0.8	0.4			1.3	0.3	2.2	0.4
11/5/92	0.6	0.3	0.8	0.2					1.3	0.3
11/7/92	0.7	0.2			1.5	0.3	0.6	0.2	1.0	0.2
11/11/92	2.4	0.3	1.1	0.3	2.7	0.2	0.8	0.3	3.3	0.5
11/12/92	2.0	0.4	2.4	0.3	0.7	0.3	0.9	0.4		
11/14/92	1.3	0.4			2.2	0.2	1.6	0.3	1.6	0.3
11/18/92	2.3	0.3	0.7	0.2	1.6	0.1	1.3	0.3	1.1	0.3
11/19/92	2.2	0.4	0.7	0.2	1.5	0.2	1.4	0.3	1.8	0.3
11/21/92	2.8	0.3	1.0	0.2			0.8	0.3	1.1	0.3
11/25/92	2.3	0.5								
11/26/92	2.3	0.4	1.4	0.3						
11/28/92	2.6	0.3	1.3	0.2						
12/2/92	1.9	0.1	1.2	0.1	1.3	0.1	1.1	0.1	0.9	0.0
12/3/92	3.4	0.2	1.4	0.1	1.2	0.1	1.9	0.1	1.4	0.1
12/5/92	2.2	0.2	1.6	0.1			1.2	0.1	1.4	0.1
12/9/92	3.0	0.2	1.4	0.1			3.4	0.2		
12/10/92	1.5	0.1	2.4	0.2	2.4	0.1				
12/12/92	1.0	0.1	2.4	0.2			1.9	0.1		
12/16/92	1.6	0.1	3.0	0.2	1.7	0.1	1.9	0.2	1.6	0.2
12/17/92	1.7	0.1	2.7	0.1	1.7	0.1	2.9	0.2	1.8	0.3
12/19/92	1.8	0.1	3.6	0.2	2.2	0.3	1.9	0.3	1.6	0.2
12/23/92	2.3	0.2	2.2	0.1	2.6	0.2	2.0	0.2	2.4	0.4
12/24/92	2.5	0.3	2.7	0.2	3.0	0.3	3.0	0.2	3.3	0.2
12/26/92	3.1	0.2	3.3	0.2	3.3	0.3	2.7	0.2	2.6	0.2
12/30/92	3.4	0.2	3.8	0.2	4.7	0.3	3.5	0.3	2.9	0.2
12/31/92	3.5	0.2	3.4	0.2	3.3	0.3	4.0	0.3	5.0	0.5
1/2/93	4.0	0.3	3.8	0.3	4.2	0.3	3.4	0.2	3.6	0.3
1/6/93	3.4	0.4	3.8	1.1	5.4	1.2	3.3	0.3	2.9	0.4
1/7/93	3.5	0.7	2.0	0.1	3.9	0.6	4.1	0.3	3.5	0.6
1/9/93	3.0	0.8	3.6	1.1	2.5	0.8	3.4	0.3	2.8	0.2
1/13/93	3.5	0.2	4.4	0.2	6.3	0.4	3.8	0.2	3.5	0.2
1/14/93	4.3	0.3	5.2	0.3	6.8	0.4	4.3	0.3	4.3	0.2
1/16/93	4.5	0.3	4.4	0.3	5.7	0.3	3.7	0.2	3.0	0.2
1/20/93	3.4	0.2	3.9	0.2	5.3	0.3	8.9	0.5	2.9	0.2

Vapor Phase Mercury Concentrations In Upstate New York (ng/m<sup>3</sup>, ± 1σ).

Date/Site	BE	±	ML	±	PR	±	WE	±	WI	±
1/21/93	3.5	0.2	4.0	0.3	5.7	0.3	6.3	0.3	2.9	0.2
1/23/93	3.7	0.2	3.3	0.2	5.8	0.3	5.7	0.3	4.7	0.2
1/27/93	3.0	0.2	7.1	0.4	5.2	0.3	7.2	0.4	6.0	0.3
1/28/93	3.1	0.2	4.5	0.3	6.7	0.4	5.1	0.3	5.3	0.3
1/30/93	3.6	0.2	3.6	0.2	6.3	0.3	5.7	0.3	6.4	0.3
2/3/93	3.0	0.2	2.3	0.2	4.3	0.3				
2/5/93	3.9	0.3	3.2	0.2	4.1	0.3			2.6	0.2
2/6/93	3.5	0.2	5.2	0.3	5.1	0.3			2.5	0.3
2/10/93	2.7	0.2	3.8	0.2	5.0	0.3			3.4	0.2
2/12/93	2.9	0.2	2.5	0.2	4.5	0.5			2.1	0.2
2/13/93	4.0	0.3	3.2	0.3	6.2	0.4			3.3	0.3
2/17/93	1.0	0.2	1.3	0.1	2.0	1.3			2.0	0.3
2/19/93	2.6	0.5	1.7	0.3	2.5	0.4			1.2	0.3
2/20/93	2.2	0.3	2.6	0.3	1.2	0.3			2.2	0.6
2/24/93	2.1	0.6	0.9	1.1	2.3	0.3	1.2	0.1	2.5	0.2
2/26/93	2.2	0.3	0.9	2.0	2.9	0.3	1.9	0.3	2.6	0.2
2/27/93	1.4	0.2	2.1	0.3	3.3	0.3	2.1	0.3	1.7	0.2
3/3/93	1.4	0.1	1.6	0.3	4.6	1.1	1.9	0.3	1.0	1.3
3/5/93	1.0	0.2	0.9	0.4	1.8	0.8	1.2	0.9	1.4	0.4
3/6/93	0.9	0.2	1.3	0.2	1.5	0.4	5.4	2.5	1.2	1.3
3/10/93	3.3	0.6	0.8	0.1	2.9	0.4	1.3	1.9	3.1	1.5
3/12/93	4.3	0.6	2.0	0.6	4.4	2.1	1.8	1.6	1.3	0.7
3/13/93	1.4	0.2	1.9	0.6	2.1	1.7	3.9	1.1	2.4	2.1
3/17/93	3.4	0.8	1.9	0.3	2.5	0.2	1.9	0.3	3.3	0.3
3/19/93	5.0	1.2	2.6	0.2	1.9	0.2	1.9	0.2	3.7	0.4
3/20/93	2.8	1.9	1.3	0.2	1.8	0.2	1.1	0.2	4.1	0.4
3/24/93	1.2	0.2	1.8	0.2	2.6	0.3	0.8	0.1	0.8	0.3
3/26/93	0.9	0.3	2.4	0.5	2.0	0.3	2.8	0.3	2.0	0.3
3/27/93	2.1	0.1	3.0	0.3	2.0	0.4	2.1	0.4	3.1	0.2
3/31/93	2.1	0.4	2.6	0.4	2.3	0.7	1.8	0.3	1.4	0.3
4/2/93	1.0	0.5	1.9	0.3	1.7	0.5	1.8	0.3	1.3	0.3
4/3/93	1.7	0.3	2.5	0.6	2.8	0.6	1.4	0.3	3.2	0.3
4/7/93	0.7	1.2	1.9	0.3	2.7	0.6	5.7	0.3	3.4	0.7
4/9/93	1.0	0.3	2.7	0.2	2.2	0.2	1.8	0.4	2.0	0.7
4/10/93	1.4	0.3	3.7	0.8	2.3	1.1	1.4	0.3	2.2	0.6
4/14/93	0.7	0.1	0.9	0.2	0.7	0.2	1.6	0.1	1.9	0.2
4/16/93	1.1	0.3			2.4	0.4	0.7	0.2	0.6	0.3
4/17/93	2.6	0.6			1.4	0.1	3.4	0.5		
4/21/93	2.0	0.2			2.0	0.2	1.5	0.3	0.8	0.1
4/23/93	1.2	0.2	1.5	0.2	5.2	0.4	3.3	0.5	1.1	0.3

Vapor Phase Mercury Concentrations In Upstate New York (ng/m<sup>3</sup>, ± 1σ).

Date/Site	BE	±	ML	±	PR	±	WE	±	WI	±
4/24/93	1.7	0.4	1.3	0.3	1.7	0.2	1.2	0.3	2.0	0.4
4/28/93	2.5	0.3	1.9	0.3	2.3	0.4	5.6	0.5	3.0	0.4
4/30/93	3.1	0.2	1.9	0.3	3.1	0.5	2.6	0.2	2.2	0.2
5/1/93	0.9	1.1	2.3	0.4	2.6	0.4	1.2	0.3	2.2	0.4
5/5/93	0.7	0.4	1.4	0.3	1.0	0.3	1.7	0.3	0.7	0.1
5/7/93	1.4	0.3	1.4	0.1	1.6	0.4	1.7	0.2	1.5	0.2
5/8/93	1.5	0.2	1.7	0.2	1.7	0.2	1.9	0.2	1.4	0.1
5/12/93	2.1	0.5	7.3	4.2	3.7	1.1	4.5	0.7	2.3	0.5
5/14/93	1.7	0.5	3.1	0.6	3.0	0.4	3.4	0.6	2.0	0.7
5/15/93	2.2	0.4	3.7	1.5			1.6	0.4	3.2	0.6
5/19/93	1.8	0.4	2.5	0.8	1.2	0.4	0.7	0.2	2.2	0.6
5/21/93	0.8	0.2			0.9	0.8	1.9	27.7	0.7	0.6
5/22/93	1.8	0.2	1.5	0.6			2.2	0.2	2.4	0.3
5/26/93			0.8	0.2			1.2	0.2	2.2	0.3
5/28/93	1.9	0.4			1.2	0.1	1.7	0.2	0.8	0.5
5/29/93	1.4	0.4	1.0	0.2			1.8	0.7	1.2	0.2
6/2/93	2.2	0.6	2.1	0.6	5.0	1.0	3.3	0.8	2.4	1.2
6/4/93	2.9	1.0	2.5	1.3	3.0	1.5	1.9	1.6	1.7	0.8
6/5/93	2.2	0.6	1.5	1.1			3.2	0.8	1.3	0.6
6/9/93			1.2	0.4	1.2	0.6	2.1	0.5	0.8	0.1
6/11/93			1.4	0.2	1.2	0.3	2.0	0.5	0.9	0.4
6/12/93			1.2	0.1			1.2	0.1	1.9	0.2
6/16/93	0.8	0.2	1.1	0.2	1.1	0.3	2.1	0.1	1.4	0.1
6/18/93	1.5	0.1			1.5	0.8			0.6	0.2
6/19/93	1.4	0.2					1.6	0.3	2.0	0.2
6/23/93	1.6	0.2			0.6	0.3	1.1	0.7	0.6	0.3
6/25/93	1.2	0.3					1.4	0.3	1.3	0.2
6/26/93			1.7	0.6			0.9	0.2		
6/30/93	1.2	0.2	2.2	0.4	1.6	0.2	3.5	0.3	1.5	0.2
7/2/93	0.9	0.2	1.1	0.3	1.2	0.4	1.6	0.2	1.3	0.3
7/3/93			0.7	0.1			1.9	0.5	1.1	0.5
7/7/93	1.1	0.3					1.5	0.2	1.3	0.3
7/9/93					1.1	0.4	2.2	0.2	1.4	0.3
7/10/93	1.0	0.2			0.8	0.2	1.2	0.3	2.0	0.6
7/14/93	0.8	0.2	1.4	0.7	1.3	0.2	1.8	0.6	0.8	0.1
7/16/93	0.8	0.1	1.1	0.2	0.8	0.1	1.9	0.2	1.1	0.3
7/17/93	1.1	0.3	1.2	0.3	0.7	0.1	2.2	0.4	1.7	0.3
7/21/93			0.7	0.2	1.6	0.2	0.8	0.3	1.9	0.3
7/23/93	0.7	0.2	1.7	0.3	1.6	0.3	1.3	0.3	1.1	0.3

Vapor Phase Mercury Concentrations In Upstate New York (ng/m<sup>3</sup>, ± 1σ).

Date/Site	BE	±	ML	±	PR	±	WE	±	WI	±
7/24/93	1.2	0.3	1.1	0.3	1.0	0.2	1.3	0.3	2.2	0.4
7/28/93	2.5	0.3	1.6	0.2	1.1	0.2	1.8	0.2	2.2	0.3
7/30/93	4.3	0.4	1.3	0.2	1.4	0.2	2.1	0.2	1.7	0.4
7/31/93	3.4	1.0	1.1	0.2	1.2	0.2	2.0	0.1	1.4	0.5
8/4/93					2.4	0.4	4.2	0.5	2.1	1.2
8/6/93	1.6	1.3			2.5	0.3	2.7	0.5	3.7	1.2
8/7/93	1.3	0.8					3.5	0.6	1.8	0.2
8/11/93	2.9	0.2					3.3	0.3	3.7	1.2
8/13/93	2.2	0.2	2.5	0.3	1.9	0.1	3.3	0.3	2.0	0.1
8/14/93	2.1	0.1	4.1	0.3	2.2	0.2			3.1	0.2
8/18/93	1.8	0.8	1.8	0.4	2.1	0.1	2.3	0.2	2.3	0.1
8/20/93	2.0	0.6	1.5	0.4	2.1	0.1	2.7	0.3	2.5	0.2
8/21/93	2.6	0.4	4.0	0.7	2.9	0.3	2.9	0.2	2.7	0.8
8/25/93	1.1	0.4	1.8	0.3	2.1	0.1			2.2	0.1
8/27/93	1.7	1.0	1.7	0.1	2.1	0.2			3.2	0.2
8/28/93	1.5	0.4	1.0	0.2	1.9	0.1			4.4	0.6
9/1/93	1.8	0.2	2.3	0.3	1.7	0.1	1.9	0.2	3.5	0.2
9/3/93			2.1	0.2	1.6	0.1	2.2	0.3	3.3	0.2
9/4/93			2.1	0.2	1.8	0.2	2.9	0.2	2.4	0.3
9/8/93	1.9	0.2	1.5	0.2	3.1	0.2	0.9	0.4	1.9	0.1
9/10/93	3.0	0.2			3.5	0.2	2.0	0.1	1.8	0.1
9/11/93							2.0	0.2	1.8	0.1
9/15/93	3.3	0.5	2.4	0.9	2.0	0.4	7.6	0.6	4.0	0.4
9/17/93			0.9	0.2	1.1	0.1	4.2	0.2	2.0	0.1
9/22/93	1.5	0.6	5.1	1.3	4.0	0.9			3.0	0.5
9/24/93	0.9	0.3	1.7	0.3	1.4	0.1	3.9	0.2	1.7	0.3
9/29/93	2.8	0.4	3.6	1.1	3.6	1.1	2.9	0.6	3.9	0.6
10/1/93	1.8	0.1	1.5	0.3	0.7	0.1	3.8	0.2	1.2	0.1
10/6/93	1.6	0.3	3.3	0.3	1.8	0.2	2.0	0.4	0.9	0.5
10/8/93	2.0	0.2	3.0	0.7	5.2	0.3	2.6	0.5	2.3	0.2
10/13/93	3.0	0.4	5.1	0.4	3.8	0.3	4.9	1.2	1.7	0.3
10/15/93	3.4	0.4	5.0	0.3	3.2	0.5	1.1	1.9	1.6	0.1
10/20/93	1.5	0.4	3.0	0.2	2.7	0.2	2.5	0.4	2.7	0.3
10/22/93	2.2	0.1	5.6	0.4	2.2	0.6	0.9	0.2	2.2	0.3
10/27/93	1.8	0.2	5.8	0.3	4.0	0.3	3.4	0.4	2.9	0.2
10/29/93	3.7	0.6	5.1	0.5	4.4	0.7	2.4	0.5	3.5	0.3
11/3/93	1.1	0.1	2.1	0.2	2.1	0.2			0.8	0.1
11/5/93	3.1	0.5			3.3	0.8			1.5	0.1



Vapor Phase Mercury Concentrations In Upstate New York (ng/m<sup>3</sup>, ± 1σ).

Date/Site	BE	±	ML	±	PR	±	WE	±	WI	±
11/10/93	2.5	0.2	2.3	0.2	2.3	0.1	2.7	0.2	1.0	0.1
11/12/93	3.4	0.3	2.6	0.4	1.8	0.3	3.3	0.4	2.2	0.1
11/17/93	1.8	0.1	4.2	0.4	2.2	0.3	3.3	0.2	2.2	0.1
11/19/93	2.3	0.3	4.2	0.8	2.1	0.5	4.2	0.5	2.1	0.1
11/24/93	3.2	0.2	4.5	0.3	1.4	0.2	4.5	0.4	1.9	0.2
11/26/93	5.3	0.9	7.3	0.6	3.4	0.3	3.5	0.7	2.8	0.2
12/1/93	4.9	0.3	2.7	0.2	1.9	0.2	3.9	0.2		
12/3/93	0.8	0.2	3.2	0.2	2.4	0.3	1.4	0.2		
12/8/93	2.7	0.2	3.2	0.3	3.4	0.4	3.9	0.4	2.0	0.1
12/10/93	2.0	0.4	5.6	0.8	6.2	0.6	2.4	0.4	1.3	0.3
12/15/93	1.8	0.1	3.7	0.4	3.1	0.2	3.2	0.5	3.8	0.3
12/17/93	3.9	0.3	4.5	0.5	3.9	0.7	3.3	0.3	2.9	0.4
12/22/93	2.1	0.2	2.8	0.2	1.4	0.2	2.3	0.3	3.1	0.5
12/24/93	2.4	0.2	4.6	0.3	3.0	0.2	4.4	0.3	3.7	0.3
12/29/93					1.2	0.1	0.9	0.1		
12/31/93	2.1	0.2	5.3	0.4	2.4	0.3	3.0	0.2	4.3	0.3
1/5/94	2.0	0.1			2.7	0.1	4.6	0.3	3.0	0.2
1/7/94	6.0	0.6	4.6	0.3	5.4	0.5	6.4	0.4	4.3	0.3
1/12/94	2.2	0.1	3.0	0.2	2.6	0.2	5.5	0.3	3.6	0.2
1/14/94	5.5	0.3	8.0	0.6	3.8	0.2	4.6	0.4	5.2	0.4
1/19/94			4.2	0.2	6.2	0.3	4.2	0.2	4.1	0.2
1/21/94	3.8	0.2	4.6	0.2	3.1	0.2	3.6	0.2	2.3	0.1
1/26/94	4.5	0.2	5.0	0.3	3.4	0.2	3.9	0.2	5.3	0.3
1/28/94	3.7	0.2	2.0	0.1	3.3	0.2	3.2	0.2	5.6	0.3
2/2/94	1.9	0.1	4.4	0.2	5.0	0.3	7.4	0.6	3.7	0.2
2/4/94	4.3	0.2	4.5	0.2	3.2	0.2	6.4	0.5	4.3	0.2
2/9/94			4.7	0.3	4.0	0.2	6.0	0.3	4.4	0.3
2/11/94	5.5	0.3	2.8	0.2	5.2	0.3	4.5	0.3	3.3	0.2
2/16/94	1.4	0.1	2.5	0.1	4.5	0.2	2.5	0.2	2.5	0.1
2/18/94	3.6	0.2	1.7	0.1	2.9	0.2	5.3	0.3	4.3	0.2
2/23/94			2.8	0.2	1.0	0.1	5.2	0.3	4.3	0.3
2/25/94	1.5	0.1	2.4	0.1	1.7	0.1	2.5	0.2	3.2	0.2
3/2/94	2.3	0.2	1.5	0.1	3.1	0.2	2.7	0.5	2.8	0.2
3/4/94	1.7	0.1	2.5	0.1	0.9	0.1	2.2	0.1	5.5	0.4
3/9/94	1.6	0.2	2.0	0.1	1.8	0.2	1.5	0.1	2.0	0.2
3/11/94	2.9	0.2	2.0	0.1	1.9	0.2	2.0	0.2	3.8	0.2
3/16/94	2.1	0.1	3.0	0.3	3.8	0.2	1.4	0.1	2.8	0.2

Vapor Phase Mercury Concentrations In Upstate New York (ng/m<sup>3</sup>, ± 1σ).

Date/Site	BE	±	ML	±	PR	±	WE	±	WI	±
3/18/94	2.3	0.2	2.1	0.1	2.8	0.2	3.7	0.2	2.8	0.2
3/23/94	4.7	0.3	2.9	0.2	2.3	0.3	2.2	0.2	1.3	0.4
3/25/94	3.8	0.6	1.8	0.2	2.1	0.2	2.0	0.2	5.3	0.7
3/30/94	2.2	0.1	2.7	0.2	1.9	0.5	1.9	0.1	1.4	0.1
4/1/94	3.0	0.3	2.7	0.3	2.1	0.2	4.6	2.0	1.7	0.4
4/6/94	1.3	0.1	1.5	0.2	0.8	0.1	1.0	0.1	1.5	0.1
4/8/94	2.2	0.3	1.3	0.2	1.5	0.3	3.3	0.4	1.5	0.3
4/13/94	3.6	0.2	1.9	0.2	3.1	0.2	1.2	0.1	1.4	0.1
4/15/94	3.4	0.3	2.3	0.1	1.9	0.1	1.2	0.2	1.2	0.1
4/20/94	3.0	0.2	1.4	0.1	2.0	0.1	1.9	0.1	2.4	0.2
4/22/94	2.8	0.4	1.7	0.2	2.0	0.2	2.6	0.2	1.7	0.1
4/27/94	2.8	0.3	1.9	0.2	1.9	0.1	1.8	0.2	1.5	0.1
4/29/94	2.1	0.1	1.0	0.1	2.5	0.6	1.6	0.1	1.6	0.1
5/4/94	1.1	0.1	2.0	0.2	1.9	0.1	2.5	0.4	1.5	0.1
5/6/94	1.4	0.1			1.1	0.1	0.6	0.1	1.0	0.1
5/11/94	1.1	0.1	1.9	0.1	0.8	0.1	0.8	0.1	1.8	0.1
5/13/94	1.1	0.1	2.6	0.3	1.0	0.1	3.4	0.4	1.4	0.1
5/18/94	1.3	0.1	2.1	0.2	0.8	0.2	1.6	0.1	2.3	0.2
5/20/94	1.2	0.2	1.7	0.1	1.7	0.2	1.7	0.2	2.4	0.2
5/25/94	1.7	0.2	2.9	0.2	3.6	0.4	2.0	0.1	1.8	0.2
5/26/94	1.5	0.2	1.7	0.2	1.8	0.1	1.6	0.2	1.2	0.2
5/28/94	1.7	0.2	3.8	0.3	4.1	0.4	1.4	0.2	1.6	0.2
6/1/94	1.2	0.2	2.2	0.2	1.6	0.1			2.0	0.2
6/2/94	2.1	0.1	3.3	0.2	2.4	0.2			1.4	0.1
6/8/94	2.3	0.1	1.7	0.1	2.2	0.3	1.8	0.2	1.4	0.1
6/9/94	1.1	0.1	1.4	0.1	1.3	0.1	0.6	0.1	1.4	0.1
6/15/94	0.7	0.1	1.7	0.2	1.6	0.2	0.9	0.2	1.4	0.2
6/16/94			1.5	0.1	0.7	0.1	1.3	0.2	1.0	0.1
6/22/94	0.9	0.1	2.2	0.1	1.7	0.2	1.0	0.1	1.0	0.1
6/23/94			1.8	0.1	1.4	0.1	0.6	0.1	1.4	0.1
6/29/94	0.8	0.1	1.9	0.1	1.9	0.1	1.1	0.2	0.9	0.1
6/30/94	2.1	0.2	1.6	0.2	1.5	0.1			2.2	0.2
7/6/94	2.3	0.2	1.4	0.2	1.3	0.1			0.9	0.1
7/7/94			0.8	0.1	2.1	0.1	0.9	0.1	0.8	0.1
7/13/94	2.7	0.2	2.3	0.2	2.2	0.2	2.0	0.6		
7/14/94	1.0	0.1	1.3	0.1	0.9	0.1	1.3	0.1		
7/20/94	3.0	0.2	2.0	0.1	5.8	1.7	2.0	0.2	1.2	0.2
7/21/94			1.9	0.1			0.8	0.1	1.9	0.2
7/27/94			1.1	0.3	2.0	0.3	1.7	0.1	3.8	0.2
7/28/94			0.8	0.1	0.9	0.2	2.9	0.2		

